Polyethylene Devices and the Effects of Sediment Resuspension on the Cycling of PAHs and PCBs in the Lower Hudson Estuary

by

Rachel G. Adams

S.M., Civil and Environmental Engineering, Massachusetts Institute of Technology, 2000
B.S. Chemical Engineering, University of Michigan, Ann Arbor, 1994

Submitted to the Department of Civil and Environmental Engineering in Partial Fulfillment of the Requirements of the Degree of

DOCTOR OF PHILOSOPHY
IN CIVIL AND ENVIRONMENTAL ENGINEERING

at the

MASSACHUSETTS INSTITUTE OF TECHNOLOGY

February 2003

Signature of the Author _____
Department of Civil and Environmental Engineering
October 3, 2002

Certified by _____
Philip M. Gschwend
Professor of Civil and Environmental Engineering
Thesis Supervisor

Accepted by _____
Professor Oral Buyukozturk
Chairman, Departmental Committee on Graduate Studies

Polyethylene Devices and the Effects of Sediment Resuspension on the Cycling of PAHs and PCBs in the Lower Hudson Estuary

by

Rachel G. Adams

Submitted to the Department of Civil and Environmental Engineering on October 3, 2002 in partial fulfillment of the requirements for the Degree of Doctor of Philosophy in Civil and Environmental Engineering

ABSTRACT

In order to examine the importance of sediment resuspension on the sediment bed-to-water column transport of hydrophobic organic contaminants (HOCs) in the lower Hudson Estuary, the following areas of research were pursued: 1) a passive, *in situ* sampler, a polyethylene device (PED), for measuring HOCs in the aquatic environment was developed; 2) the desorption rate of pyrene, a polycyclic aromatic hydrocarbon (PAH), from native Hudson River sediments was measured, and 3) pyrene and 2,2',5,5'-tetrachlorobiphenyl (PCB #52), a polychlorinated biphenyl (PCB), concentrations were measured in the lower Hudson Estuary so that the input of these chemicals as a result of sediment resuspension could be compared to modeling expectations and the contribution of sediment resuspension to these chemicals' cycling could be quantified.

The use of a new passive, *in situ* sampler, a polyethylene device (PED), for measuring hydrophobic organic contaminants (HOCs) in the aquatic environment was demonstrated. Like semipermeable membrane devices (SPMDs) and solid-phase microextraction (SPME), PEDs passively measure the concentration of chemical present in the dissolved phase. PEDs provide for *in situ,* time-averaged measurements with fast equilibration times (on the order of days) and simple laboratory extraction. Polyethylene-water equilibrium partitioning constants (K_{PEW}s) and polyethylene diffusivity coefficients (D_{PE}s) were measured in the laboratory so that dissolved concentrations could be calculated subsequent to PED extraction. K_{PEW}s for eleven PAHs and PCBs were found to correlate closely with octanol-water equilibrium partitioning constants (K_{OW}s; $\log K_{PEW} = 1.1 \log K_{OW} - 0.45$, $R^2 = 0.85$). Temperature and salinity dependence of K_{PEW} for the chemical of interest can be predicted with that chemical's excess enthalpy of solution and Setschenow constant, respectively. D_{PE}s for several HOCs were measured in the laboratory so that the time for equilibrium uptake in the field could be predicted. PEDs allowed for quick, *in situ*, time-averaged measurements of phenanthrene and pyrene at pM concentrations and PCB #52 at fM concentrations in Boston Harbor seawater.

Observations of disequilibrium between sorbed HOCs (e.g., PAHs & PCBs) and the surrounding environmental waters indicate that the times for desorption are important for understanding the fate of HOCs. Settling and resuspended particles can play a significant role in the cycling of HOCs. For PAHs, like pyrene, these chemicals' strong affinity for black carbon in the environment makes the rate of desorption less certain. The desorption rate for pyrene from native Hudson River sediment was measured in the laboratory and a diffusion rate constant (effective diffusivity/particle radius^2) ranging from 1.0E-7 to 5.6E-7 s^{-1} was measured. The results were in good agreement with a physically- and chemically-based model for estimating effective diffusivity and the rate of desorption.

The elevated levels of PAHs and PCBs in the sediments of the lower Hudson Estuary coupled with the tidally-driven sediment resuspension that occurs there, provide for the transport of these HOCs to and from the overlying water column. PED-measured dissolved concentrations of pyrene and PCB #52 were quantified during both neap and spring tides during April and October field campaigns in order to assess the impact of increased sediment resuspension. The chemical potential in the sediments was found to be higher than that of the overlying waters for both pyrene and PCB #52. The input due to sediment resuspension to the lower Hudson Estuary was estimated to be 640 – 2200 g/day for pyrene and 12 - 32 g/day for PCB #52 during April 1999, and 62 – 800 g/day for pyrene and 4.4 – 10 g/day for PCB #52 during October 2000. A comparison to other sources and sinks suggest that sediment resuspension is an important source. A one-box model was used to estimate the dissolved concentration within the estuary. This allowed for the validity of the model to be assessed and for missing sources or sinks to be examined. In April 1999 resuspended sediments appear to have served as a source of pyrene to the estuary, while during October 2000 the sediments and water were close to equilibrium suggesting a diminished source of pyrene to the overlying water. In contrast, mixing diagrams in April 1999 suggest that the resuspended sediments were serving as a sink, scavenging PCB #52. However, the sediment and water samples indicate that there was a driving force from the sediments to the water. A possible explanation for this observation may be the scavenging of PCB #52 by "cleaner" sediments throughout the estuary. In October 2000, as with pyrene, the sediments and water were more closely equilibrated with respect to PCB #52. These results show that sediment resuspension is important to the cycling of PAHs and PCBs in the lower Hudson Estuary.

Thesis Supervisor: Philip M. Gschwend
Title: Professor of Civil and Environmental Engineering

ACKNOWLEDGMENTS

This work was supported by the Office of Naval Research Grant Nos. N00014-93-1-0883 and N00014-99-0039 and Grant No. 006/01A of the Hudson River Foundation. I would also like to thank the Hudson River Foundation for support by a graduate fellowship (Grant No GF/01/01).

The completion of this thesis would not have been possible without the help of many people.

I cannot thank John MacFarlane enough for all that he has taught me and all of the help he has given me in the lab. He has helped me throughout my years at MIT and was invaluable to the April 1999 sampling campaign for which we were able to perform extensive sampling despite the rainy, cold weather and boat engine problems we experienced. Above all John has been a pleasure to work with and has provided me with invaluable advice and support.

Rocky Geyer is the driving force behind the Hudson sampling trips. Without him, none of these trips would be possible. He has kindly shared with me his knowledge of sediment transport and the estuarine behavior of the lower Hudson Estuary.

I wish to thank Terry Donoghue for piloting the *Mytilus* in April 1999. Thanks also go to Rainer Lohmann, Linda Kalnejais, Jay Sisson, Chris Sommerfield, and all of the researchers and crew aboard the *Samantha Miller* in October 2000 for their tireless efforts in the field.

Rainer Lohmann has also been working on PEDs and provided some of the polyethylene-water partitioning coefficients and organic and black carbon results presented in this thesis. I am thankful to him for sharing his laboratory expertise and his data with me.

I would also like to thank Chris Swartz, Allison MacKay, and Örjan Gustafsson for sharing their knowledge and showing me the ropes as a new graduate student. I have also enjoyed discussions with the many post docs that I have worked with: Lukas Wick, Carol Johnson, Kris McNeill, Goran Ewald, and Greg Noonan.

Steve Rudnick and Bob Chen helped me to use their time-resolved, laser-induced fluorescence spectrometer system and helped me to evaluate some of the data. They and the others in their lab made me feel very welcome, and I really appreciate all of their help.

I thank my thesis committee Phil Gschwend, Rocky Geyer, Harry Hemond, and Chris Reddy. They provided many thoughtful ideas and suggestions as to how to improve my work and this thesis.

I owe a great deal of thanks to my advisor Phil Gschwend. He has been the driving force behind this work and has provided a myriad of ideas and suggestions that have greatly improved it. He has taught me so much, and his enthusiasm for learning has been inspiring.

I must also thank Sheila Frankel. She has provided me with invaluable advice and support. She is always available to help a student in need, and I am so thankful to her for her encouragement.

Thanks also to Vicki Murphy, Sheila Anderson, and Jim Long. They are the people that keep Parsons running. I am especially lucky to have worked with Vicki

Murphy. I can always count on her to help me straighten out a bureaucratic debacle and to be just really friendly and helpful.

I am so thankful to Steve Margulis. He has always been there to listen to my latest idea or help me think through an obstacle in my research. He has helped me in more ways than I can begin to list.

Finally, I want to thank all of my friends at Parsons. There are too many great people to list, and I'm afraid I might forget someone. I appreciate all of the smiles and kind words I got from the friends I have made here. They have significantly enhanced my graduate school experience.

TABLE OF CONTENTS

LIST OF TABLES

LIST OF FIGURES

CHAPTER 1: INTRODUCTION

Once in the aquatic environment, the hydrophobic nature of polycyclic aromatic hydrocarbons (PAHs) and polychlorinated biphenyls (PCBs) causes them to preferentially sorb to the sediments (1). Consequently, even after the input of these contaminants has ceased or diminished, the sediments can remain a source of pollutants to the surrounding water. Recent studies indicate that the sediments of urban bodies of water are a source of hydrophobic organic contaminants (HOCs) to the overlying water column (2-6). The significant resuspension events that occur in the lower Hudson Estuary (7-9) may result in large fluxes of PAHs and PCBs to the surrounding waters. Recent studies in the Hudson (3,10) suggest that this is the case. It is important to improve our understanding of the extent to which sediment resuspension and subsequent chemical desorption play a role in the release of PAHs and PCBs to the water column so that we may improve our understanding of the mechanisms governing the fate of these chemicals in the environment. This improved understanding will aid environmental regulators and scientists in understanding the effects of these chemicals on the surrounding ecosystem and organisms and allow for the selection of appropriate sediment quality criteria (11,12).

The U.S. Environmental Protection Agency (EPA) estimates that approximately 10% of the sediment underlying U.S. surface waters is sufficiently contaminated with toxic pollutants to pose potential risks to fish and to humans and wildlife who eat fish (12). The U.S. EPA has studied data from 1,372 of the 2,111 watersheds in the continental U.S., and 96 of these studied watersheds have been identified to contain "areas of probable concern" where potential adverse effects of sediment contamination

are more likely to be found (12). Similarly, out of 22 coastal embayments sampled by the U.S. National Oceanographic and Atmospheric Administration (NOAA) 11% of the surveyed area was found to be toxic in an amphipod survival test (13). Because of the contaminated sediments present throughout the United States as well as other parts of the world, the transfer of HOCs from the sediments to the surrounding waters is an important area of study.

The suspension of contaminated particles is of particular concern as it allows for direct contact between sorbed pollutants and the surrounding water. Several researchers have studied the importance of particle cycling on the fate of PAHs and PCBs in lakes (14-16) and estuaries (17-19). Depending on the difference in chemical potential between the sediments and water, particles may serve as a source or sink for HOCs in the surrounding waters.

The scavenging of PCBs onto settling particles has been observed in the aquatic environment. Jeremiason et al. (20) used sediment traps to estimate that over 50% of the total Lake Superior water PCB burden is transported each year by settling particles to within 5 m of the lake bottom. However, they estimate that only 2-5% of the settling PCBs accumulate in bottom sediments, suggesting that most of the PCBs are recycled in the bottom waters. In contrast, sediments with a greater chemical potential than the surrounding water may provide for the bed-to-water transfer of PAHs and PCBs. Capel and Eisenreich (21) observed elevated PCB concentrations in Lake Superior during the spring months when sediments are resuspended tens of meters into the water column. They observed the water column to have a PCB signature closely aligned to the PCB signature observed in the sediments during the spring months, while the summer PCB

water column signature was dissimilar to the underlying sediments. Maskaoui et al. (22) measured PAH porewater concentrations that were greater than surface water levels in the Jiulong River Estuary suggesting that the sediments may, in fact, serve as a source of PAHs to the overlying waters. In the Hudson River Estuary, sediment-bound PCBs were above equilibrium with the overlying water, suggesting that Hudson River sediments are a source of PCBs to the surrounding waters (3). Achman et al. have estimated that the sediment-exchange fluxes of PCBs are 2 to 100 times greater than the advective fluxes.

The overall goal of this research was to further our understanding of the fate of PAHs and PCBs in the aquatic environment, specifically, the importance of sediment resuspension on the sediment-water transport of HOCs in the lower Hudson Estuary. In order to accomplish this goal the following tasks were completed: 1) a passive, *in situ* sampler, a polyethylene device (PED), for measuring HOCs in the aquatic environment was developed; 2) the desorption rates of pyrene, a PAH, from native Hudson River sediments were measured, and 3) using chemical concentrations measured in the lower Hudson Estuary, the input of pyrene and 2,2',5,5'-tetrachlorobiphenyl (PCB #52), a PCB, due to sediment resuspension was quantified.

In Chapter 2, the parameters necessary for PED use were measured in the laboratory, and their use in the aquatic environment was demonstrated. PEDs, which are simply strips of low-density polyethylene, provide for *in situ*, time-averaged measurements with fast equilibration times and simple laboratory extraction. Polyethylene-water equilibrium partitioning constants and polyethylene diffusivity coefficients were measured in the laboratory so that dissolved concentrations could be calculated subsequent to PED extractions. PED sampling in Boston Harbor provided for

time-averaged measurements of phenanthrene and pyrene at pM concentrations and PCB #52 at fM concentrations.

In Chapter 3, the desorption kinetics of pyrene from native Hudson River sediments were measured. Laboratory desorption experiments were performed using time-resolved, laser-induced fluorescence and the results were modeled with the physically-based desorption model proposed by Wu and Gschwend (23,24). The measured rate constant was then used to estimate the time for pyrene desorption in the lower Hudson Estuary.

In Chapter 4, the importance of sediment resuspension to the inputs of dissolved pyrene and PCB #52 were examined. PED-measured dissolved concentrations were collected during both neap and spring tides in order to assess the impact of increased sediment resuspension. Dissolved concentrations were examined with respect to salinity, which was used as an index of conservative mixing, in order to observe conservative or non-conservative behavior within the estuary. The magnitudes of the predominant sources and sinks of pyrene and PCB #52 were estimated. Finally, dissolved concentrations of each chemical in the estuary were models with a one-box model approach in order to assess the validity of the model and check for any missing sources or sinks.

Finally, major conclusions and areas of future work are discussed in Chapter 5.

CHAPTER 2: POLYETHYLENE DEVICES: SAMPLERS FOR MEASURING TRACE DISSOLVED HYDROPHOBIC ORGANIC CONTAMINANTS IN THE AQUATIC ENVIRONMENT

INTRODUCTION

Many hydrophobic organic contaminants (HOCs) including polycyclic aromatic hydrocarbons (PAHs) and polychlorinated biphenyls (PCBs) are toxic. Unfortunately, these toxic chemicals are prevalent in the aquatic environment. While only a small fraction of the HOCs in the environment are present in the dissolved phase, it is the chemical's activity, which is closely related to this dissolved level, that controls the diffusive transport into other surrounding phases (i.e., volatilization, sorption, and passive uptake into organisms). Until recently, measuring the concentrations of dissolved HOCs has required the extraction of large volumes of water due to their low dissolved concentrations in the environment. This water must also be filtered in order to remove particulate matter; however, depending on the size of filter used, colloids and even larger particles may still be present in this "dissolved" fraction.

In the 1970's, scientists began Mussel Watch (25) a program where the concentrations of pollutants in mussels were measured in order to monitor the quality of the waters in which the mussels lived. Because mussels concentrate chemicals by up to factors of 10^5 depending on the chemical, a much smaller sample can be analyzed than could be if the water is extracted. However, differences in biological or biochemical activities of the mussels were believed to result in some of the temporal and spatial variations observed in the mussel data.

Recently, two samplers based on the passive partitioning of HOCs into a hydrophobic phase have been used to measure HOCs in the dissolved phase. Huckins et al. (26) developed lipid-containing polyethylene tubes called semipermeable membrane devices (SPMDs) to passively monitor the concentration of HOCs dissolved in the water. Arthur and Pawliszyn (27) developed solid phase microextraction (SPME) for the concentration of organic chemicals onto chemically modified fused silica fibers followed by thermal desorption directly into an analyzing instrument. Both samplers are widely used.

SPMDs can serve as a surrogate to organisms living in the aquatic environment. They measure a chemical's activity in the environment while limiting variability due to biological activity (28). SPMDs allow for a time-averaged measurement of the concentrations of HOCs present (29). The chemicals of interest are concentrated into the triolein *as well as the polyethylene tubing* allowing for the recovery of large quantities of these chemicals (30). Laboratory experiments have been performed to measure the partitioning of HOCs into SPMDs and the rate of HOC uptake, allowing water concentrations to be calculated (29,30). At water flow rates less than 0.28 cm/s, chemical uptake may be limited by a water-controlled boundary layer (31). However, recovery compounds can be added to the SPMD prior to deployment in order to correct for variations in analyte uptake (32,33).

While SPMDs have proven to be useful samplers of the aquatic environment, many sampling difficulties still exist. SPMDs require protective housing for their deployment in order to avoid damage (32). We have found them to tear in the field resulting in a loss of an unknown quantity of the lipid inside. This loss makes it difficult

to calculate the HOC concentration that was in the water. Separating the triolein and its component fatty acids (i.e., oleic acid) from the HOC requires extra separation steps (32). Lengthy deployment times (14-30 days) required for SPMDs can be inconvenient and can enable biofouling which alters the uptake rates for the analytes of interest (32).

Another sampling method, SPME, has also been used for the passive measurement of HOCs in environmental samples (34). SPME allows for the desorption of the concentrated extract directly into the analyzing instrument. First, a polymer-coated silica fiber is exposed to the sample allowing the chemical of interest to absorb into the polymer. The fiber is then placed into the hot injector of a gas chromatograph or other instrument and thermally desorbed. This method does not require solvents and allows for simplified sample extraction (35). Varying polymer types and thicknesses have been used to suit the chemicals of interest (35). SPME fibers can be reused in order to limit cost. However, SPME fibers are fragile (35) so that sampling the environment directly is not always practical. In fact, high percentages of suspended matter in moving water can cause fiber damage (35). Typically, environmental samples are collected and then SPME sampling is done in the laboratory. Unfortunately, this method does not yield time-averaged concentration results. The reuse of fibers is limited by carryover of chemicals from previous extractions, and a blank of the fiber should be run at least once between samples (34). Potter & Pawliszyn (34) found carryover to be significant for benz(a)anthracene, benzo(a)pyrene, and pentachlorobiphenyl even after four fiber blanks. Because the volume of polymer coated on the fibers is less that that of the triolein and polymer volume used in SPMDs, detection limits for SPME are generally not as low as those for SPMDs.

In our study, a new passive sampler called a polyethylene device (PED) is introduced. PEDs, which are simply strips of low-density polyethylene, provide a simple and effective method for the passive, *in situ* sampling of HOCs dissolved in water. They combine the best of SPMDs and SPME. If tearing occurs, this is not a problem as there is no triolein to leak out. Also, the single layer of plastic exposed on both sides allows for faster equilibration times. This enables environmental observations to be made in shorter times. It also results in less time for the formation of biofilms. Similar to SPMDs, reference compounds can be impregnated into the PEDs in order to correct for any variations in uptake rate that may be caused by biofouling or a water-controlled boundary layer. The absence of triolein greatly simplifies the extract cleanup procedure. While PEDs cannot be inserted directly into the detector as SPME fibers are, their larger volume allows for a greater mass of chemical to be collected. Because they are easily used *in situ*, time-averaged environmental concentrations can be measured. As polyethylene is inexpensive, there is no need to reuse PEDs, eliminating any carryover problems that occur with SPME.

Because PEDs sample by diffusive uptake, an understanding of the polyethylene-water partitioning (K_{PEW}) as well as the diffusivity in polyethylene (D_{PE}) for the chemical of interest is needed. Here we report K_{PEW} and D_{PE} values for several PAHs and PCBs. Temperature and salinity effects on the K_{PEW} for selected chemicals were examined, and the temperature dependencies of D_{PE} were also tested. Finally, we used K_{PEW}s and D_{PE}s to quantify HOC concentrations for PED samples from Boston Harbor.

THEORY

In order to solve for the concentration of chemical present in the water of interest, the K_{PEW} (L^3/M) must be known. The K_{PEW} is the ratio of the concentration of chemical in polyethylene (C_{PE}; M/M) and the concentration of chemical in water (C_w; M/L^3) at equilibrium:

$$K_{PEW} = \frac{C_{PE}}{C_W} \tag{2.1}$$

With this K_{PEW} and the measured C_{PE}, the concentration of the chemical in the water at equilibrium can be estimated.

Because it may not always be possible or convenient to keep the PEDs in the environment for the time required for equilibration, it is important to understand the kinetics of uptake. When a plane sheet is suspended in a large volume of solution such that the amount of solute taken up by the sheet is a negligible fraction of the total solute mass, the concentration in the solution remains constant (36). This is the case for a PED in a large body of water (e.g. a lake, river, harbor, etc.). However, for a limited volume of solution (as is typical in laboratory experiments), a decrease in the concentration of solute in the solution will result because a significant fraction of solute will diffuse into the polyethylene (PE) sheet. Consequently, the empirically observed uptake rate varies as a function of the percentage of total chemical finally taken up by the sheet. The time for equilibration increases as the size of the water body increases. For example, for pyrene diffusing into polyethylene with a 78 μm thickness, it takes 3.4 days to reach 50% of equilibrium in an infinite bath (i.e., large body of water), while it only takes 1.3 hours to reach 50% equilibrium when 90% of the total solute mass is finally taken up by the

sheet. The total mass of pyrene diffused into the PE in the first case is ten times greater than in the latter case, which results in longer equilibration times.

The limited volume case (i.e., the laboratory) allows one to measure the change in concentration in the solution over time. Assuming there is no water boundary limitation to transfer, the results can be used to estimate the diffusivity of the solute in the PE sheet. Crank (36) solved Fick's second law for the diffusion of a chemical from a stirred solution of limited volume into both sides of a plane sheet:

$$\frac{M_t}{M_\infty} = 1 - \sum_{n=1}^{\infty} \frac{2\alpha(1+\alpha)}{1+\alpha+\alpha^2 q_n^2} \exp\left(-Dq_n^2 t / l^2\right) \qquad (2.2)$$

where M_t and M_∞ are the total amount of chemical in the sheet at time t and at infinite time, respectively (M), D is the diffusion coefficient (L^2/T), t is time (T), and l is one-half of the sheet thickness (L). The values of q_n are the non-zero positive roots of:

$$\tan(q_n) = -\alpha \cdot q_n \qquad (2.3)$$

and α is the ratio of the volume of solution, V_W (L^3), to the mass of the PE sheet, $Mass_{PE}$ (M), divided by the partition coefficient:

$$\alpha = \frac{(V_W / Mass_{PE})}{K_{PEW}} \qquad (2.4)$$

In other words, α is the ratio of the dissolved to sorbed chemical at equilibrium. The fractional uptake, f_{PE}, into the PE sheet at equilibrium may also be used to solve for α. The f_{PE} is equivalent to $1/(1+\alpha)$. For example, if 75 percent of the chemical in the PE-water system is in the sheet at equilibrium, f_{PE} is 0.75, and α is 0.33. Equation 2.2 can be used to estimate D by solving for the best fit with experimental data.

When there is an infinite amount of solute or a bath that is so large that the solution concentration does not change due to PED uptake (an infinite bath case), the following equation, also from Crank (36), can be used to solve for M_t/M_∞:

$$\frac{M_t}{M_\infty} = 1 - \sum_{n=0}^{\infty} \frac{8}{(2n+1)^2 \pi^2} \cdot \exp\left\{ -D\left(n+\frac{1}{2}\right)^2 \cdot \frac{\pi^2 t}{l^2} \right\} \tag{2.5}$$

By combining Eqs. 2.1 and 2.5, one can solve for C_w as a function of C_{PE}, K_{PEW}, D, t, and l:

$$C_W = \frac{C_{PE}}{K_{PEW} \cdot \left[1 - \sum_{n=0}^{\infty} \frac{8}{(2n+1)^2 \pi^2} \cdot \exp\left\{ -D\left(n+\frac{1}{2}\right)^2 \cdot \frac{\pi^2 t}{l^2} \right\} \right]} \tag{2.6}$$

As t approaches infinity, C_w approaches C_{PE}/K_{PEW}. Diffusivity and K_{PEW} can be obtained from lab experiments; and C_{PE}, t and l can be measured in field-deployed PEDs allowing one to solve for C_w in an infinite bath (i.e., an environmental case).

EXPERIMENTAL SECTION

Materials

Methanol (MeOH), acetone, methylene chloride (DCM), and hexane solvents were all JT Baker Ultra-resi-analyzed (Phillipsburg, NJ).

Low-density polyethylene (0.92 g/cm^3) from two different manufacturers was used in the experiments. The first polyethylene (Brentwood Plastics, Inc., Brentwood, MO) was 70 ± 1 μm thick. The second (Carlisle Plastic, Inc., Minneapolis, MN) was 51 ± 3 μm thick. Prior to use, PE was pre-cleaned with 500 mL of methylene chloride for a

minimum of 48 hours, followed with methanol (24 hr), and finally clean water (24 hr). PEDs were kept in clean water (treatment explained below) until use.

All water was reverse osmosis pretreated and run through an ion-exchange resin and activated carbon filter system (Aries Vaponics, Rockland, MA) until a resistance of 18 MΩ was achieved. The water was then treated with ultraviolet light (Aquafine total organic carbon reduction unit, Valencia, CA) and filtered with a 0.22 μm filter (Millipore, Bedford, MA). This low-carbon water was found to have less than 0.3 mg/L of total organic carbon (TOC) upon analysis on a Shimadzu TOC-5000 (Columbia, MD).

Water Sampling Experiment

In order to sample a PED-water system multiple times so that the time-dependence of concentration could be repeatedly observed, a closed incubation apparatus that allowed for the sampling of a small fraction of water was developed. Phenanthrene and pyrene were examined in the first set of experiments and 2,2',5,5'-tetrachlorobiphenyl (PCB #52) was measured in the following experiments. One polyethylene device (PED) was placed in one of two opaque 13-L stainless-steel beakers with stainless steel lids (Polar Ware, Sheboygan, WI). Each beaker was filled with 10 L of water. Phenanthrene and pyrene beaker concentrations were 150 μg/L (300 μL of 5000 μg/mL in MeOH, Supelco, Bellefonte, PA) and 20 μg/L (200 μL of 1000 μg/mL in MeOH, Supelco), respectively. The PCB # 52 concentration was 16 μg/L (400 μL of 400 μg/mL in acetone prepared by dissolving 10 mg PCB #52, UltraScientific, N. Kingstown, RI). No PED was added to the second beaker, which served as a control.

The beaker solutions were allowed to equilibrate overnight after the chemicals of interest had been added. The PAH solutions were subsampled (3 mL) over time and analyzed via fluorescence spectroscopy (see below). The PCB #52 solutions were subsampled (10 mL) over time, extracted into 0.5 mL hexane, recovery corrected with hexachlorobenzene (10 μl of 1 μg/mL in acetone, Kodak Eastman, Rochester, NY), and analyzed with a gas chromatograph-electron capture detector (GC-ECD; see below). Several subsamples were taken and analyzed over a period of several hours to measure the initial water concentration.

The PEDs were punctured with sixteen-gauge stainless-steel or copper wire approximately every 3 cm in an accordion fashion. The wire was then bent into a circle

(~11 cm in diameter) and attached to a stainless steel rod, which could be rotated. The PED was pulled flat against the wire in a circle. Then the PED was added to the first beaker and spun at speeds ranging from approximately 1 m/s (90 rev/min) to 0.3 m/s (30 rev/min) in order to mimic a typical water flow in the field. Because no change in uptake rate was observed upon changing the spinning from 1 m/s to 0.3 m/s, the chemical uptake rate is not thought to have been water-boundary controlled with in this range of spinning rates. Approximately 500 mg of PED was used in the PAH experiment, and 90 mg in the PCB experiment. The beakers were subsampled every 20 to 30 minutes initially and at longer time intervals after the PED and water in the first beaker had reached equilibrium (Figure 2.1).

Lab experiments allowed for the determination of the fraction of chemical present in the water at equilibrium (Figure 2.1). Assuming that the chemical is present only in the water or the PED (i.e., there are no wall effects, transformations, or losses), one may solve for the K_{PEW} as a function of the fraction of the chemical in the water f_w at equilibrium:

$$K_{PEW} = \frac{(1/f_w) - 1}{r_{PEW}} \tag{2.7}$$

where r_{PEW} is the polyethylene-to-water phase ratio (M/L^3). Any losses observed in the control beaker were used to correct the f_w. This control-corrected f_w was calculated as:

$$f_W = \frac{C_{W,t,PED}}{C_{W,0,PED}} \cdot \frac{C_{W,0,Control}}{C_{W,t,Control}} \tag{2.8}$$

where $C_{W,t,PED}$ is the water concentration in the PED beaker at time t, $C_{W,0,PED}$, is the water concentration in the PED beaker just before the PED is added, $C_{W,0,Control}$ is the water concentration in the control beaker at time zero just before the PED is added to the

PED beaker, and $C_{W,t,Control}$ is the concentration in the water in the control beaker at time *t*.

In order to measure the temperature dependence of K_{PEW}, partitioning experiments were performed at several temperatures. The temperature was gradually decreased and finally increased to rule out chemical degradation as the cause for the decreased water concentrations. Several PAH uptake experiments were also performed at varying temperatures to investigate the importance of temperature on kinetics. The temperature of the beakers was maintained by placing them in a 40-L insulated tank attached to a refrigerated 28-L recirculator (Forma Scientific, model 2100, Marietta, OH) and kept constant at temperatures ranging from 3 ± 0.3 to 24 ± 0.3°C for 24 hours before the water concentrations were measured.

In order to measure the salinity dependence of K_{PEW} on the PAHs, sodium chloride (NaCl) was added to the beakers to create a 0.1 M NaCl solution. Phenanthrene and pyrene calibration solutions with 0.5 M NaCl were made and fluorescence intensities were measured to insure that salinity had no effect on fluorescence.

Fluorescence intensities for phenanthrene and pyrene were measured over time for the PED laboratory experiments performed at 23°C. Over this period 1.4% of the water was removed for sampling purposes. A linear fit of the control beaker concentration data showed the fluorescence intensities decreasing by 6% for both phenanthrene and pyrene over the course of the experiment (130 hours; Figure 2.1). This small loss from the control beaker suggests that losses due to biodegradation, volatilization, etc. were small compared to uptake by the PED. As the stainless-steel

beakers are opaque, photodegradation can also be excluded as a possible decay mechanism.

A PAH mass balance was performed at the end of the 2-day 22°C lab experiment (Table 2.1). The PED was extracted in 540 mL of hexane for 48 hours, and the phenanthrene and pyrene fluorescences were measured. For both phenanthrene and pyrene, the total mass measured was in good agreement with the mass added. For phenanthrene extracted from the beaker wall, an overlapping peak (d_{10}-phenanthrene which had been added as a mass spectrometer recovery standard) prohibited us from measuring the intensity of phenanthrene. It can only be said that it was less than the height of the shoulder of the overlapping peak. However, the mass of phenanthrene and pyrene measured on the beaker walls of the experiment performed at 14°C was found to be 2 μg of phenanthrene for both the control beaker extract and the PED beaker extract. If this was the value of phenanthrene on the wall at the end of the 22°C experiment, the total phenanthrene recovered was 1471 μg, which is 98% of the mass added. For pyrene, 99% of the chemical added was in the water or in the PED. These mass balances indicate that there was little or no photodegradation or biodegradation. Because 98% of phenanthrene and 99% of pyrene was found to be in one of two phases (water and PED), our assumption that this was a two-phase system appears to be a valid one.

The concentrations of PCB #52 were measured in both the PED and the control beaker throughout the course of the PCB experiment. A linear fit of the control beaker concentration data indicated that the PCB #52 concentration increased by 5% over the first 160 hours of the experiment (Figure 2.1). This is within the standard deviation of the measurements. However, over the entire course of this 71-day experiment, there was

considerable loss of PCB #52. The water, PED (if present), and beaker walls were extracted for both the PED beaker and the control beaker, so that a mass balance on each beaker and its contents could be performed (Table 2.1). The PED was extracted in hexane for 48 hours. Water samples from each of the beakers were extracted as discussed previously, and the beaker walls were extracted with DCM. Cl_6-benzene was used as a recovery standard for all of the extracts. The samples were analyzed on a gas chromatograph-mass spectrometer (see below).

Approximately 50% of the PCB #52 initially added was recovered at the end of the 71-day experiment. We estimate that between 6 and 24% of PCB #52 was lost due to volatilization over the time period of the experiment. This assumes that the PCBs in the water and air have equilibrated, and that each time the beaker is sampled, the PCBs in the headspace are lost. However, as the beaker lids were not airtight, it is possible that there was greater PCB loss due to volatilization over the 71-day period. Between 1 and 3% of the PCB was removed from the beaker due to sample removal. Because of the agreement between the total beaker extracts in both beakers, PCB concentrations were corrected with the control beaker (see above).

PED and Water Extraction Experiment

In order to measure *multiple* K_{PEW}s in the same experiment, multiple round-bottom flasks were prepared with water containing known concentrations of several PCBs or several PAHs and one small piece of PED (~ 4 mg) per flask. All of the experiments were performed at room temperature (23°C), unless otherwise noted.

The PCB PED and water extraction experiments were performed by Rainer Lohmann in the Gschwend laboratory. A 4-L aqueous solution containing PCBs (# 29 and 69 at 20 pg/mL, UltraScientific) was prepared from a 200-pg/μL PCB solution in acetone and transferred into 250 mL flasks. A small piece of PED (~ 4 mg) was added to each flask. The flasks were then tumbled for increasing time intervals (6, 12, 24 hrs, 2, 4, 7 days, and three were removed at 14 days) in order to ensure equilibrium. The PEDs were extracted in 5 mL of DCM followed by 5 mL of hexane. For most samples, the aqueous phase was also solvent-extracted. A 25 μL internal PCB-standard (# 35, 60, 114, and 169 at 200 pg/μL) was added prior to extraction, and a 10-μL aliquot of a 10 ng/μL m-terphenyl solution was used as an injection standard.

A 4-L water solution containing 60 ng/L phenanthrene, 30 ng/L 2-methyl-phenanthrene and pyrene, 20 ng/L benz(a)anthracene, 40 ng/L chrysene, 200 ng/L benzo(a)pyrene, and 90 ng/L perylene was prepared. The phenanthrene and pyrene solutions were the same used in the water sampling experiment. Chrysene (95%), 2-methyl-phenanthrene (99%), perylene (>99%), benzo(e)pyrene (99%; all from Aldrich, Milwaukee, WI) and benz(a)anthracene (Accustandard Inc.; New Haven, CT) were dissolved in acetone, and subsequently added to the water solution. Approximately 500 mL of this solution was added to each of six 500-mL glass round-bottom flasks.

Prior to the partitioning experiment, six 7-mg PED circles were stirred in a 50 mL glass round-bottom flask with 50 mL of acetone containing 4 μg/mL d_{12}-benz(a)anthracene (2000 μg/mL dissolved in DCM from UltraScientific) and fluoranthene (98% from Aldrich). Impregnating the plastic with these PAHs allowed us to ensure that equilibrium had been reached at the end of the experiment. For example,

one would expect the K_{PEW}s for the deuterated and non-deuterated benz(a)anthracene to be equal at equilibrium. The circles and acetone solution were stirred with a glass-covered stir bar for 26 hr. The PED circles were then placed in 50 mL of water and stirred for 1 hr. This process was repeated two more times to insure that all of the acetone had been removed. While a small quantity of PAHs may also have been removed, their low solubility and higher molecular weight allowed for a minimal loss.

Each circle was then cut into two pieces. Approximately three-fifths of each circle was added to one of the six round-bottom flasks, and the remaining two-fifths was extracted (see below). Each of the flasks was stirred on a stir plate with a glass-covered stir bar and covered in foil to avoid photodegradation. The water and PED of each flask was extracted and analyzed at increasing time intervals (9.9, 18, and four flasks at 28 days).

The PED pieces were extracted in 10 mL of hexane for at least 48 hours. A solution of d_{10}-phenanthrene, d_{10}-pyrene, and d_{12}-perylene (100-µl of 200-pg/µl in hexane for PED extracts; in acetone for water extracts) was added as a recovery standard. The water was extracted in 500 mL glass volumetric flasks (3 x 10 mL of hexane). The extracts were reduced to approximately 100 µl, and a 10-µl aliquot of a 4-ng/µl m-terphenyl solution was added as an injection standard for subsequent analysis.

The K_{PEW} was calculated for each HOC as the ratio of the measured concentration of the solute in the PED and the measured concentration of the solute in water at equilibrium (Eq. 2.1). The average of the K_{PEW}s measured at equilibrium was taken in order to calculate the best value.

Infinite Bath Experiment

In order to evaluate the diffusivity values measured in the non-infinite bath water sampling experiments, the same water sampling system (see above) was set up with a very small mass of PED such that the water concentration would remain constant (phenanthrene: 25 μg/L and pyrene: 0.85 μg/L), mimicking the field. In contrast to the previous experiments, only 1.1 mg of PED was added. This allowed for a predicted 1% and 0.2% fractional uptake at equilibrium for pyrene and phenanthrene, respectively. The experiment was performed at 20 °C. After 7.3 hr before equilibrium was reached, the PED was removed and extracted in a quartz cuvette (NSG Precision Cells Inc., Farmingdale, NY) in 3 mL of hexane for 48 hr. Synchronous fluorescence (see below) was used to measure the mass of phenanthrene and pyrene present in the PED as well as in the water before and after the PED was added. Throughout the experiment, the water concentration of phenanthrene and pyrene remained constant (C_{phen0} = 25.0 ± 0.4 μg/L, C_{phenF} = 24.9 ± 0.4 μg/L; C_{pyr0} = 0.84 ± 0.3 μg/L; C_{pyrF} = 0.85 ± 0.03 μg/L).

PED Deployment in Boston Harbor

In order to test the applicability of PED use in the aquatic environment, sampling was performed in Boston Harbor, MA, in December 2000. PEDs (85 cm x 5 cm x 51 μm) were deployed at two locations within the Harbor. The first PED was hung from a navigational buoy (#12) across from Logan Airport (N 42° 20.955 min, W 71° 01.124 min), 2m below the water surface. The second PED was attached to our own float near the mouth of the Charles River (N 42° 22.261 min, W 71° 03.382 min), also 2 m from the surface. The water temperatures at the airport and Charles River locations were 2 and

3°C, respectively, and the water salinity was 33 psu at both locations. Both PEDs were deployed for 15 days, and 4-L water samples were taken at the same location at the time of PED recovery.

In the laboratory, the PEDs were rinsed in low-carbon water, wiped with a Kim wipe in order to remove any visible biofilm, and extracted in DCM. The water samples were also extracted in DCM, and recovery standards were added to both extracts. The samples were analyzed on the GC-MS as described below. Particulate organic carbon from the total water samples was measured by filtering a known volume of the sample on a glass fiber filter (Whatman, Maidstone, England). The filtered solids were then dried (80°C), weighed, and analyzed with a PE 2400 CHN elemental analyzer (Perkin Elmer Corp., Norwalk, CT).

Synchronous Fluorescence

Synchronous fluorescence (37) allowed for the simultaneous measurement of the concentrations of pyrene and phenanthrene in both water and hexane. The samples were scanned at room temperature (23 °C) in quartz cuvettes (NSG Precision Cells Inc.) on a Perkin Elmer Luminescence Spectrometer LS 50B between 250 and 350 nm with an offset of 55 nm, slit widths for the emission and excitation beams of 7 nm, and a scan speed of 1500 nm/min. Phenanthrene and pyrene intensity were measured at 292 nm and 319 nm, respectively. The measurement error (one standard deviation, s.d.) for phenanthrene and pyrene were 0.6 and 1.3%, respectively. A calibration curve for phenanthrene and pyrene dissolved in water as well as hexane was completed each day in order to account for variations in the lamp. The s.d. for the equilibrium concentrations

measured before the PED was added was within 0.3% (phenanthrene) and 0.2% (pyrene) of the mean. The s.d.'s for the concentrations measured once the PED and water had equilibrated were on average within 1% and 3% of the mean for phenanthrene and pyrene, respectively. The measured intensities were at least 15 times greater than intensities measured for water only.

GC-ECD

The PCB #52 extracts from the water sampling experiment were separated on a Carlo Erba high-resolution gas chromatograph (HRGC-5300) with a DB-5 column (J&W Scientific; Folsom, CA; ID 0.32 mm; 0.25 μm film, 30 m length) and analyzed using an electron capture detector (ECD-40; Milan, Italy). The extract (1 μL) was injected cold on-column, and the GC was temperature programmed from 70°C to 300°C at 20°C/min and held at 300°C for 3 minutes. The ECD was run with a 95% argon and 5% methane make-up gas at 300°C. A calibration curve for PCB # 52 and Cl_6-benzene was completed each day in order to account for instrument variations.

PCB #52 concentrations were recovery corrected with Cl_6-benzene recoveries (78 ± 6%). The s.d. (n = 4) for the PCB #52 beaker equilibrium concentrations measured before the PED was added was within 0.9% of the mean. The s.d. (n = 5) for the concentrations measured once the PED and water had equilibrated was within 7% of the mean. The peak heights were at the least 50 times greater than the baseline.

GC-MS

Extracts from PED and water extraction experiments were analyzed on a gas chromatograph (GC; Hewlett Packard 6890 Series) -mass spectrometer (MS; JEOL MS-

GCmate). The extracts (1 μl) were injected splitless and separated on a J&W Scientific (Folsom, CA) 30 m x 0.32 mm DB-5 (0.25 μm film thickness) fused-silica capillary column. For PCBs, the injection port was at 300°C, and the GC-temperature program started at 70°C, ramped at 20°C/min to 180°C, increased by 4°C/min to 260°C, reached 280°C in a minute where it was held for 4 min. For PAHs, the injection port was at 280°C, and GC was temperature programmed from 70°C to 180°C at 20°C/min and continued to 300°C at 6°C/min. The MS was operated at a resolution of 500 in EI+ mode and selected ion monitoring (SIM) was used. PCBs and PAHs were quantified relative to the internal recovery standards.

RESULTS AND DISCUSSION

Equilibrium Constants

The K_{PEW}s measured in both experimental setups (the water sampling experiment and the PED and water extraction experiments explained above) for phenanthrene and pyrene match within error [Table 2.2, (38-41)]. The water sampling K_{PEW} measured for PCB #52 was also consistent with the PCB K_{PEW}s measured in the PED and water extraction experiment. The K_{PEW} for phenanthrene estimated by Huckins et al. (29)is in good agreement with the numbers presented here; however, the K_{PEW} for PCB #52 is not. The experiments performed by Huckins et al. (29) did not reach equilibrium, and the K_{PEW}s were estimated by modeling the uptake data. The differing PCB #52 K_{PEW} estimated in their work may be due to modeling error.

Within both compound classes, the K_{PEW}s increase with increasing molecular weight. This is to be expected since van der Waal's forces are a function of size, and as

the volume of these hydrophobic molecules increase, so does their affinity for the PE and their aversion to the water. Because of the large body of literature on octanol-water partition coefficients (K_{OW}) and the limited importance of hydrogen bonding on the K_{PEW} of these HOCs, the correlation between K_{PEW} and K_{OW} was examined (Figure 2.2). The measured K_{OW}s for PAHs cited in Mackay et al. (40) were averaged and 1 s.d. was calculated (Table 2.2). There were no K_{OW} values for 2-methyl-phenanthrene referenced in Mackay et al. (40) so a value from Hansch et al. (41) was used. Because the K_{OW} value cited for perylene was significantly lower than the K_{OW} for PAHs of comparable and smaller molecular weights, the K_{OW} reported here is from Sangster (39). There was a good linear correlation between log K_{PEW} and log K_{OW} for the combined set of HOCs (R^2 = 0.85; Figure 2.2). The linear fit of the log K_{PEW} and log K_{OW} for the individual compound classes was still better. For example, PAHs improved to R^2 = 0.95 (n = 8) and PCBs to R^2 = 0.99 (n = 3). Interestingly, the log K_{PEW}-log K_{OW} correlations indicate that the K_{PEW}'s for PAHs are greater than K_{PEW}'s for PCBs with the same K_{OW}. One explanation for this observation may be that the planar structure of the PAHs enhances their partitioning into the hydrocarbon chains of the polymer over that of the non-planar PCBs measured in this study. It is conceivable that the linear nature of the polyethylene is more compatible with the planar PAHs than the non-planar PCBs. These K_{PEW}-K_{OW} correlations allow one to estimate an HOC's K_{PEW} with a K_{OW}.

By assuming that the aqueous activity coefficient is the only variable governing K_{PEW} that has significant temperature dependence (i.e., the excess enthalpy of solution in PE $\approx$ 0), K_{PEW} was related to the excess enthalpy of solution in water, ΔH_s^e(kJ/mol).

$$\ln(K_{PEW}) \cong -\frac{\Delta H_s^e}{RT} + C \qquad (2.9)$$

where R is the gas constant (kJ/molK), T is the absolute temperature (K), and C is a constant. Examining the partition data as a function of *1/(RT)* yielded estimates of corresponding ΔH_s^e values (Figure 2.3). The ΔH_s^e for phenanthrene was found to be 18 ± 1 kJ/mol. This is the value that Schwarzenbach et al. (42) estimate for the ΔH_s^e of phenanthrene. We also measured an ΔH_s^e for pyrene of 29 ± 2 kJ/mol. This is also comparable to the ΔH_s^e for pyrene estimate by Schwarzenbach et al. [25 kJ/mol; (42) Finally, the ΔH_s^e for PCB #52 was found to be 12 ± 5 kJ/mol, comparing reasonably well with 16 kJ/mol estimated for 2,3,4,5 tetrachlorobiphenyl [calculated with values from (43) These measurements indicate that a chemical's K_{PEW} can be adjusted for temperature with that particular chemical's ΔH_s^e.

Salinity can also affect a chemical's partition coefficient. Assuming that salt only influences PE-water partitioning due to effects in the aqueous solution, we expect:

$$\frac{K_{PEW,salt}}{K_{PEW}} = 10^{K^S \cdot [Salt]} \qquad (2.10)$$

where K^S is the Setschenow constant (M^{-1}), and *[Salt]* is the salt concentration (M). Assuming K^S is 0.28 for phenanthrene and 0.29 for pyrene (42) and calculating $K_{PEW,salt}$ / K_{PEW} for a 0.1 M NaCl water solution, one finds that the $K_{PEW,salt}$ is expected to be 1.07 times greater than K_{PEW} for both phenanthrene and pyrene. Experimental measurements indicate that $K_{PEW,salt}$ was 1.07 times greater than K_{PEW} for phenanthrene and 1.05 times greater for pyrene. These findings indicate that the Setschenow correlation can be used for adjusting K_{PEW} for salt effects. While the effect of a 0.1 M NaCl solution is only 7%,

correcting for salt effects becomes more important at higher salinities. For example, a 0.5 M NaCl solution, which is similar to the salinity of ocean water, will result in a 40% increase in the K_{PEW} for pyrene.

Diffusivity Constants

In order to solve for HOC diffusivities in PE, a mass balance was used to fit Eq. 2.2 for observed C_W:

$$C_W = C_{W@t=0} - \left(1 - \sum_{n=1}^{\infty} \frac{2\alpha(1+\alpha)}{1+\alpha+\alpha^2 q_n^2} \exp\left(-Dq_n^2 t / l^2\right)\right) \cdot \left(C_{W@t=0} - C_{w@t=\infty}\right) \quad (2.11)$$

The concentration data collected during the lab experiments were fit to Eq. 2.11, and the sum of the squared differences were minimized to solve for the diffusivity of each chemical (phenanthrene, pyrene, and PCB #52) in polyethylene at 23°C (Figure 2.4; Table 2.3). The PAH and PCB experimental data were obtained from the water sampling experiments. Equation 2.11 appears to fit the phenanthrene data quite well, but does not fit the higher molecular weight pyrene and PCB #52 as well. For these HOCs, diffusion is slower than the fitted value initially and then becomes greater than the calculated diffusivity in the second half of the time course. This trend is also visible for phenanthrene, but to a lesser extent. The best fits for the PAHs measured in the experiments at 5, 14, and 22°C show the same results as the experiment at 23°C. The concentration data for the laboratory experiments suggest that the diffusivities of the HOCs increased with time. It is possible that the chemical of interest may be acting as a plasticizer, causing diffusivity to increase with increasing absorbate concentration.

The diffusivities measured above along with K_{PEW}s were used to predict the dissolved concentrations of phenanthrene and pyrene in an infinite bath lab experiment

(see above). The PED concentration, D_{PE}, and K_{PEW} were used to calculate C_W according to Eq. 2.3. For phenanthrene, this value compared favorably to the directly-measured water concentration (Table 2.4). For pyrene, Eq. 2.3 over-predicted the water concentration by about a factor of two. This was likely caused by an under-prediction of the fractional uptake (31% uptake predicted with Eq. 2.5 vs. 56% measured fractional uptake; Table 2.4). A diffusivity of 6 E-11 cm^2/s would provide for the observed 56% fractional uptake. This is consistent with the greater-than-calculated diffusivity observed in the second half of the water sampling time courses (Figure 2.4).

Several researchers have measured the diffusivities of hydrocarbons in polyethylene (44-47). However, there are many difficulties in comparing experimental data on diffusion in polymers. These comparisons are difficult because of the variations in morphological characteristics (e.g., degree of crystallinity) of the polymer. Only one value for the diffusivity of phenanthrene in polyethylene, one for pyrene, and one for PCB #52 were found in the literature (29,48). Huckins et al. (29) measured diffusion coefficients for phenanthrene and PCB #52 in SPMDs in an open system (Table 2.3). Although the diffusivity measured by Huckins et al. is for diffusion through triolein and polyethylene, one might expect the diffusion through a plastic to be much slower than that through a liquid. Consequently, the "total" diffusivity should be similar to the diffusivity in polyethylene alone. The phenanthrene and PCB #52 diffusivities measured here and by Huckins et al. are well within a factor of three.

Simko et al. (48) measured the diffusivity of pyrene in low-density polyethylene to be 5 E-10 cm^2/s; this is more than an order of magnitude greater than the measured value of 2 E-11 cm^2/s in this study. It is important to note, however, that the

experimental setup of Simko et al. was very different from the one used here. They measured the concentrations of pyrene in a polyethylene sheet composed of five layers. In order to prepare this five-layer sheet, they heated and pressed the polyethylene for several minutes. This heating and cooling may have a significant effect on the crystallinity of the polymer, which may have affected the diffusivity (49).

The diffusivities calculated with Eq. 2.11 were used to calculate the time for 90% of equilibrium in an infinite bath diffusing into a PED with a 51 μm thickness (Eq. 2.5; Table 2.3). These times illustrate the importance of the kinetics on PED uptake. For example, a field experiment of 7 days (23°C) will allow phenanthrene and pyrene to come to equilibrium; however, PCB #52 will not have equilibrated and Eq. 2.6 will be needed to correct for uptake kinetics.

The diffusivities of chemicals in various media have been observed to relate to the molar volume of the chemical (50). We examined the correlation between the D_{PE} for our measured values as well as literature values (44-46) and LeBas molar volumes (Figure 2.5). In general, our measured D_{PE}s are lower than the literature values. However, it is important to consider that the majority of the literature studies measure the uptake of a chemical into a semi-infinite sheet. This method assumes a constant concentration at the sheet surface and uses a different method of solution. Considering our lower-than-literature-reported values and the apparent diffusivities increasing with time, it is possible that our D_{PE} are underestimated, and that the time for equilibrium may be less than we have predicted.

Our laboratory experiments suggest that the D_{PE}s measured for our chemicals were, in fact, increasing with time. This may be an experimental problem where late time

losses have been attributed to uptake when, in fact, they are due to other loss mechanisms. The increasing chemical uptake rate may be a real phenomenon due to the absorbate itself serving as a plasticizer. Future work is needed to understand this increasing diffusivity with time.

The D_{PE}s measured in this study also appear to be less than those measured in other studies. These lower-than-literature values may be due to sampling artifacts (e.g. losses inferred to represent PE uptake are actually due to other loss mechanisms). Alternatively, the observed D_{PE}s may be lower because of differences in PE structure. For example, the plastic used in this study may be more crystalline than the other plastics studied. Our current kinetic observations serve as a good starting point for estimating the time for equilibrium, which will aid in predicting the required sampling exposure time. In order to account for these D_{PE} inaccuracies and possible biofouling that may occur in the field, impregnating PEDs with internal standards (see above) will allow for the fractional uptake to be estimated. For example, one would expect d_{10}-phenanthrene to desorb from the PED at the same rate phenanthrene was absorbed. With this rate constant, the fractional uptake of phenanthrene could be estimated based on field conditions.

In order to adjust diffusivity for temperature, it is necessary to know the diffusivity activation energy. The Arrhenius equation can be used to solve for this energy:

$$D = A\exp(-E/RT) \qquad (2.12)$$

where A is a pre-exponential factor (cm^2/s) and E is the activation energy (kJ/mol). A plot of $ln(D)$ vs. $1/(RT)$ allowed for the use of the slope to solve for the activation energy

of diffusion for phenanthrene and pyrene (Figure 2.6). With this method, the activation energies ± 1 s.d. for phenanthrene and pyrene were estimated to be 46 ± 10 kJ/mol and 45 ± 12 kJ/mol, respectively. Activation energies for the diffusivity of about 40 different hydrocarbons in low-density polyethylene compiled by Flynn (44) ranged from 34 to 87 kJ/mol. Our estimated activation energies are within this range. An activation energy of diffusivity of 45 kJ/mol and a temperature drop of 10°C will cause the diffusion coefficient to decrease by a factor of two.

Environmental Measurements

To demonstrate the effectiveness of PEDs for environmental sampling, we used them to assess HOCs in Boston Harbor seawater in December 2000. Total water extracts were used to calculate dissolved concentrations (Table 2.5). The dissolved fraction was estimated with particulate organic carbon measurements and organic matter-water partitioning coefficients corrected for water temperature and salinity. K_{PEW}s measured at 23°C were corrected for temperature and salt effects and used to calculate the dissolved HOC concentrations corresponding to the PED extracts. The previously measured diffusivities were corrected for temperature, and the PCB #52 concentration was corrected to account for the percentage of equilibrium that had been attained within 15 days at 2 and 3°C (Table 2.5). Considering that total water extracts measure one point in time and are therefore not directly comparable to PED measurements, which provide for a time average, the total water extracts and PED measurements are in good agreement. HOC concentrations for PEDs and total water extraction measurements for phenanthrene

as well as pyrene in Boston Harbor were similar, although not identical (Table 2.5). PCB #52 total water extracts were within a factor of three of the PED-measured concentration. In order to remove the temporal variability present in Boston Harbor, several liters of harbor water should be collected for laboratory experiments. Subsamples could then be measured with a PED or extracted in the lab, and the resulting concentrations could be compared. This approach would help to remove temporal variability assuming that any laboratory sources and sinks could be eliminated or corrected for. As discussed previously, we believe there is greater error associated with those HOC concentrations that are measured with PEDs that have not yet equilibrated (i.e., PCB #52) with the surrounding water and must be corrected with diffusivity. This error may help to explain the higher PED sample concentrations.

The phenanthrene concentrations measured in December 2000 (40 and 80 pM) are comparable to the 100 pM phenanthrene concentration measured by Flores (4) with a SPMD at the airport location in February 1998. The pyrene concentrations we measured (20 pM) at the airport are several times less than the 100 pM concentration measured with *in situ* fluorescence detection by Rudnick (51) near the airport in November 1997. This apparent decrease in PAH concentration may be partially explained by the implementation of secondary treatment for Boston's municipal wastewater in July 1998 and the relocation of the wastewater outfall to 9.5 miles off-shore in September 2000. PCB #52 particulate samples collected in outer Boston Harbor near the airport in July of 1996 by Gustafsson (52) were used to estimate dissolved concentrations of 400 fM. This value is comparable to the PCB #52 concentrations we measured in December 2000 in

the inner harbor (100 to 200 fM). In this instance, the temporal and spatial differences in these samples make them difficult to compare.

Applications

Initial experiments indicate that PEDs are useful devices for the measurement of dissolved HOCs in the water column. Polyethylene is readily available in varying thicknesses and is inexpensive. K_{PEW}s can be estimated with K_{OW}s and adjusted for temperature and salinity. Diffusivities can be used to estimate the time for equilibrium. PEDs can be impregnated with internal standards so that the rate of desorption within the surrounding environment can be measured and used to correct for the uptake rate of the chemicals of interest.

PEDs allow for the measurements of HOCs that are "truly dissolved." "Truly dissolved" refers to those chemicals which are not sorbed to particulate matter or colloids. This dissolved fraction controls the diffusive transport into the surrounding environment. Consequently, it is an important fraction to measure.

As PEDs require days (depending on the chemical and temperature) to reach equilibrium with the surrounding water, they allow for a time-averaged measurement. This is useful for determining the level of pollutant exposure for organisms living in the sampled environment. Using different PED thicknesses will allow for the measurement of varying lengths of time. For example, decreasing the PED thickness from 80 to 40 μm cuts the uptake time by 75%.

The large polyethylene-water partition coefficients for HOCs make the measurement of small concentrations of HOCs much less labor intensive than the

extraction of large volumes of water. In our hands, we have been able to measure concentrations as low as 200 fM (e.g., PCB #52). These large partition coefficients will facilitate the extraction of a mass of chemical that is greater than the analyzer's detection limit. Additionally, these larger concentrations generally allow for more accurate measurements.

Table 2.1. Masses of chemicals measured at the end of a PAH and a PCB water sampling lab experiments.

Chemical	PED or Control Beaker	Incubation Time (day)	Mass in Water (μg)	Mass in PED (μg)	Mass on Wall (μg)	Total (μg)	Mass Added (μg)
phenanthrene	PED Beaker	2	998	471	<24	1469 - 1493	1500
pyrene	PED Beaker	2	56	142	3	201	200
PCB #52	PED Beaker	71	14 ± 1	69 ± 10	0.6	84 ± 11	160
PCB #52	Control Beaker	71	70 ± 10	—	4	74 ± 10	160

Table 2.2. Polycyclic aromatic hydrocarbon (PAH) and polychlorinated biphenyl (PCB) equilibrium partitioning coefficients @ 23°C[a]

Chemical	Log Kpew[b] PED & Water Extraction Exp.	Log Kpew[b] Water Sampling Experiment	Log Kpew[b] Huckins et al.	Log Kow[c]	Source
PAHs					
Phenanthrene	4.3 ± 0.1	4.23 ± 0.02	4.2	4.5 ± 0.1	Mackay et al. (1992)
2-Methyl Phenanthrene	4.8 ± 0.2			5.2	Hansch et al. (1995)
Fluoranthene	4.9 ± 0.1			5.1 ± 0.2	Mackay et al. (1992)
Pyrene	5.0 ± 0.1	5.02 ± 0.03		5.0 ± 0.2	Mackay et al. (1992)
Benz(a)anthracene	5.7 ± 0.1			5.62 ± 0.02	Mackay et al. (1992)
d_{12}-Benz(a)anthracene	5.7 ± 0.1				
Chrysene	5.7 ± 0.1			5.9 ± 0.1	Mackay et al. (1992)
Benzo(e)pyrene	6.2 ± 0.1			6.3 ± 0.2[d]	Mackay et al. (1992)
Perylene	6.5 ± 0.2			6.3	Sangster (1989)
PCBs					
2,4,5 TriCB (#29)	5.1 ± 0.1[e]			5.6	Hawker & Connell (1988)
2,2',5,5' TetraCB (#52)		5.4 ± 0.1	4.6	5.8	Hawker & Connell (1988)
2,3',4,6 TetraCB (#69)	5.6 ± 0.2[e]			6.0	Hawker & Connell (1988)

[a]Errors shown are ± 1 s.d. [b]log [(mol/kg_{PE})/(mol/L_W)]. [c]log [(mol/L_O)/(mol/L_W)]. [d]The K_{OW} for benzo(a)pyrene is used for comparison as there were no experimental data available for benzo(e)pyrene. [e]These values were measured by Rainer Lohmann in the Gschwend Laboratory.

Table 2.3. Diffusivities in polyethylene measured for phenanthrene, pyrene, and 2,2',5,5'- tetrachlorobiphenyl (PCB #52).

Chemical	This study (cm^2/s @ 23°C)	Time for 90% equilibrium in an infinite bath (day)	Huckins et al., 1993 (cm^2/s @ 18°C)	Simko et al., 1999 (cm^2/s @ 24°C)	LeBas Molar Volume (cm^3/mol)
phenanthrene	2 E-10	0.4	7 E-11		199
pyrene	2 E-11	3		5 E-10	214
PCB #52	7 E-12	10	2 E-11		268

Table 2.4. Measured and calculated values for phenanthrene and pyrene in the infinite-bath experiment.

Chemical	Water Concentration (μg/L)		Fractional Uptake		Diffusivity (cm^2/s)	
	Measured	Predicted with Eq. 2.6 and D_{PE} from Table 2.3[a]	Measured[b]	Predicted with Eq. 2.5 and D_{PE} from Table 2.3	Table 2.3	Required for measured fractional uptake[c]
phenanthrene	25	23	0.85	0.79	2 E-10	1 E-10
pyrene	0.85	1.5	0.56	0.31	2 E-11	6 E-11

[a]C_{PE} measured with synchronous fluorescence following extraction in hexane. Log K_{PEW} for phenanthrene: 4.23 and pyrene: 5.02. [b]Calculated as $(C_{PEmeasured}/K_{PEW})/C_{Wmeasured}$. [C]Using this diffusivity in Eq. 2.5 results in the measured fractional uptake.

Table 2.5. Phenanthrene, pyrene, and 2,2',5,5'-tetrachlorobiphenyl (PCB #52) concentrations measured with both total water extraction and PED methods.

Chemical	Location	Dissolved Conc. from total water extracts[c] (pM)	Estimated dissolved fraction[e]	Dissolved Conc. from PED extracts[f] (pM)	Estimated equilibrium percentage at 15 days
phenanthrene	Airport[a]	40	0.99	80	100%
	Charles River[b]	70	0.99	70	
pyrene	Airport[a]	20	0.98	20	100%
	Charles River[b]	40	0.98	10	
PCB # 52	Airport[a]	< 0.1[d]	0.93	0.2	60%
	Charles River[b]	< 0.07[d]	0.94	0.2	

[a]Water temperature 2°C, 2 m depth, particulate organic carbon 0.2 mg/L, and salinity 33 psu. [b]Water temperature 3°C, 2 m depth, particulate organic carbon 0.2 mg/L, and salinity 33 psu. [c]Dissolved concentrations were calculated from total water extracts and corrected for the predicted fraction of chemical in dissolved phase. [d]The ion ratio measured indicated that there may have been an interfering ion, and that peak area may overestimate the mass present. [e]The fraction of chemical present in the dissolved phase was estimated with particulate organic carbon measurements and organic-matter partitioning coefficients corrected for water temperature and salinity. [f]Dissolved concentrations were calculated from PED extracts with K_{PEW} corrected for water temperature and salinity effects.

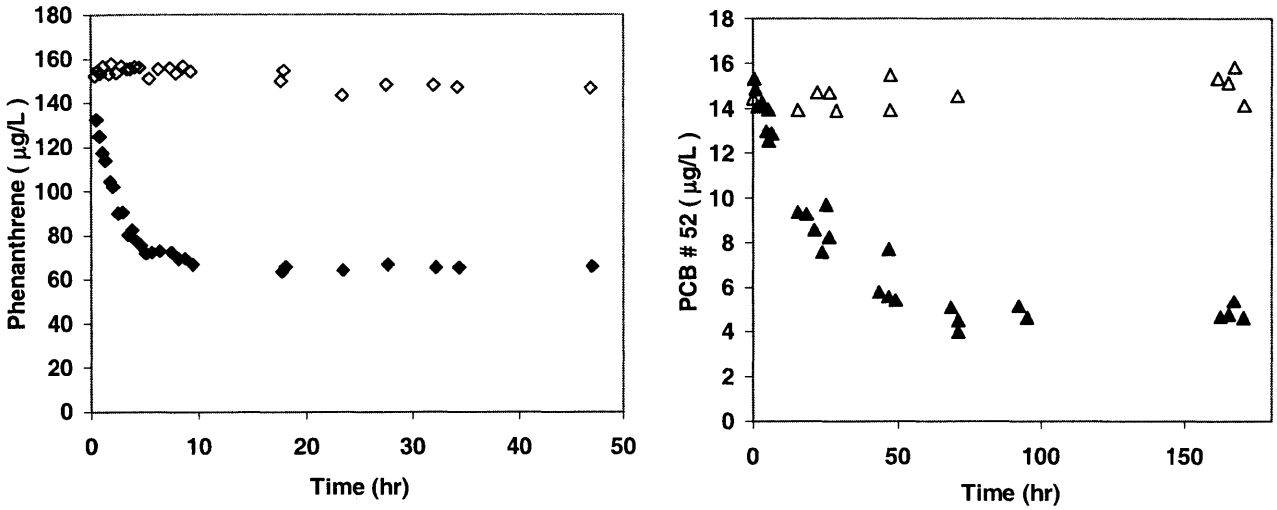

Figure 2.1. Water concentration vs. time for phenanthrene (solid diamonds) and 2,2',5,5'-tetrachlorobiphenyl (#52; solid triangles) measured in laboratory experiments with spinning PED show that the system has reached equilibrium. Control beaker concentrations for phenanthrene (open diamonds) and 2,2'5,5'-tetrachlorobiphenyl (open triangles) show no other significant losses.

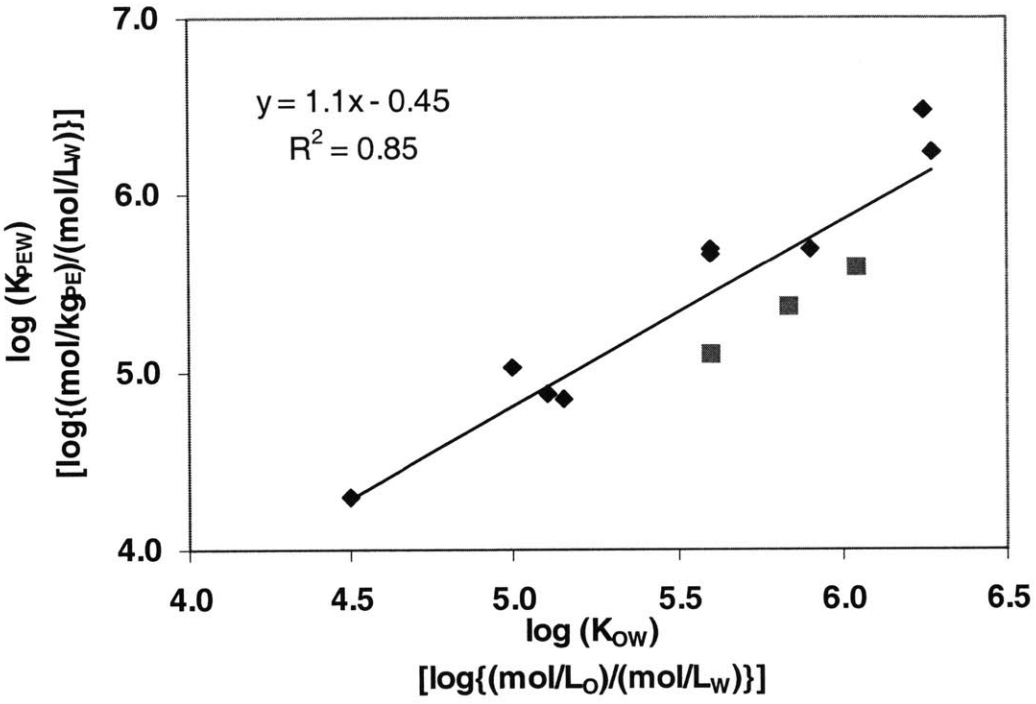

Figure 2.2. Log K_{PEW} vs. Log K_{OW} at 23°C for PAHs (solid diamonds) and PCBs (solid squares). The best-linear equation for each chemical group is: PAHs: 1.2x- 0.97 (R^2 = 0.95); PCBs: 1.1x-1.3 (R^2 = 0.99)

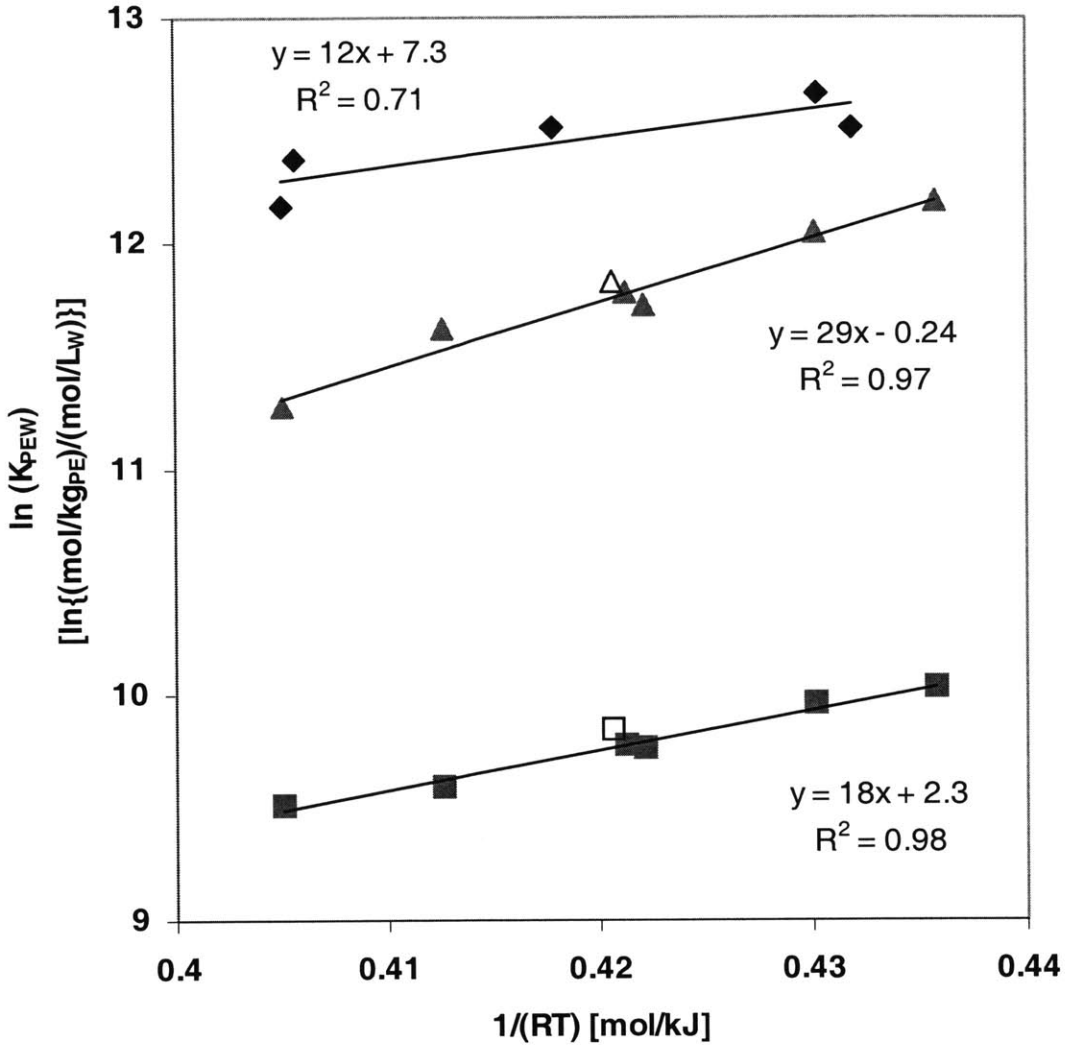

Figure 2.3. ln K_{PEW} vs. 1/(RT) for 2,2',5,5'-tetrachlorobiphenyl (PCB #52; solid diamond), pyrene (solid triangle), and phenanthrene (solid square). The effect of 0.1 M NaCl on K_{PEW}s for pyrene (open triangle) and phenanthrene (open square) are indicated with open symbols.

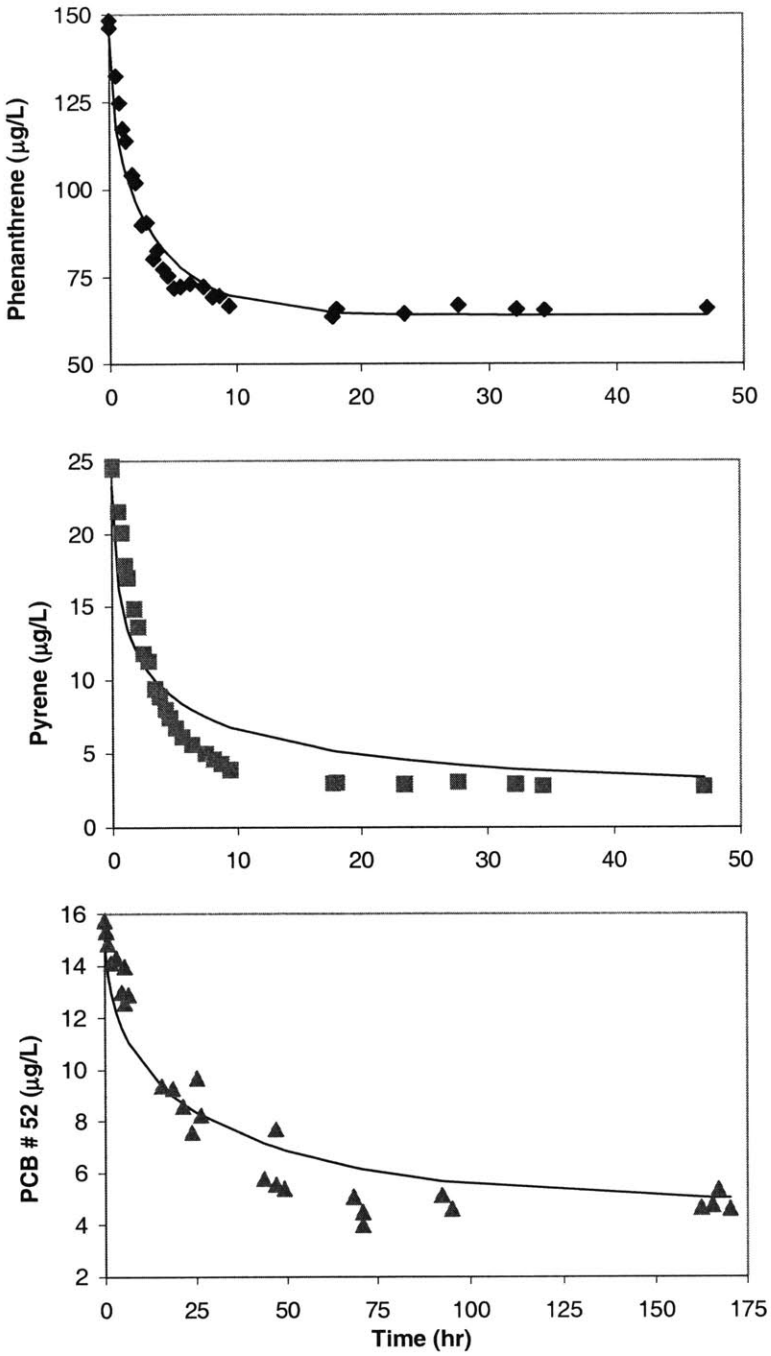

Figure 2.4. Phenanthrene (solid diamond), pyrene (solid square), and 2,2',5,5'-tetrachlorobiphenyl (solid triangle) concentration in water vs. time at 23°C. The Crank equation (2.11) fit is depicted as a solid line.

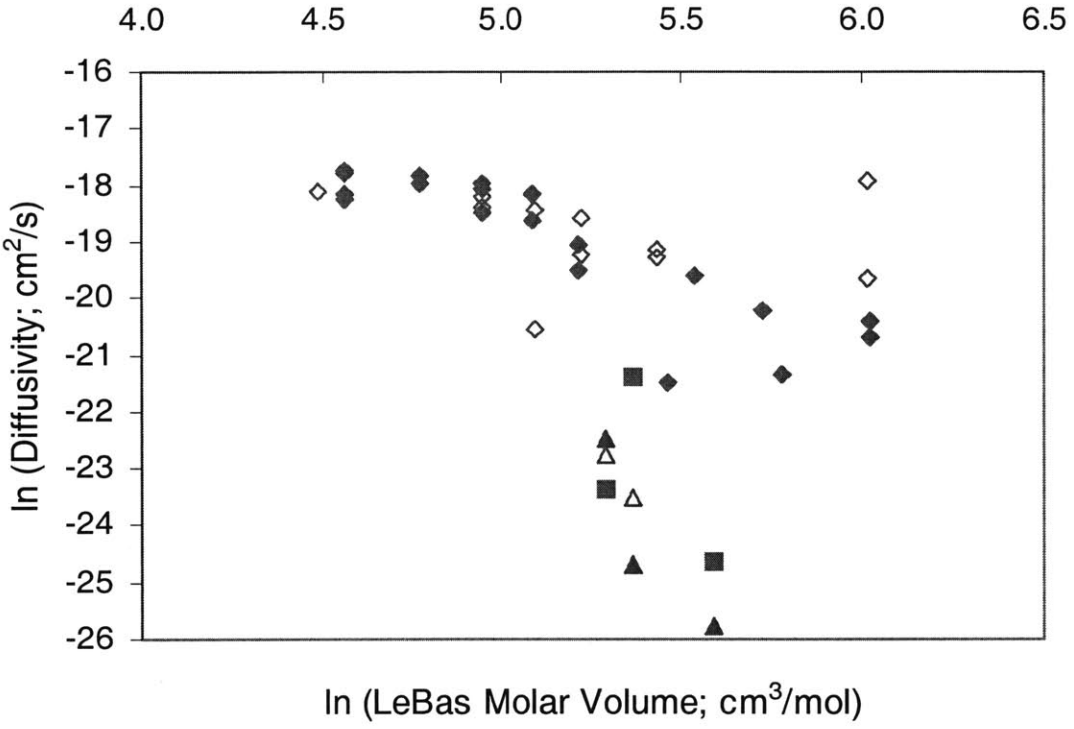

Figure 2.5. ln Diffusivity vs. ln LeBas molar volume for chemicals measured in this work (Table 2.3: solid triangle; Table 2.4: open triangle), polycyclic aromatic hydrocarbons in the literature (solid square), aromatic hydrocarbons in the literature (solid diamond), saturated hydrocarbons in the literature (open diamond).

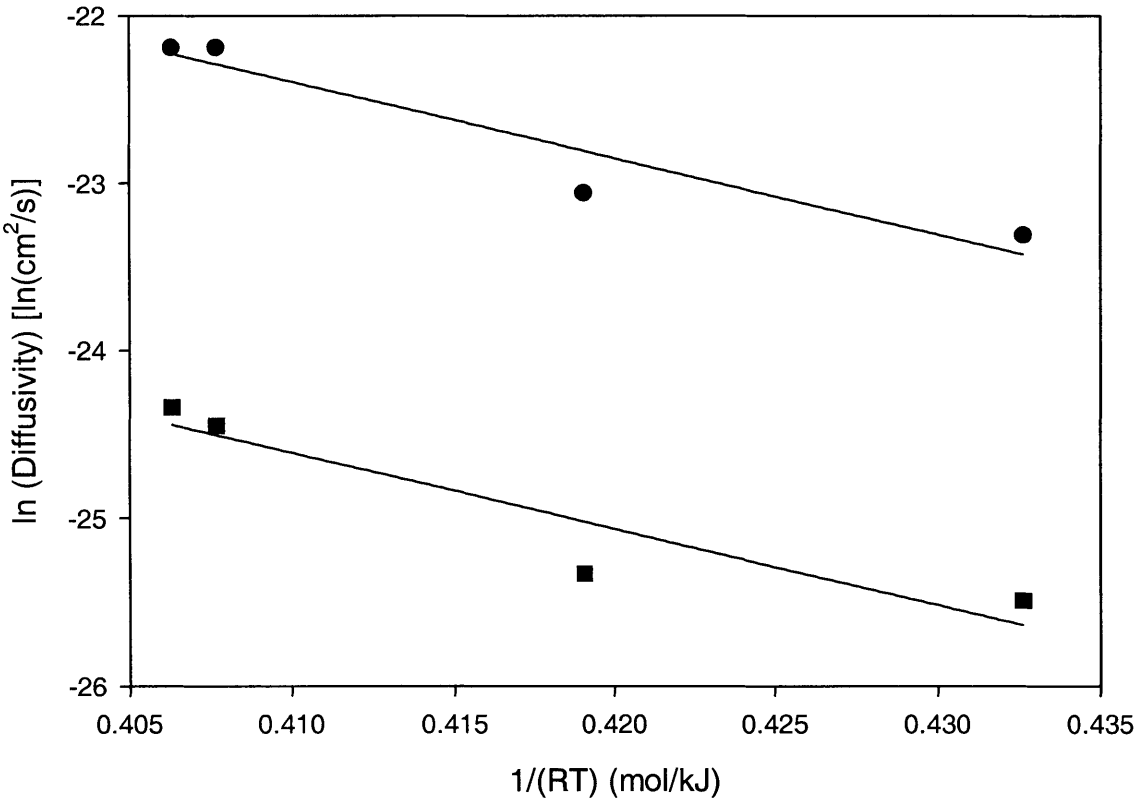

Figure 2.6. ln diffusivity vs. 1/(RT) for phenanthrene (solid circle) and pyrene (solid square). R is the gas constant (kJ/molK) and T is temperature (K). The best linear fits for each chemical were: phenanthrene [$y = (-46 \pm 10$ kJ/mol)$x + (-3.7 \pm 4.1)$ $R^2 = 0.91$] and pyrene [$y = (-45 \pm 12$ kJ/mol)$x + (-6.0 \pm 5.0)$ $R^2 = 0.88$].

CHAPTER 3: DESORPTION KINETICS OF PYRENE FROM NATIVE LOWER HUDSON ESTUARY SEDIMENTS

INTRODUCTION

Observations of disequilibrium between sorbed hydrophobic organic contaminants [HOCs; e.g., polycyclic aromatic hydrocarbons (PAHs) and polychlorinated biphenyls (PCBs)] and the surrounding environmental waters (3,53,54) indicate that the time for desorption is important for understanding the fate of HOCs. The settling and resuspension of particles can play a significant role in the cycling of HOCs (15,55,56). In areas of significant sediment resuspension, depending on the time of solid-water contact, the desorption of HOCs from suspended particles may be a significant source or sink of contaminants to or from the surrounding waters. For example, Achman et al. (3) have estimated that the input due to the desorption of PCBs from resuspended sediments in the lower Hudson Estuary is similar in magnitude to the boundary-layer-diffusion-controlled release from the bed.

For PAHs, these molecules' strong affinity for black carbon in the environment (19,57-59) makes their desorption kinetics more complicated. For example, in laboratory experiments, Accardi-Dey & Gschwend (59) found the sorption of pyrene onto black carbon had a half-life of approximately 1 day in contrast to a half-life on the order of hours for pyrene sorption onto natural sediment. Our current understanding of the desorption kinetics of PAHs from native sediments is limited and is an area where more study is needed.

Many models have been developed to simulate sorption kinetics. The one-box model is the simplest of the models. This model assumes that the sorption rate is a first-

order function of the difference in concentration between the bulk solution and the solution equilibrated with the sorbent is quantified with a single rate constant, k. This model implies that only one process is the limiting step for mass transfer across a boundary. Unfortunately, this simplified model does not fit experimental data well. Several researchers have observed a rapid initial uptake followed by a slower uptake rate (60,61) In order to account for these differing rates of desorption, a two-box model is often applied (62,63). This model applies to situations where there are two types of sorbents, two chemical reactions, or a more accessible sorbing site paired with one that is less accessible.

Wu and Gschwend (23,24) developed a model of sorption kinetics based on known physical and chemical processes (i.e., molecular diffusion and phase partitioning). Their model describes the kinetics of solution-solid exchange as a radial diffusive penetration of organic pollutants into or out of porous natural aggregates. The sorbate molecules are assumed to diffuse through the pore fluids in the interstices of natural silt aggregates while undergoing microscale equilibrium partitioning between the mobile and immobile phases of the silt aggregates. They developed a model to explain the time rate of change of the sorbed compound per unit volume:

$$\frac{\partial S(r)}{\partial t} = D_{eff}\left[\frac{\partial^2 S(r)}{\partial r^2} + \frac{2}{r}\frac{\partial S(r)}{\partial r}\right] \qquad (3.1)$$

where $S(r)$ is the local total volumetric concentration in porous sorbent (mol/cm^3), r is the radial distance, and

$$D_{eff} = \frac{D_m n}{(1-n)\rho_S K_d} \cdot f(n,\tau) \qquad (3.2)$$

where D_m is the pore fluid diffusivity of the sorbate (cm^2/s), n is the porosity of the sorbent (cm^3 of fluid/cm^3 total), ρ_S is the specific gravity of the sorbent (g/cm^3), K_d is the solid-

water partition coefficient ([mol/kg]/[mol/L]), and f is a correction factor which is a function of intraaggregate porosity and tortuosity (τ). The model was found to fit laboratory sorption data for chlorobenzenes to soils and river sediments once the fitting porosity n was adjusted (23). Using a correction factor of n^1, an empirical choice of n = 0.13 allowed for a fit of reasonable accuracy. Using the Wu and Gschwend model, Eq. 3.1 can be solved analytically for diffusion into a well-stirred bath with particles that are uniform in size (36):

$$\frac{M_t}{M_\infty} = 1 - \sum_{n=1}^{\infty} \frac{6\alpha(\alpha+1)\exp(-D_{eff} q_n^2 t / a^2)}{9 + 9\alpha + q_n^2 \alpha^2} \qquad (3.3)$$

where M_t and M_∞ are the total amount of chemical in the water at time t and at infinite time, respectively (M), t is time (T), and a is the particles' spherical radius (L). The values of q_n are the non-zero positive roots of:

$$\tan(q_n) = \frac{3q_n}{3 + \alpha q_n^2} \qquad (3.4)$$

and α is the ratio of the volume of solution to the mass of solids divided by the partition coefficient:

$$\alpha = \frac{(V_W / Mass_P)}{K_d} \qquad (3.5)$$

where V_W is the volume of water (L^3) and $Mass_p$ is the dry mass of the sediment particles (M). Simply stated, α is the ratio of the dissolved to the sorbed chemical at equilibrium. The fractional uptake, f_W, into the water at equilibrium may also be used to solve for α. The f_W is equivalent to $1/(1+1/\alpha)$ or $1/(1+ r_{SW}*K_d)$ where r_{SW} is the ratio of solid to water or $Mass_P/V_W$. For example, if 25% of the chemical in the particle-water system is in the water at equilibrium, f_W is 0.25, α is 0.33, and $r_{SW}*K_d$ is 3. Eq. 3.3 can be used to

estimate D_{eff}/a^2 by solving for the best fit with experimental data. The limited volume case (i.e., the laboratory) allows one to measure the change in concentration in the solution over time. The results can be used to estimate the effective diffusivity of the solute within the particles. Once the D_{eff}/a^2 has been solved for in the laboratory case, the α can be adjusted for the solid-to-water ratio in the field, and the time for sorption or desorption in the field can be estimated.

In this study we examined pyrene, a PAH, in order to estimate the desorption rates of pyrene from native Hudson Estuary sediment. The use of native sediments allowed for the study of the effects of black carbon on PAH desorption. Due to the slower sorption times for PAHs to black carbon, PAHs that are added to sediments in the laboratory may not be representative of the PAHs sorbed to environmental sediments. On shorter time scales, these added PAHs may not partition into the sediments in the same manner as native PAHs. Laboratory experiments were performed and the results evaluated with the physically-based desorption model proposed by Wu and Gschwend (23,24) with respect to pyrene desorption from natural sediment (i.e., unaltered sediment with no pyrene addition). The most abundant size class (38-88 μm) of a Hudson River sediment from an area of significant resuspension was used in the experiment. Finally, the measured D_{eff}/a^2 was used to estimate the time for pyrene desorption in the lower Hudson Estuary. To our knowledge, this is the first study on the desorption of a PAH from native sediment.

EXPERIMENTAL SECTION

Materials

Sediment was collected with a 50x50 cm box corer from the lower Hudson Estuary in an area of significant sediment resuspension approximately 14 km north of the Battery (40° 49.209'N, 73° 58.270'W) on October 4, 2000 (Southern Estuarine Turbidity Maximum, SETM; Figure 4.1). The sediment was divided into one-centimeter depth intervals and stored in glass amber jars at 4°C. The 0 to 2 cm depth fraction was wet-sieved with standard sieves (sizes: 710, 250, 177, 149, 105, 88, and 38 μm). Clean water (see below) was used to rinse the sediment through each of the sieves. Each size fraction was then rinsed into an amber jar where the particles were allowed to settle, and the excess water was decanted off. Each size class was weighed and a subsample of each size class was weighed, dried at 75°C, and weighed again so that the solid mass fraction could be determined. The particle density of the 38 – 88 μm size class was measured with a specific gravity flask (64).

All water was reverse osmosis pretreated and run through an ion-exchange resin and activated carbon filter system (Aries Vaponics, Rockland, MA) until a resistance of 18 MΩ was achieved. The water was then treated with ultraviolet light (Aquafine total organic carbon reduction unit, Valencia, CA) and filtered with a 0.22 μm filter (Millipore, Bedford, MA). This low-carbon water was found to have less than 0.3 mg/L of total organic carbon (TOC) upon analysis on a Shimadzu TOC-5000 (Columbia, MD). Methanol (MeOH), acetone, methylene chloride (DCM), and hexane solvents were all JT Baker Ultra-resi-analyzed (Phillipsburg, NJ).

Desorption Experiments

In order to sample the sediment-water mixture multiple times so that the change in pyrene water concentration could be measured over time, two opaque 13-L stainless-steel beakers with stainless steel lids (Polar Ware, Sheboygan, WI) were used. Each beaker was filled with 10 L of clean water. The control beaker contained 30 ng/L of pyrene (added via 10 mL of 30 μg/L in water from dilution of 1000 μg/mL in MeOH, Supelco, Bellefonte, PA) and was allowed to equilibrate overnight. Once the baseline concentration (0 ng/L pyrene) in the experimental beaker, had been established, 5.15 g of the 38-88 μm fraction of wet sediment (3 g dry weight) were added and continuously stirred with a motor-driven stainless steel stirring rod. This experiment was performed twice. The first experiment was performed at 23.8 ± 0.5°C and the second was performed at 25.2 ± 0.4°C.

For both experiments, the pyrene water concentration was measured in both beakers over time with time-gated, laser-induced fluorescence (LIF; see below). Unfortunately, difficulties with the LIF optical trigger (see below) made the measurements over the initial 20 hr of the first experiment suspect. Consequently, we only have confidence in the data collected after hour 20 of this experiment. No trigger problems were experienced in the second experiment. In order to measure fluorescence in the beaker with sediment, the stirring was stopped for approximately 10 min in order to allow for particle settling. A Stokes settling calculation [particle density = 2.66 g/cm^3 (measured as discussed above), T = 25°C] indicated that 38 μm particles should settle within 4 min; however, as the water was murky even after 10 minutes, it is suspected that the particles became smaller with stirring. The end of the LIF fiber optic probe (stainless steel casing; 1.3 cm diam. x 10 cm long; see below for optical fiber specifications) was placed in the beaker and three or more

pyrene measurements were taken; each measurement takes approximately 1 min to perform. As soon as the measurements were completed, the stirring in the beaker was reinitiated with the stir rod. The stirring was fast initially in order to resuspend any particles that may have settled. After a minute of fast stirring, the speed was lowered to approximately 150 rev/s. The control beaker was measured at similar time intervals to the beaker with sediment.

For the first experiment, calibration curves using 10, 20, 40, and 60 ng/L pyrene solutions in 1-L amber bottles were completed within 4 hr or less of each measurement. During the second experiment, a 0 ng/L pyrene measurement was added to further constrain the lower portion of the calibration curves, and a calibration curve was completed immediately before or after each pair of desorption and control beaker measurements. Deviations in the calibration-curve-derived control beaker concentrations were used to correct the concentration in the beaker with sediment. The calibration curve was first used to calculate the pyrene concentration present in the beaker with sediment. Then this value was divided by the calibration-curve-derived concentration in the control beaker and multiplied by the spiked concentration (30 ng/L).

Inner Filter Effects

Attenuation of the excitation beam and/or absorption of emitted radiation by an excess concentration of fluorophore or by the presence of an additional absorbing species in solution is commonly called the "inner filter effect." Additional pyrene fluorescence measurements were made with and without particles present in order to test for inner filter effects. Following the desorption experiment, the particles in the beaker were allowed to settle for 15 days. After this time, the solution was clear, and particles were visible on the

bottom of the beaker. A Stokes settling calculation [particle density = 2.66 g/cm^3 (measured as discussed earlier), T = 25°C] indicated that particles as small as 1 μm should settle within 4 days. Several LIF measurements were taken over an hour. The particles were resuspended by first manually stirring the beaker with a stainless steel stirring rod and subsequently using the motor-driven stirrer for several minutes of continuous stirring. Then stirring was stopped and LIF measurements were taken at multiple particle-settling times.

Over the period of the fluorescence measurement checks, a gradual increase in the LIF system response over time was observed in all of the calibration standards. For example, the 10 ng/L standard intensity increased from 5800 @ 1:20 PM to 7300 at 3:30 PM. This increase in response is believed to be due to instrument "warm-up" and has been experienced previously by other instrument users.

Sediment and Water Extraction

After 10 days, the water-sediment mixture from the first experiment was centrifuged, so that the water and sediment could be separated for subsequent extraction. A 500 mL subsample of the water was extracted in a 1-L separatory funnel with 50 mL of DCM followed by two more 30 mL extractions. d_{10}-Pyrene (50 μl of 500 pg/μl in MeOH) was added prior to extraction for recovery correction. The extract was dried with anhydrous sodium sulfate (Na_2SO_4), transferred to hexane, and reduced to approximately 2 mL.

A 1.2 g (dry weight) subsample of sediment was extracted in a 50-mL glass centrifuge tube with 2 mL of acetone and 30 mL of DCM. d_{14}-p-Terphenyl was added prior to extraction for recovery correction. The sediment-solvent mixture was agitated with

a Vortex mixer for 1 min, the sediment was allowed to settle for 30 min, and the solvent was decanted into a 250-mL round-bottom flask. This process was repeated twice, and repeated two more times with only 3 mL of acetone in order to remove any residual pyrene. The extract was concentrated and exchanged into approximately 3 mL of hexane. A 50-μL aliquot of a 3 ng/μL m-terphenyl solution was added to both the water and sediment extracts as an injection standard.

GC-MS

Sediment and water extracts were analyzed on a gas chromatograph (GC; Hewlett Packard 6890 Series) -mass spectrometer (MS; JEOL MS-GCmate). The extracts (1 μl) were injected splitless and separated on a J&W Scientific (Folsom, CA) 30 m x 0.32 mm DB-5 (0.25 μm film thickness) fused-silica capillary column. The injection port was at 280°C, and GC was temperature programmed from 70°C to 180°C at 20°C/min and continued to 300°C at 6°C/min. The MS was operated at a resolution of 500 in EI+ mode and selected ion monitoring (SIM) was used. Pyrene was quantified relative to the internal recovery standards. Recoveries for the added d_{10}-pyrene and d_{14}-p-terphenyl were quantified relative to an m-terphenyl injection standard and were 66% for the sediment extraction and 68% for the water extraction.

Laser Induced Fluorescence

A time-resolved, laser-induced fluorescence spectrometer system (65)was used to measure the dissolved pyrene concentration *in situ*. While the system can be used to measured fluorescence as a function of time (time-resolved), here pyrene intensity was measured at one delayed time (time-gated). The system consists of a pulsed nitrogen laser

(λ = 337 nm, 600 ps pulse width, 1.3 mJ pulse^{-1}, Photon Technology, Model PL2300) lens focused onto a 400 μm diameter silica optical delivery fiber. A concentric ring of 9 x 200 μm diameter fibers delivers the emission radiation to a ¼-m imaging spectrograph (SPEX, Model 270M) whose output is focused on the input lens of a gated, intensified 1024 x 256 pixel charge-coupled camera (Princeton, Model ICCD-1024). The camera is thermo-electrically cooled and controlled by a Princeton Instruments Model ST130 controller and CSMA software. A time delay unit (Princeton Instruments Model PG-200) controls the time gating via a 100 μm fiber connecting the laser and the optical trigger on the delay unit (65). Pyrene intensity was measured at a 128 ns delay with a gate width of 50 ns at 391 nm. The pyrene detection limit for this system is on the order of 5 ng/L (51).

The ICCD was read after each pulse and the fluorescence responses to 100 pulses from the laser were summed to create the fluorescence spectra. The CSMA software provided for a spectral display of emission fluorescence from 350 to 550 nm with a resolution of approximately 0.3 nm. The data was extracted from the CSMA files to a flat ASCII format using a C-program written by Steven Rudnick (51). The data was then filtered (smoothed with a low-pass filter) and plotted using a Matlab code written by Steven Rudnick and modified by Steven Margulis (Appendix A). The peak height of interest (Raman @ 371 nm; pyrene @ 391 nm) was quantified using a Matlab code written by Steven Margulis (Appendix A).

Organic and Black Carbon Analysis

A subsample of the sediment that was collected from the desorption experiment (38 – 88 μm) was analyzed for both organic and black carbon. The sediment was dried (70°C) and crushed with a metal spoon. A 40 mg sample was combusted in a precombusted

crucible in a Sybron F-A1730 Thermolyne muffle furnace (Dubuque, IA) under air for 24 hr at 375°C. This method combusts the more labile organic carbon (OC) leaving the recalcitrant black carbon [BC; (58,59)].

Combusted (BC) and untreated (OC & BC) sediment were subsampled and weighed (~ 10 mg) into Ag capsules. In order to remove any inorganic carbon (IC) that may be present, 50 μl of clean water and 50 μl of sulfurous acid (>6% SO_2 by weight; Fisher Scientific, Fair Lawn, NJ) were added to each subsample. No effervescence was observed suggesting that there was little to no IC present. The samples were dried at room temperature overnight in a laminar flow hood.

The samples were then analyzed for carbon with a Perkin-Elmer 2400 CHN Elemental Analyzer (Norwalk, CT). Response factors were determined using an acetanilide standard (reproducible to within ±0.3%). Sample blanks were found to have less than 3 μg of carbon and were subtracted from the sample carbon measurements. Three replicates for both the combusted and untreated samples were run and found to have a relative standard deviation of ± 0.05%. The weight percent carbon in the combusted samples (BC) was subtracted from the weight percent carbon measured in the untreated samples (OC & BC) to quantify the weight percent of OC.

RESULTS AND DISCUSSION

Sediment Particle Distribution

The sediment particles were dominated by the smaller size fractions (Figure 3.1). The 38 – 88 μm size class made up 62% of the particles on a dry mass basis, while the < 38 μm size class was the second most abundant group (13%). The 105 – 149 μm size class

made up 12% and the 88 – 105 μm size class was 5% of the total. The remaining 9% of the particles were all larger than 149 μm. Because the 38 – 88 μm particle size class was the most abundant class present at this Hudson site, it was used in the desorption experiments for estimating representative rates of pyrene desorption in the lower Hudson Estuary.

Laboratory Desorption

The first desorption experiment indicated that the pyrene had reached equilibrium within the first 22 hr (Figure 3.2). The pyrene concentration in the system was measured up to 140 hr and appeared to remain constant over the 22 to 140 hr period suggesting that no further pyrene desorption was occurring. Control-corrected equilibrium pyrene concentrations in the beaker with sediment averaged 13 ± 2 ng/L. This value is consistent with the equilibrium pyrene concentration measured in the desorption beaker of the 2nd experiment (15 ± 2 ng/L). In this experiment, there were no problems with the trigger, and the system appeared to reach equilibrium within 2 hr. In the 1st experiment, the LIF-measured control beaker concentrations (after hour 20) ranged from 26 to 34 ng/L with an average concentration of 32 ± 2 ng/L (n = 7). In the second experiment, the concentrations ranged from 27 to 33 ng/L with an average concentration of 30 ± 2 ng/L (n = 12), implying very good accuracy and ±7% precision. Adding the 0 ng/L concentration to the calibration curve and an increase in the frequency with which calibration curves were completed may have helped to improve the measurement accuracy in the second experiment.

Fluorescence Measurement Checks

Within error, fluorescence measurements with the LIF were not affected by particle-derived inner filter effects (Figure 3.3). Pyrene fluorescence intensities in particle-

free water (15 days of settling; 7200 ± 500) were 5% less than the intensities measured in water with particles (6 to 13 min of settling; 7600 ± 600). However, as these measurements are within 1 standard deviation (s.d.) of the other, fluorescence measurements with the LIF are not believed to have been affected by particle-derived inner filter effects. If inner filtering were occurring, one would expect intensities to decrease in the presence of particles; however, in this experiment, the intensity increased slightly. This increase is believed to be the result of instrument warm-up because an increase in response for the pyrene standards was also observed.

Dissolved organic carbon quenching effects were calculated to be minimal. The total organic carbon concentration in our experiment was 6 mg/L (3 g sediment * 2% organic carbon / 10 L). If we assume that 10% of this carbon became dissolved (0.6 mg/L) and that the pyrene-DOC partition coefficient is 10^5 L/kg_{DOC} (66,67)only 6% of the pyrene would be bound to DOC. This percentage is comparable to the error for our measurements in the control beaker; however this error would be systematic rather than random.

Solid-Water and Black-Carbon Partitioning

The solid-water partitioning coefficient was calculated as the ratio of the pyrene sediment concentration and the dissolved pyrene concentration. The dissolved pyrene concentrations at equilibrium were measured independently with LIF and via a water extraction followed by GCMS analysis (both discussed previously). The LIF-measured pyrene concentrations measured were 13 ± 2 ng/L (1st experiment) and 15 ± 2 ng/L (2nd experiment; Table 3.1). The GCMS-analyzed concentration in the water extract was 15 ng/L. Replicate GCMS measurements in our laboratory suggest that this number is accurate to within approximately 20%. Because of the improved calibration curve protocol

in the 2nd desorption experiment, and the GCMS-measured value, the dissolved concentration was assumed to be 15 ng/L. Using this value and the measured sediment concentration (800 ng/g), we calculated a K_d of 53,000 ± 12,000 (L/kg). The error (1 s.d.) was propagated from the measurement error in each of the variables following the general method for error propagation (68).

The black carbon-water partitioning coefficient K_{BC} ([μg/kg$_{BC}$]/[μg/L]$^{\nu}$) for the 38 – 88 μm size class of Hudson River sediment was estimated according to (59):

$$K_{BC} = \frac{K_d - f_{OC}K_{OC}}{f_{BC}C_W^{(\nu-1)}} \qquad (3.6)$$

where f_{OC} is the weight fraction of organic carbon in the solid phase, K_{OC} is the OC-normalized partitioning coefficient ([mol/kg$_{OC}$]/[mol/L]), f_{BC} is the weight fraction of BC in the solid phase, and ν is the Freundlich exponent appropriate for the specific BC-PAH pairing of interest. This assumes that both pyrene sorbed fractions had equilibrated after 10 days. Based on the constant pyrene concentration measured over time (Figure 3.2), this assumption seems appropriate. The parameters K_d, f_{BC}, f_{OC}, and C_W were measured (see above). A log K_{OC} value of 4.7 (69,70) and a Freundlich exponent of 0.62 (59) measured by others were used in the calculations. The weight percentage of OC and BC were measured as 1.85 ± 0.01 and 0.17 ± 0.01, respectively. Using these values, the log K_{BC} is 6.8 ± 0.4 according to Eq. 3.8. Again error was propagated with measurement errors (68). This log K_{BC} is 0.5 log units greater than the log K_{BC} (6.25 ± 0.14) measured in Boston Harbor sediments (59) However, given the large error associated with our K_{BC}, these values are just within the error of the other. However, the K_{BC} measured in this study is more closely aligned with log K_{BC} measured for diesel particulate using a batch sorption method (6.6)

and column experiments [7.0; (71)]. This finding may indicate that the black carbon associated with our smaller size class of sediment (38 – 88 μm) is more similar to diesel-combustion derived black carbon.

Rearranging Eq. 3.6 to solve for K_d, one can calculate the magnitude of each "piece" of K_d: $f_{OC}K_{OC}$ and $f_{BC}K_{BC}C_W^{(n-1)}$. According to this equation, only 2% of the pyrene was sorbed to organic carbon, while 98% of the pyrene was black carbon-sorbed. Interestingly, 6% of the pyrene in the system desorbed from the sediments. Consequently, the desorption rate measured in our system is thought to include both organic and black carbon desorption. At least 66% of the pyrene is desorbing from black carbon; however, if equilibrium partitioning is maintained throughout the desorption, 98% of the pyrene is desorbing from black carbon. Using the same organic and black carbon partitioning model, Lohmann et al. (72) estimated that 95% of the pyrene in a sediment sample from the same location (all size fractions) at the 0-4 cm depth was black carbon-sorbed. In Boston Harbor sediments, they estimated that 92% of the pyrene was sorbed to black carbon.

Radial Diffusion Rate Constant

In order to estimate the radial diffusion rate constant, D_{eff}/a^2, with the desorption measurements, a mass balance was used to solve Eq. 3.3 for the concentration in the water as a function of time, $C_W(t)$:

$$C_W(t) = C_{W@t=\infty}\left(1 - \sum_{n=1}^{\infty} \frac{6\alpha(\alpha+1)\exp(-D_{eff}q_n^2 t/a^2)}{9+9\alpha+q_n^2\alpha^2}\right) \qquad (3.7)$$

The water concentration data collected during the lab experiments were fit to Eq. 3.7 with the exception of the initial water concentration (time = 0). The following equation, which is derived from a solution discussed in Crank (36) and is suitable for small times, was used

to fit the initial water concentration values because the use of 30 terms in Eq. 3.7 was not sufficient to bring the M_t/M_∞ term to zero at t = 0:

$$C_W(t) = C_{W@t=\infty}(1+\alpha)\left[1 - \frac{\gamma_1}{\gamma_1+\gamma_2} eerfc\left\{\frac{3\gamma_1}{\alpha}\left(\frac{D_{eff}t}{a^2}\right)^{1/2}\right\} - \frac{\gamma_2}{\gamma_1+\gamma_2} eerfc\left\{-\frac{3\gamma_2}{\alpha}\left(\frac{D_{eff}t}{a^2}\right)^{1/2}\right\}\right] \quad (3.8)$$

where

$$\gamma_1 = \frac{1}{2}\left\{\left(1+\frac{4}{3}\alpha\right)^{1/2}+1\right\}, \qquad \gamma_2 = \gamma_1 - 1$$

and

$$eerfc(z) = \exp z^2 erfc(z)$$

Each set of pyrene water concentration measurements taken within a 5 min period of time were averaged and the standard deviation calculated. The sum of the squared differences between the measured and estimated (Eq. 3.7 & 3.8) values were minimized to solve for the D_{eff}/a^2 for pyrene in the sediment particles. Fitting the first four data points in this manner provided for a D_{eff}/a^2 of 5.6E-7 s^{-1} (Figure 3.4). When only the first two data points were fit to Eq. 3.7 and 3.8, the D_{eff}/a^2 was 1.0E-7 s^{-1}.

The K_d measured at equilibrium (Table 3.1) was used to estimate α based on Eq. 3.5. However, it should be noted that K_d is believed to be a function of C_W (Eq. 3.6). According to Eq. 3.6, K_d decreases as C_W increases. Consequently, the K_d at the earlier desorption times may have been smaller in magnitude. Because lower values of K_d correspond to longer times of desorption (see below), the D_{eff}/a^2 rate constants estimated here may be low estimates.

As we discussed previously, desorption can be modeled with a first-order rate constant. While this model does not fit experimental data as well as an intraparticle

diffusion model, its simplicity and single fitting parameter make it a desirable model for a first approximation or use with box-model systems. In a closed system, the fractional uptake can be modeled with a first-order desorption rate constant according to:

$$\frac{M_t}{M_\infty} = 1 - \exp[-k_2(1+\alpha)t] \qquad (3.9)$$

where k_2 is the desorption first-order rate constant. Both k_2 and D_{eff}/a^2 are directly related to the reciprocal of the sorption time scale (24). Based on this, Wu and Gschwend (24)matched the first-order solution with the radial diffusion model at half-equilibration time ($M_t/M_\infty = 0.5$). In a closed system, k_2 is related to D_{eff}/a^2 by the following:

$$k_2 = \frac{\left[\left(\frac{10.56}{\alpha} + 22.7\right) D_{eff}/a^2\right]}{\alpha} \qquad (3.10)$$

Fitting the first two experimental data points to Eq. 3.9 provided for a first-order desorption half life of 0.80 hr (2.4 E-4 s^{-1}; Table 3.2). Using Eq. 3.10 to solve for the k_2 corresponding to the D_{eff}/a^2 for the first four data points (5.6 E-7 s^{-1}) resulted in a first-order desorption half life of 0.11 hr. This smaller half-life is consistent with the greater rate of desorption observed for this fit (Figure 3.4). The k_2 half-life corresponding to the radial diffusion rate constant fit to the first two data points was estimated as 0.64 hr with Eq. 3.10. This value is well within a factor of two of the first-order desorption half-life estimated with Eq. 3.9. One would expect these values to be the similar as they were both fit with the two initial data points.

In an effort to assess the validity of our radial diffusion rate constant, D_{eff}/a^2, the model for effective diffusivity proposed by Wu and Gschwend (23)was used to estimate a

D_{eff}. In order to calculate the D_{eff} in Eq. 3.2., the pore geometry factors, $f(n,\tau)$ was related to porosity in sediment beds as:

$$f(n,\tau) = n^i \tag{3.11}$$

where the exponent, i, is between 1 and 2 (73). For simplicity, Wu and Gschwend (23)take the i to be 1, and solve for D_{eff} as:

$$D_{eff} = \frac{D_m n^2}{K_d (1-n)\rho_s} \tag{3.12}$$

Using the intraaggregate porosity as a fitting parameter, they found the intraaggregate porosities in their sediments to range from 0.07 to 0.17 (0.13 on average). The diffusivity of pyrene in water (D_m) was estimated according to Hayduk and Laudie [7.7 E-6 cm^2/s; (50)]. Using a porosity of 0.13 for the sediment used in this study, the D_{eff} is 1.1 E-12 cm^2/s (Table 3.3).

Using the range of particle radii present in the experimental sediment and the D_{eff} calculated according to Eq. 3.12 (1.1 E-12 cm^2/s), the radial diffusion rate constant, D_{eff}/a^2 ranges from 5.5 E-8 – 2.9 E-7 s^{-1} (Table 3.4). The D_{eff}/a^2 corresponding to a 38 μm particle diameter (2.9 E-7 s^{-1}) is within the span of the radial diffusion constants estimated (1.0 E-7 and 5.6 E-7s^{-1}). The 64 μm particle diameter corresponds to a D_{eff}/a^2 of 1.0 E-7 s^{-1} and is equivalent to the radial diffusion rate constant estimated by fitting the first two data points of experimental data with Eq. 3.7 and 3.8. Considering the positive correlation between shrinking particle sizes and the energy input to the system, one might argue, that the average particle diameter in our experimental system with continuous stirring may be on the lower end of the particle range (e.g., 38 μm). If this is true, then the physically-based

model proposed by Wu and Gschwend (23) is a reasonable predictor of the D_{eff} for pyrene in the native sediments tested.

Time for Desorption in the Lower Hudson Estuary

The rate of desorption is dependent on the solid-to-water ratio $Mass_p/V_W$ or r_{SW} in the system as well as the solid-water partition coefficient, K_d. Using Eq 3.3 and Eq. 3.8 at small times, the analytical solution for the radial diffusive desorption from or uptake by spherical particles suspended in a closed system was solved for and is presented graphically (Figure 3.5) in order to illustrate the importance of the ratio of the solid-to-water on the rate of desorption. For example 300 mg/L of total suspended solids (TSS) corresponds to a K_d*r_{sw} of 15.9, so the dimensionless time for 50% of equilibrium ($M_t/M_\infty = 0.5$) is 2 E-4. However, if the TSS is only 10 mg/L, the K_d*r_{sw} is 0.53, and the corresponding dimensionless time is 1.5 E-2. This value is almost two orders of magnitude greater than the desorption rate for 300 mg/L of TSS and illustrates the importance of the solid-to-water ratio as well as the partitioning coefficient on the rates of desorption and sorption.

The D_{eff}/a^2 measured in the laboratory were used to estimate the time for 50% and 90% desorption equilibrium for representative solid-to-water ratios measured in the lower Hudson Estuary. This approach assumes that the D_{eff}/a^2 for all of the sediments in the estuary are similar to the D_{eff}/a^2 measured for the 38 – 88 μm size class. Eq. 3.3 was used to solve for the time at which M_t/M_∞ was equal to 0.5 and 0.9. The range of D_{eff}/a^2 ratios measured in the laboratory for the 38 – 88 μm sediment fraction (1.0 E-7 s^{-1} – 5.6 E-7s^{-1}) was used to calculate the time for 50% and 90% equilibrium. If we assume that the high-TSS bottom waters of the lower Hudson Estuary have 300 mg/L TSS on average, it is

estimated that it will take between 5 and 30 min to reach 50% equilibrium (Table 3.5). Using the same approach, the time for 90% equilibrium ranges from 4 to 20 hr. Given the 2 to 7 day residence times for the waters of the lower Hudson Estuary (74), the sediment and bottom water pyrene fractions are expected to be in equilibrium. If we assume an average 10 mg/L TSS for surface waters of the lower Hudson (7), the time for 50% equilibrium will range from 8 to 40 hr, while the time for 90% equilibrium is estimated to range from 3 to 10 days. Depending on the residence time for the estuary, the sediment and surface waters may or may not reach equilibrium. These findings illustrate the importance of the solid-to-water ratio and the partitioning coefficient on predicting appropriate rates of sorption and desorption.

Implications

Our findings suggest that the physically and chemically-based model for effective diffusivity put forth by Wu and Gschwend (23,24) is appropriate for estimating the desorption kinetics of pyrene in native sediments. Despite the fact that between 66 and 98% of the pyrene is believed to have been desorbing from black carbon, the retarded radial diffusion model allowed for the estimation of an effective diffusivity that fit experimental results. An improved understanding of the pyrene desorption rates in native sediments is important for predicting the inputs of pyrene that may result from the disequilibrium observed between the pyrene fractions in the sediments and overlying water column. Based on the reasonable agreement between measured and modeled sorption rates for chlorobenzenes observed by Wu and Gschwend (23,24) and the agreement between the measured and modeled sorption rates for pyrene observed in this study, the physically and

chemically-based model for effective diffusivity may be useful for estimating rates of sorption and desorption for other HOCs as well.

Table 3.1. Measured values used to calculate solid-water and black-carbon normalized partitioning coefficients.

Pyrene sediment concentration, C_S (ng/g)	800			
Pyrene water concentration, C_W, (ng/L)	15 ± 2[a]	15 ± 3[b]		
Solid-water partitioning coefficient), K_d (L/kg)	53,000 ± 12,000[c]			
Weight percentage of OC in solid phase, f_{OC}	1.85 ± 0.01[d]			
Weight percentage of BC in solid phase, f_{BC}	0.17 ± 0.01[e]			
Log (OC-normalized partitioning coefficient), log K_{OC} (L/kg$_{OC}$)	4.7[f]			
Freundlich exponent, ν	0.62 ± 0.12[g]			
Log (Black carbon-normalized partitioning coefficient), Log K_{BC} (L/kg$_{BC}$)	6.8 ± 0.4[h]	6.25 ± 0.14[i]	6.6[j]	7.0[k]
Organic carbon-sorbed fraction	0.02			
Black carbon-sorbed fraction	0.98			

[a]Measured in beaker experiments with LIF. [b]GCMS-analyzed centrifuged water extract; 20% error assumed. [c]Calculated as C_S/C_W. [d]Measured with CHN analyzer and calculated as weight percent (average ± 1 s.d.; n = 3) untreated sediment less the weight percent of combusted sediment. [e]Weight percent (average ± 1 s.d.; n = 3). [f]Value from correlation reported by Karickhoff (69). [g]Measured value from Accardi-Dey & Gschwend (59). [h]Calculated using Equation 3.6. [i]Measured for Boston Harbor sediments (59). [j]Measured for diesel particulate matter (NIST standard reference material) using batch sorption method (71). [k]Measured for diesel particulate matter (NIST standard reference material) using column experiments (71).

Table 3.2. First-order desorption and radial diffusion rate constants.

	D_{eff}/a^2 (s^{-1})	1st-order desorption rate constant, k_2 (s^{-1})	Half-life, $t_{1/2}$ (hr)
Estimated with Eq. 3.9		2.4 E-4	0.80
Estimated with Eq. 3.10 & 4-data-point-fit radial diffusion rate constant	5.6 E-7	1.7 E-3	0.11
Estimated with Eq. 3.10 & 2-data-point-fit radial diffusion rate constant	1.0 E-7	3.0 E-4	0.64

Table 3.3. Values used to calculate the effective diffusivity for 38 – 88 μm Hudson River sediment.

Diffusivity of pyrene in water, D_m (cm^2/s)	7.7 E-6[a]
Solid-water partitioning coefficient, K_d (L/kg)	53,000
Particle density, ρ_s (g/cm^3)	2.66[b]
Intraaggregate porosity, n (Wu & Gschwend, 1986)	0.13[c]
Calculated Effective Diffusivity, D_{eff}, (cm^2/s)	1.1 E-12[d]

[a]Calculated according to Hayduk & Laudie (50); molar volume =158.9 cm^3/mol; viscosity = 0.8904 centipoise. [b]Measured with a specific gravity flask according to method in Blake (64). [c]Typical intraporosity reported in Wu & Gschwend (23). [d]Calculated according to Eq. 3.12.

Table 3.4. Assumed particle radii with corresponding D_{eff}/a^2.

Particle Radius (μm)	Corresponding D_{eff}/a^2 (D_{eff} = 1.1E-12 cm^2/s)[a]
19	2.9E-7
32	1.0E-7
44	5.5E-8

[a]D_{eff} calculated according to Eq. 3.12.

Table 3.5. Range of total suspended solids in the lower Hudson Estuary and the corresponding equilibration times for pyrene.[a]

Total suspended solids[b] (mg/L)	Time for 50% equilibrium[c] (hr)	Time for 90% equilibrium[c] (hr)
10	8 - 40	3 – 10 days
300	5 - 30 min	4 - 20

[a]This assumes the D_{eff}/a^2 for all of the sediments in the estuary are similar to the D_{eff}/a^2 for the 38 – 88 μm size class measured here. [b]These are the end-members of the range of total suspended solids measured in the lower Hudson Estuary. [b]Calculated according to Eq. 3.3; the first number corresponds to a D_{eff}/a^2 = 5.6 E-7 s^{-1}, and the second number corresponds to a D_{eff}/a^2 = 1.0 E-7 s^{-1}.

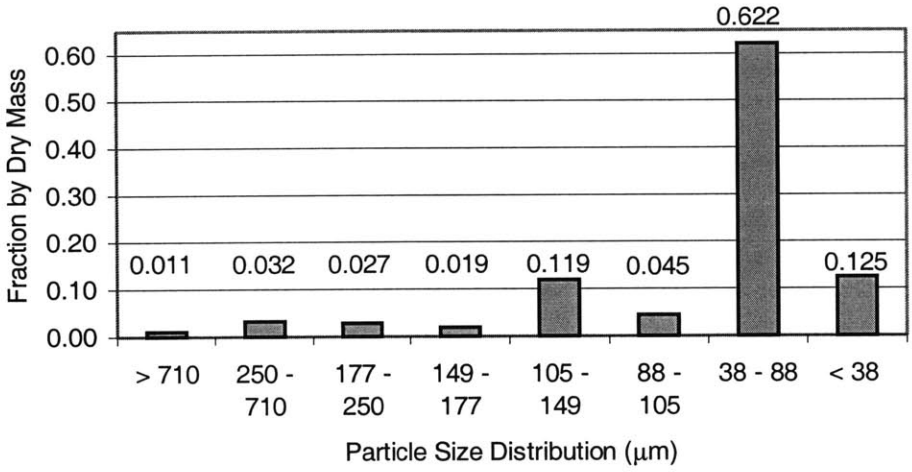

Figure 3.1. Size distribution by dry mass of sediment from the lower Hudson Estuary approximately 14 km north of the Battery (40° 49.209' N, 73° 58.270' W).

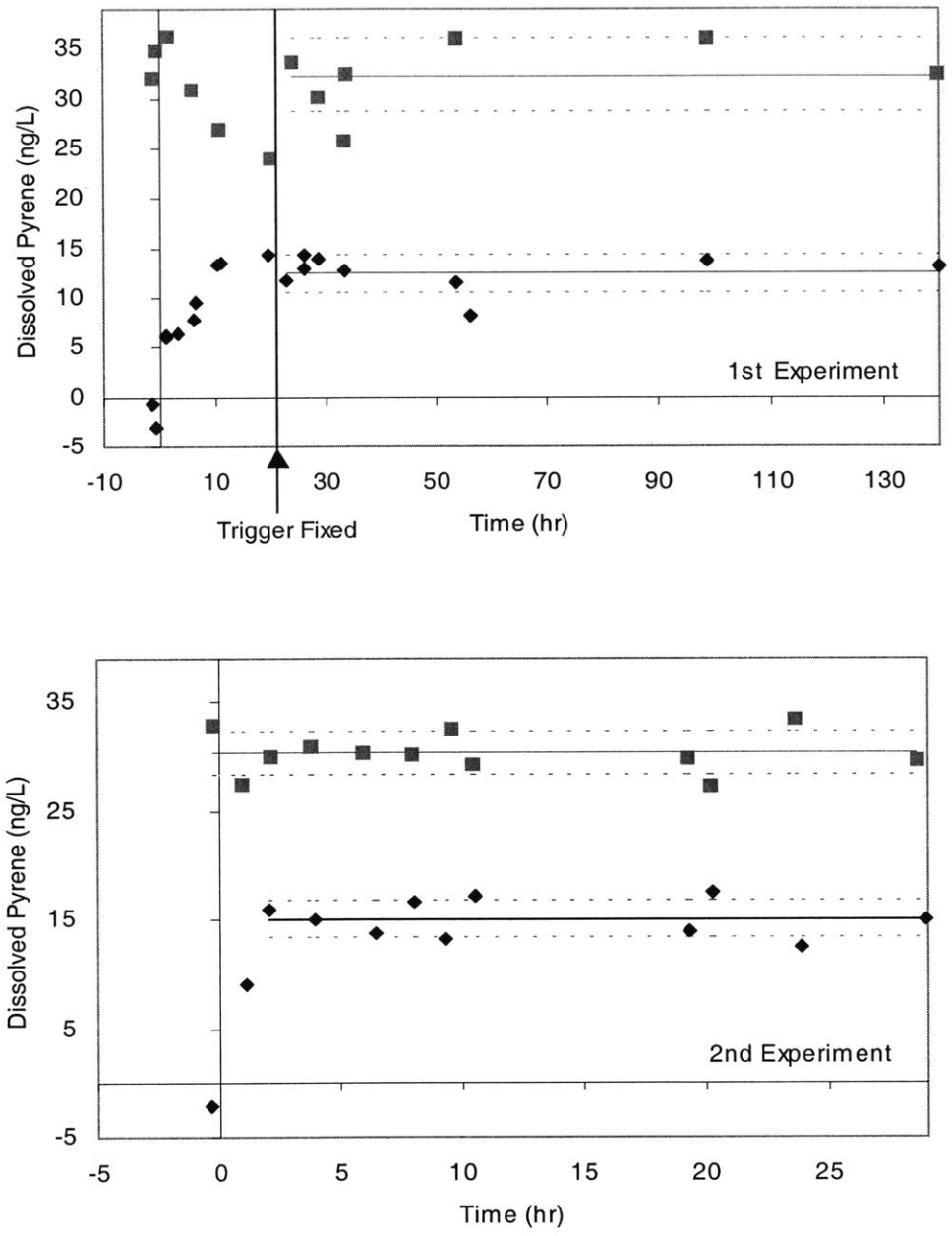

Figure 3.2. Pyrene water concentration vs. time measured in laboratory experiments with suspended sediment (solid diamond) show that in the 1st experiment (trigger difficulties), the system reached equilibrium within 22 hr with an average concentration of 13 ± 2 ng/L. The pyrene concentration in the control beaker (solid square) was 32 ± 4 ng/L. In the 2nd experiment (no trigger difficulties), the system with suspended sediment (solid diamond) reached equilibrium within approximately 2 hr with an average concentration of 15 ± 2 ng/L. Pyrene water concentrations in the control beaker (solid square; 2nd experiment) show that the laser induced fluorescence measurements are consistent and accurate (30 ± 2 ng/L).

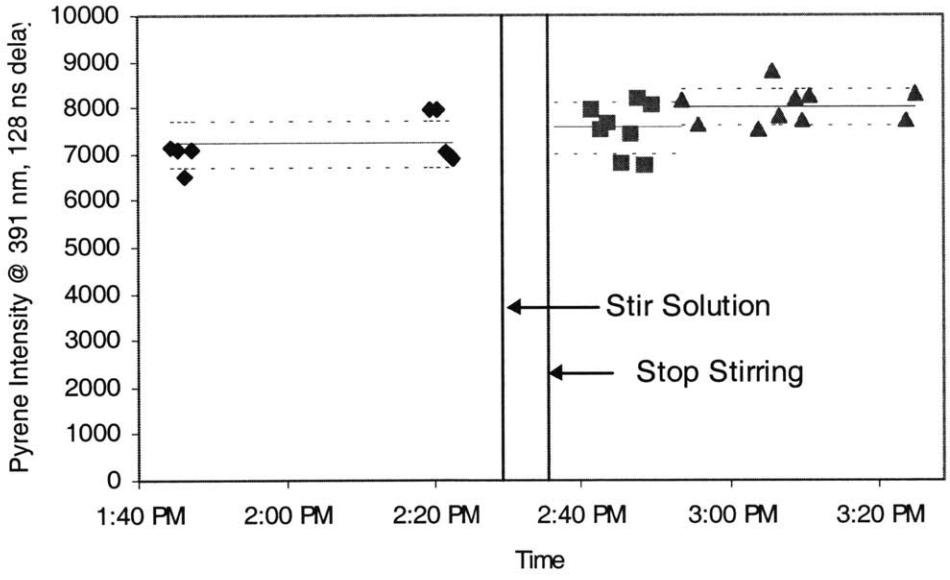

Figure 3.3. Pyrene fluorescence measured with laser induced fluorescence as a function of time. First, the pyrene fluorescence intensity was measured after 15 days of particle settling (solid diamond; 7200 ± 500; n=8). Following this measurement, the system was stirred and the particles were suspended. The average of the pyrene intensities measured between 6 and 13 min of particle settling (solid square) was 7600 ± 600 (n=8). The average after 17 to 45 min of settling (solid triangle) was 8000 ± 400 (n=10).

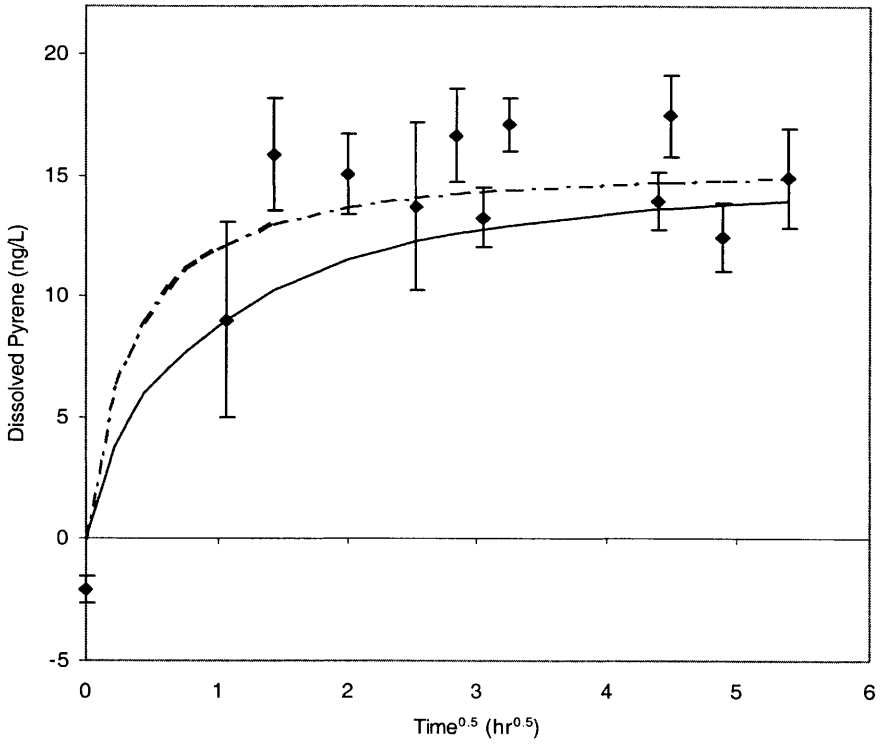

Figure 3.4. Dissolved pyrene (ng/L) (solid diamond) vs. time$^{0.5}$ at 25°C (2nd experiment). The error bars are ± 1 s.d. When the first four experimental data points were fit to Eq. 3.7 and 3.8, the resulting D_{eff}/a^2 was 5.6E-7s^{-1} (dotted line). When only the first two data points were used to fit Eq. 3.7 and 3.8, the D_{eff}/a^2 was 1.0E-7 s^{-1} (solid line).

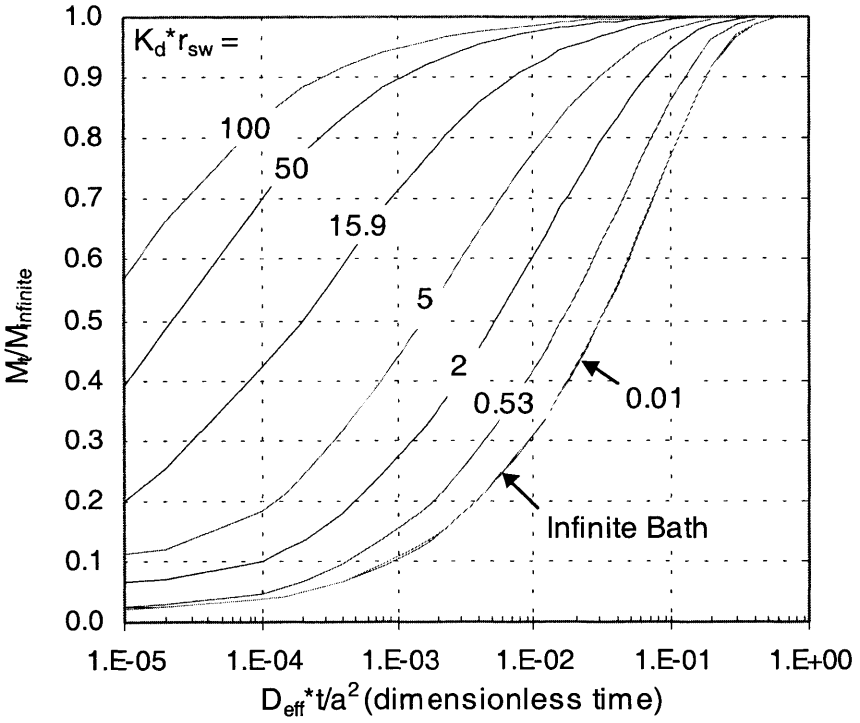

Figure 3.5. Analytical solutions for the radial diffusive desorption from or uptake by spherical particles. The numbers on the curves (K_d*r_{sw}) are the ratio of the mass sorbed on solids to the mass dissolved in solution at equilibrium. The K_d*r_{sw} value of 15.9 corresponds to a r_{sw} of 300 mg/L (K_d = 53,000 L/kg), and the K_d*r_{sw} = 0.53 corresponds to a r_{sw} = 10 mg/L.

CHAPTER 4: THE IMPORTANCE OF SEDIMENT RESUSPENSION TO THE SEDIMENT-WATER EXCHANGE OF PAHS AND PCBS IN THE LOWER HUDSON ESTUARY

INTRODUCTION

Once in the aquatic environment, the hydrophobic nature of polycyclic aromatic hydrocarbons (PAHs) and polychlorinated biphenyls (PCBs) causes them to preferentially sorb to the sediments (1). Consequently, even after the input of these contaminants has ceased or diminished, the sediments can remain a source of pollutants to the surrounding water. Recent studies indicate that the sediments of urban bodies of water are a source of hydrophobic organic contaminants (HOCs) to the overlying water column (2-6). The significant resuspension events that occur in the lower Hudson Estuary (7-9) are expected to result in large fluxes of PAHs and PCBs to the surrounding waters. Recent studies in the Hudson (3,10) suggest that this is the case. It is important to improve our understanding of the extent to which sediment resuspension plays a role in the release of PAHs and PCBs to the water column so that we may model the transport of pollutants. This improved understanding will aid environmental regulatory agencies in establishing appropriate guidelines. Specifically, understanding the mechanisms for and the magnitude of PAH and PCB fluxes caused by sediment resuspension will aid the Environmental Protection Agency in selecting appropriate sediment quality criteria (11,12).

Because of elevated concentrations of PAHs and PCBs in sediments, parts of the lower Hudson Estuary are considered to be areas of environmental concern (75). Several researchers have measured PAHs and PCBs in and near the lower Hudson River Estuary (6,10,75-78). The average total PAH sediment concentration for the Hudson-Raritan Estuary (40 μg/g) reported by Wolfe et al. (75) is ten times the "high" value (4 μg/g: 85th

percentile of the national concentration range) reported by NOAA (79). The input of an estimated 100 to 650 tons (80) of PCBs between the late 1940's and 1977 from electrical capacitor manufacturing plants approximately 300 km from the mouth of the river may have provided for elevated PCB concentrations in the lower Hudson Estuary. However, it should be noted that due to the non-reactive nature of PCBs they are still abundant throughout the environment and several other sources (e.g., wastewater, run-off, atmospheric deposition, etc.) may contribute to PCB loading in the estuary. The average total PCB sediment concentration for the Hudson-Raritan Estuary [300 ng/g; (75)] was greater than the "high" value (200 ng/g) reported by NOAA (79). Because of the large PAH and PCB concentrations measured in the sediments of the Hudson Estuary, an improved understanding of how environmental processes like resuspension affect the fate of PAHs and PCBs is needed.

The lower Hudson River estuary has been observed to have two estuarine turbidity maxima on the western side of the river [Figure 4.1; (7)]. Geyer (8) observed near-bottom suspended solids concentrations between 100 and 200 mg/L in the summer of 1992 and between 100 and 400 mg/L concentrations during high discharge in 1993 at the southern estuarine turbidity maximum site (Figure 4.1). However, these elevated suspended solid concentrations were observed to drop to below 20 mg/L at slack tide, indicating the tidal influence of sediment resuspension. Tidal cycles also influence suspended solid concentrations. During spring tides, which are tides of greater-than-average change in water level around the times of new and full moon, near-bottom suspended sediment concentrations were found to reach values as high as 1800 mg/L. In contrast, near-bottom, suspended sediment levels during neap tide, which is a tide of minimum change in water

level occurring during the first and third quarters of the moon, were approximately six times less (81).

The distance of salt-water intrusion up the Hudson from the Battery varies from approximately 30 km during high freshwater discharge in the spring to approximately 100 km during low discharge in the fall (82). The flow in the Hudson Estuary is dominated by tidal flow even during times of high discharge; tidal flow is between 10 and 100 times greater than freshwater flow (83). Geyer (8) observed maximum flood currents to be 0.8 m/s and maximum ebb currents to be 1.2 m/s during low discharge conditions in 1992. During high discharge conditions, Geyer (8) observed maximum flood and ebb currents to be 1.5 m/s.

In this study the importance of sediment resuspension to the inputs of dissolved pyrene, a PAH, and 2,2',5,5'-tetrachlorobiphenyl (PCB #52), a PCB, were examined. The PED-measured dissolved concentrations were sampled during both neap and spring tides in order to assess the impact of increased sediment resuspension. Dissolved concentrations were examined with respect to salinity, which was used as an index of conservative mixing, in order to observe conservative or non-conservative behavior. Sediment concentrations were used to predict the expected direction of chemical movement based on the concentration gradient between the sediments and the overlying water. The magnitudes of the predominant sources and sinks of pyrene and PCB #52 were estimated. Finally, the dissolved concentration of each chemical within the estuary was solved for with a simple one-box model approach in order to assess the validity of the model and check for any missing sources or sinks.

EXPERIMENTAL SECTION

Study Area

The lower Hudson River Estuary empties into New York Harbor and is bordered by northern New Jersey to the west and Manhattan Island and New York City to the east. Sampling was performed along the estuary between New York Harbor and the town of Hastings approximately 34 km up river (Figure 4.1) in April of 1999 and October of 2000. During the April campaign, sampling was performed during neap (April 9 – 11, 1999) and spring (April 15 – 18, 1999) tides at three stations: the Southern Site (SS) at the Battery which is located next to the southern tip of Manhattan where the Hudson empties into New York Harbor, the Southern Estuarine Turbidity Maximum (SETM) approximately 13 km up the river, and the Northern Site (NS) which is approximately 34 km up the river from the Battery near the town of Hastings (Table 4.1). During the October sampling campaign, samples were collected during neap (October 4-6, 2000) and spring (October 12-14, 2000) tides at four stations: the SS, the SETM, the Northern Estuarine Turbidity Maximum (NETM; approximately 22 km from the Battery), and the NS. The NS was chosen to allow for the estimation of the input of PAHs and PCBs flowing into the estuary. As the SETM and NETM were observed to be areas of maximum resuspension, they would allow for an estimate of the magnitude of PAH and PCB input from sediment resuspension. The Battery (SS) was chosen to represent the output of PAHs and PCBs from the estuary. The SS and NS also served as a sort of "control" site where the resuspended solids concentrations are lower than those observed at the SETM and NETM.

Polyethylene Devices

Polyethylene devices (PEDs) were used in order to measure the "dissolved" concentrations of PAHs (e.g., pyrene) and PCBs (PCB #52). They were deployed in the lower Hudson Estuary during the neap and spring tides of both sampling campaigns (Table 4.2). PEDs were deployed at the SS, the SETM, and the NS in April 1999 and at the SS, the SETM, the NETM, and the NS in October 2000.

In April 1999, two different types of polyethylene were used in the field. The first (Brentwood Plastics, Inc., Brentwood, MO) was 70 ± 1 μm thick, and the second (Carlisle Plastic, Inc., Minneapolis, MN) was 51 ± 3 μm thick. In October 2000, only the 51 μm-thick polyethylene was used. The PEDs used in the field were approximately 3 cm wide, 90 cm long, and 70 μm or 51 μm thick depending on the manufacturer. Prior to deployment, the PEDs for the April campaign were extracted with methylene chloride ($MeCl_2$; JT Baker Ultra-resi-analyzed) twice (2 days each time). They were then dried in a laminar flow hood for a minimum of 6 hours. After drying, the PEDs were stored in amber glass jars with screw-on, teflon-lined polypropylene covers. Prior to use, PEDs for the October campaign were pre-cleaned with 500 mL of $MeCl_2$ for a minimum of 48 hr, followed with methanol (24 hr), and finally clean water (see below; 24 hr). October PEDs were kept in clean water until use. The night before deployment, the PEDs were each punctured with a piece of $MeCl_2$-rinsed, 16-gauge, stainless steel wire in an accordion manner and stored in a 1-gallon Ziploc bag.

Water was reverse osmosis pretreated and run through an ion-exchange resin and activated carbon filter system (Aries Vaponics, Rockland, MA) until a resistance of 18 MΩ

was achieved. The water was then treated with ultraviolet light (Aquafine TOC reduction unit, Valencia, CA) and filtered with a 0.22 μm filter (Millipore).

During the April 1999 campaign, the boat was anchored, the engine turned off, and the stainless-steel wire with the PEDs was attached to a nylon rope. The nylon rope was anchored to the bottom and kept vertical with a float. PEDs were attached to the rope so that they would be at varying depths from the bottom (Table 4.2). The plastic bags were left around the PEDs until just before the each PED went into the water. During the October 2000 campaign, the same protocol was followed except the PEDs were attached to a chain anchored to the bottom. The bottom PEDs were kept vertical with a float approximately 5 m from the bottom, and the "surface" PED was attached to the chain 2 m below a surface buoy.

Extra PEDs were taken into the field and handled on deck in the same manner that the deployed PEDs were in order to determine the PAHs and PCBs present in the air that would also be in contact with the PEDs that were deployed in the water. In April, while the buoy for the PED deployment was being lowered into the water, the blank PED was exposed to the air. As this PED was exposed for the duration of the buoy deployment (approximately 15 minutes), the April blanks were exposed longer than each of the individual water-sampling PEDs. In October, the blank PEDs were exposed during the same period of exposure time as an individual water-sampling PED at each site.
The PEDs were deployed for between approximately 2 and 3 days (Table 4.2). At recovery, the rope or chain was lifted from the water and as soon as each PED left the water, it was removed from the wire and placed in a glass amber jar with a teflon-lined polypropylene screw lid. Blank PEDs were re-exposed during recovery.

Water Sampling

Water samples and hydrographic data were collected during the neap and spring tides of the April 1999 campaign as well as during the spring tide of the October 2000 campaign. During the April 1999 neap tide, hydrographic data was collected at the SS and the NS, and only a few water samples were collected (Table 4.3). During the April 1999 spring tide hydrographic data and water samples were collected. The NS near Hastings was sampled during maximum flood. The SETM was sampled during maximum ebb, and the SS was sampled during maximum flood. Samples were typically collected 2 m from the surface and then several samples were typically collected 1, 2, and 3 m from the bottom.

During the October spring tide, water and hydrographic data were collected at the SS, the SETM, the NETM, and the NS (Table 4.3). The SS was sampled during slack tide (October 12 & 14, 2000). The NETM was sampled during ebb (October 12) and flood (October 14) tide. The NS was sampled during slack (October 12) and flood (October 14) tide. Samples were typically collected at 2 m depth and 1 and 2 m from the river bottom. On October 13, 2000 (spring tide), water samples and hydrographic data were collected approximately every hour for one 12-hr tidal cycle at the SETM.

Water was collected for total suspended solids measurements, particulate organic and black carbon analysis. A positive-displacement, gear-driven pump (SP-300; Fultz Pumps, Inc., Lewistown, PA) attached to a water quality multiprobe was lowered over the side of the boat. The water was pumped through $MeCl_2$-rinsed, ¼"diameter, aluminum tubing into 300 mL, clear glass, glass-stoppered, BOD bottles pre-combusted at 450°C.

The tops of the bottles were kept covered with aluminum foil to avoid any addition of organic carbon not from the sample.

At the end of each day, between 40 and 120 mL of the water from each of the 300-mL samples for organic carbon analysis was filtered using a hand-pumped vacuum with pre-combusted 4.25-cm glass fiber filters (Whatman International Ltd., Springfield Mill, England). During the October campaign, filters were rinsed with clean water immediately following the sample filtering; however, April filters were not rinsed. Filters were then folded and wrapped in aluminum foil and kept frozen until they could be analyzed for particulate organic and black carbon. All samples were stored in ice until they could be stored in the laboratory freezer at 0°C.

As mentioned previously, the water-displacement pump was attached to a water quality multiprobe (DataSonde 4; Hydrolab Corporation, Austin, TX). This probe allowed for the measurement of the following parameters at the time of sampling: depth, temperature, conductivity, and turbidity.

Sediment Sampling

In April and June of 1999, sediment was collected at the SETM with a hydraulically dampened, gravity corer (84). Subsequent to collection the cores were stored at 6°C. Because this coring method provides for an 11-cm diameter core encased in polycarbonate, sediments from the inner section of the core were collected to avoid any organic contamination. During the October campaign, sediment was collected with a 50 x 50 cm box-corer at each of the four sites over a two-day period (October 4-5). Metal spatulas and spoons were used to collect the surface sediment at 1-cm depth intervals at the surface and

2-cm depth intervals at greater depth (2 to 7 cm). The sediment was stored in glass amber jars at 4°C.

PED Extraction

The PEDs were stored in the glass amber jars at 0°C until they were extracted. PEDs from the April campaign were extracted in 500 mL of $MeCl_2$ in glass-stoppered bottles for 1 week. PEDs from the October campaign were extracted in 60 mL of $MeCl_2$ two times for a minimum of 24 hr each time. All bottles were covered with foil to prevent photodegradation. The PEDs from the neap tide of the April campaign were spiked with d_{12}-benz(a)anthracene as a recovery standard, while the spring tide April PEDs were spiked with several recovery PAHs (d_{10}-phenanthrene, p-terphenyl, and d_{12}-perylene). The PEDs from the October campaign were spiked with a PAH and PCB recovery standard (d_{10}-phenanthrene, d_{14}-terphenyl, d_{12}-benz(a)anthracene, d_{12}-perylene, 2,3',4,6-Cl_4B, 2,2',3,4',5-Cl_5B, and 2,2',3,4,5,6'-Cl_6B). The extracts were dried with anhydrous sodium sulfate (Na_2SO_4) and stored overnight at 0°C. Subsequently, samples were concentrated with a Kuderna-Danish apparatus or via rotary evaporation followed by N_2 blow down.

GC-MS

PED extracts were analyzed on a gas chromatograph (GC; Hewlett Packard 6890 Series) -mass spectrometer (MS; JEOL MS-GCmate). The extracts (1 μl) were injected splitless and separated on a J&W Scientific (Folsom, CA) 30 m x 0.32 mm DB-5 (0.25 μm film thickness) fused-silica capillary column. For PCBs (e.g., PCB #52), the injection port was at 300°C, and the GC-temperature program started at 70°C, ramped at 20°C/min to 180°C, increased by 4°C/min to 260°C, reached 280°C in a minute where it was held for 4

min. For PAHs (e.g., pyrene), the injection port was at 280°C, and GC was temperature programmed from 70°C to 180°C at 20°C/min and continued to 300°C at 6°C/min.

The MS was operated at a resolution of 500 in EI+ mode and selected ion monitoring (SIM) was used. PCBs and PAHs were quantified relative to the internal recovery standards. Pyrene was quantified relative to the d_{12}-benz(a)anthracene, p-terphenyl, or d_{14}-terphenyl recovery standards. PCB #52 was quantified relative to the 2,3',4,6-Cl_4B recovery standard. Recoveries were calculated relative to the injection standard (p-terphenyl or m-terphenyl).

The concentration of pyrene and PCB #52 present in the water was calculated by first subtracting off the mass of the respective chemicals measured in the blanks (Table 4.4). Pyrene blanks never exceeded 2.9% of the mass measured in the water sampling PED and averaged 0.89 ± 0.76% and 0.69 ± 0.75% during the April 1999 and October 2000 campaigns, respectively. The PCB #52 blanks during the April 1999 campaign averaged 14 ± 10% of the mass measured in the water sampling PED with the highest percentage measured at 33%. The PCB #52 blanks during the October campaign were much smaller averaging 0.33 ± 0.25% and ranging from 0.01 to 1.0% of the mass measured in the sample.

The concentrations of dissolved pyrene and PCB #52 present in the water column were calculated using their respective polyethylene-water partition coefficients (K_{PEW}; Table 2.2) adjusted for temperature and salinity and temperature-adjusted diffusivities (Table 2.3). This method is presented in Chapter 2.

Total Suspended Solids

Because the turbidity probe broke during the April campaign, only filtered water samples were used to estimate the total suspended solids (TSS). During the October campaign, filtered water samples as well as Hydrolab turbidity measurements were collected. After the April campaign, each folded filter was transferred to a new aluminum foil envelope as the salt in the samples had begun to corrode the foil. The filters were first weighed, and then placed in a small utility oven (Model 1300U; VWR Scientific, So. Plainfield, NJ) at 70°C in order to dry. They were weighed each of the two following days until they had reached a constant weight indicating that they were dry. The average weight of five different clean filters was used to subtract from the total weight to calculate the mass of solids present. In order to correct for the additional mass of the salt present on the April filters, water was added to a pre-weighed, clean filter until it was saturated. The mass of the pre-weighed filter was subtracted from the saturated filter mass in order to calculate the mass of water present at saturation. The density of water was used to calculate the volume of water present, and using the salinity of the water, the additional mass due to salt was calculated. The salt mass was estimated to be between 12 and 87 % of the total suspended solid mass (including salt), depending on the salinity of the water.

The Hydrolab turbidity sensor consists of an infrared emitter and a photodiode detector. The sensor measures the intensity of light scattered at 90° from an infrared light source of 880 nm. The turbidity sensor was calibrated with clean water (0 mg/L) and a 100 mg/L kaolinite suspension in water. However, the corresponding filtered samples were measured to have consistently higher total suspended solids than the Hydrolab-measured samples. It is suspected that the kaolinite solution may not be representative of the

suspended solids observed in the Hudson Estuary. A correlation between filter-measured and Hydrolab-measured TSS (Filter-measured TSS = 1.67*Hydrolab-measured TSS + 39.5; $R^2 = 0.96$) was used to estimate the true TSS concentrations from Hydrolab measurements.

Organic and Black Carbon Analysis

Both sediments and TSS filters were analyzed for organic carbon (OC) and black carbon (BC). The sediment samples were ground with a mortar and pestle, and both sediments and filters were dried at 70°C. The dried filters were subsampled with a 4 mm-diameter cork-borer. The filter subsamples and sediments were added to tared silver capsules (D2029, 8 x 5 mm; Elemental Microanalysis Ltd., Manchester, NH) and weighed using an electrical microbalance (Cahn 25 Automatic Electrobalance; Ventron Corp., Cerritos, CA). In order to remove inorganic carbon, low-carbon water and 1 M HCl were added directly to the capsules following the procedure outlined by Gustafsson et al. (58). The samples were analyzed with a PE 2400 CHN elemental analyzer (Perkin Elmer Corp., Norwalk, CT). The instrument detection limit was approximately 3 μg of C per input. Response factors were determined using an acetanilide standard. The relative standard deviation of these response factors within batches was ± 0.3%. Blanks were prepared for each batch of samples; the average blank was 4.7 ± 1.2 μg of C (n=5).

Portions of the remaining dried filter and sediment samples were added to preweighed and low-carbon-water rinsed porcelain crucibles with a silica glazed surface (Coors Ceramics, Golden, CO). The black carbon analysis procedure developed by Gustafsson et al. (58) was used to remove the "non-black" organic carbon. The crucibles with samples were placed into a muffle furnace (Thermolyne Model F-A1730) equipped

with an auxiliary temperature controller (Thermolyne Furnatrol 133, Sybron Corp., Dubuque, IA) and covered with precombusted aluminum foil. The samples were oxidized in the presence of air for 24 hours at 375°C. After the samples had cooled, the same method outlined above for the removal of inorganic carbon was followed, and the samples were analyzed with the PE 2400 CHN analyzer as discussed above.

RESULTS AND DISCUSSION

Temperature and Salinity

The estuary is more strongly stratified during the neap tides than during the spring tides (Figures 4.2 & 4.3). A significant vertical salinity gradient was observed during both the April 1999 and October 2000 neap tides. For example, the average surface salinity (2 m depth) at the SS was 9 psu, while the average bottom-water salinity was 27 psu during the neap tide in April 1999. The vertical salinity gradient during spring tides was much smaller than the gradient observed during neap tides. During the spring tide in April 1999, the average salinity at 2 m was 21 psu, while the average salinity in the bottom waters was 22 psu.

Temperature variations within the estuary were less dramatic than the salinity gradients. The temperature difference along the vertical ranged from 0 to 0.7°C. The greatest vertical temperature gradient was observed at the NS during the April 1999 neap tide. At this time, the surface temperature was 8.8°C while the bottom-water temperature was 8.1°C. In general, the spring tide vertical temperature gradient was smaller (i.e., 0 to 0.1°C) with the largest vertical temperature gradient at the SS, where the temperature difference was 0.2°C in April 1999 and 0.6°C in October 2000. The along-estuary

temperature difference (from the NS to the SS) was as large as 1.4°C during the April 1999 neap tide. In April, the harbor waters were colder than those upstream at the NS. In contrast, the surface-water temperatures measured during the October 2000 spring tide increased from the NS to the SS. Perhaps most noticeable is the temperature difference between the April and October campaigns where April water temperatures were between 7 and 9°C and October temperatures were between 16 and 17°C.

Total Suspended Solids

The total suspended solid (TSS) concentration was found to increase during flood and ebb tide and drop to smaller levels during slack tide (Figure 4.4). This was most noticeable in the bottom waters (6.5 to 8 m depth) suggesting that presently resuspended sediments were responsible for the increased TSS. For example, approximately an hour before maximum flood, the TSS concentration was 680 mg/L at 7.9 m depth. Approximately one hour before slack tide, the TSS had dropped to 60 mg/L. Subsequently, at maximum ebb, the TSS at 6.9 m depth increased to 1000 mg/L. The average TSS over the course of the tidal cycle was 390 mg/L. These significant fluctuations in TSS illustrate the importance of the tidal cycle on sediment resuspension as well as the temporal variability within the estuary.

A much smaller TSS variability was observed at 2 m depth. At maximum flood, TSS at 2 m was 76 mg/L, while at slack tide it had dropped to 50 mg/L. The TSS levels increased to 120 mg/L at maximum ebb. The tidally-averaged TSS at 2 m depth was 71 mg/L. TSS was observed to increase with depth at the other sites during flood and ebb tides (Figures 4.5b&c). There is an increase in TSS with increasing depth at the NETM during both ebb and flood tide and at the NS during flood tide. As expected, the TSS

concentrations in the bottom waters at the NS are not as high as those in the NETM bottom waters during flood tide. The TSS concentrations measured during slack tide at the SS change very little over depth as is the case for the TSS during slack tide at the NS (Figures 4.5a&c). Again, the influence of tidal cycle on TSS is apparent. Geyer et al. (81) also observed increases in TSS with depth as well as with flood and ebb tide.

Filtered water samples also showed an increase in TSS with depth (Tables 4.6 & 4.7). For example, the TSS concentration at 2 m depth at the SS during spring tide in April was 68 mg/L, while the TSS at 7.9 m at the same location and time was 120 mg/L. In agreement with observations by Geyer et al. (81) the bottom-water neap-tide TSS during a changing tide (ebb tide at the SS) was six times smaller than the bottom-water spring-tide TSS during a changing tide (flood tide at the SS). Also in agreement with the observations of other researchers (7,81) the SETM had higher TSS levels than the NS and the SS during flood and ebb tides during the spring tide of April 1999, illustrating why it is called the Southern *Estuarine Turbidity Maximum*. Fewer comparisons can be made with the October 2000 filtered TSS as they are all spring tide measurements and the SS and NS samples were collected during slack tide in contrast to the SETM and NETM samples which were collected during flood and ebb tides. As observed in April 1999, the increasing turbidity with depth is apparent at the three sites where multiple samples were collected at varying depths.

Organic and Black Carbon

The percentage of OC measured in TSS samples collected in April 1999 ranged from 1.5 to 13% (Tables 4.6 & 4.7) with an average of 4.2 ± 2.9 % OC. The percentage of organic carbon measured on October 2000 TSS ranged from 2.0 to 4.7% with an average of

3.3 ± 0.9%. As the mass of the April filters was corrected for with an estimate of salt content, there is greater error associated with these values. This may explain the larger standard deviation associated with the average; however, it is also possible that the suspended OC was more variable within the estuary. The suspended OC percentages measured in this study are comparable to those measured by Achman et al. (3) approximately 11 km north of the Battery in 1992 and 1993. Their average TSS OC percentages ranged from 3.24 ± 0.52% to 4.07 ± 0.12%.

The TSS were measured to contain between 0.08 and 0.25% BC in April 1999 with an average of 0.13 ± 0.05%. In October 2000, the few TSS samples measured were found to range from <0.3 to 0.5% BC. These values are comparable to sediment black carbon percentages measured in the East River in August 1996 by Mitra et al. (6). These researchers found the black carbon percentages ranging from 0.25 to 0.55%. The percentages of BC in TSS measured in this study are up to an order of magnitude lower than the percentage of BC measured in TSS samples collected in the Mississippi River and the Gulf of Mexico in April and November of 1999 (85). These researchers measured between 0.47 and 7.8% BC in TSS. However, they also measured high percentages of OC in the TSS; the TSS contained between 24 and 32% OC. The Mississippi River TSS appears to have contained a much higher percentage of OC and BC than the Hudson River TSS we measured.

Dissolved Spring and Neap Pyrene and PCB #52

PED-measured dissolved pyrene concentrations in the lower estuary ranged from 1 to 10 ng/L during the April 1999 sampling campaign (Figure 4.6). The dissolved pyrene concentrations measured during the October 2000 campaign ranged from 5 to 60 ng/L (Figure

4.7). The October concentrations were an order of magnitude greater than the April concentrations in several locations within the estuary. The dissolved pyrene concentrations measured in this study are comparable to values measured in New York Harbor at the mouth of the Hudson River in July 1998 using an XAD-2 resin [10 & 16 ng/L; (86)]. They are also similar to "dissolved" pyrene measured in filtered water samples taken south of the Harlem River [nearest to the NETM; (87)] where pyrene values ranged from 11 to 19 ng/L in these filtered water samples collected between December 1998 and October 2001.

PED-measured PCB #52 concentrations ranged from 4 to 300 pg/L during the April 1999 sampling campaign (Figure 4.8). The October 2000 concentrations ranged from 100 to 400 pg/L (Figure 4.9). As with pyrene there was an order of magnitude increase in PCB #52 concentrations at multiple locations between April 1999 and October 2000. These values are comparable to measurements by Totten et al. (88) in New York Harbor at the mouth of the Hudson River in July 1998 using an XAD-2 resin. Totten et al. measured 237 and 275 pg/L concentrations for PCB # 52 & 43; however as PCB #43 is present at less than 0.05% in all Aroclor mixtures (89), the measured concentration is likely to be predominantly PCB #52. XAD-measured PCB #52 water concentrations south of the Harlem River collected between December 1998 and October 2001 ranged from 11 to 340 pg/L (87). The PED-measured dissolved concentrations for additional PAHs (phenanthrene and benzo(a)pyrene) and PCBs (#95, #105, and #128) are presented in Appendix B.

Estuarine Activity

In order to study the importance of sediment resuspension, pyrene and PCB #52 dissolved concentrations during both the neap and spring tides were examined with respect to salinity (Figures 4.10 – 4.13). In the absence of a source or a sink for the chemical, the

physical mixing of the river and ocean waters will result in a linear or conservative relationship. If all other sources and sinks of the chemical of interest remain constant during the spring and neap tides, a non-conservative behavior may be attributed to sediment resuspension. The dissolved pyrene concentration in the mid-salinity region of the estuary increased between spring and neap tides (Figure 4.10). This suggests that the sediment resuspension observed in the lower Hudson Estuary may be a source of dissolved pyrene to the estuary. In contrast, during the October sampling campaign, the along-estuary mixing appeared much more conservative (Figure 4.11). The largest dissolved concentration during the October neap tide was in the SS surface water, which is not an area of significant sediment resuspension. The October spring tide dissolved pyrene-salinity correlation is linear suggesting conservative behavior. During October the pyrene concentrations appear to be highest at the SS suggesting that the harbor waters may be a source of pyrene to the estuary.

It is important to note, that because the spring tide waters are more vertically well-mixed, spring tide mixing diagrams are more conducive to identifying sources and sinks within the estuary. The vertical stratification present during the neap tides, provides for a more pronounced bottom-water saltwater intrusion at the Battery (SS), and a freshwater outflow on the surface of the estuary. This stratification provides for a much different water path throughout the estuary than the path observed during spring tides. Consequently, sources and sinks are more difficult to identify with a mixing diagram.

During April 1999 the PCB #52 concentration in the mid-salinity region of the estuary appears to decrease between neap and spring tides (Figure 4.12). This may suggest that PCB #52 is being scavenged by the resuspended sediments, which are serving as a sink. The surface concentrations measured during the neap tide are larger than the concentrations at greater depth

with the exception of the NS sample at 3-m depth. One could hypothesize that during the neap tide when there is less resuspension and the estuary is vertically stratified, the PCB #52 in the bottom salty layer is being scavenged by particles. Then during spring tide and increased sediment resuspension, the PCB #52 at the SETM is scavenged further resulting in the small concentrations at all depths.

The dissolved PCB #52-salinity correlation in October 2000 is much more linear (Figure 4.13). Consequently, it is difficult to point to either a source or a sink for PCB #52 within the estuary. Interestingly, for both April 1999 and October 2000 the upper river appears to be the source of PCBs to the estuary. This finding may suggest that the PCB "hot spots" approximately 300 km upriver are affecting PCB loading into the lower estuary.

Sediment Concentrations

Two sediment samples from the SETM were collected in April and June 1999. The pyrene concentration was 1600 ng/g in both samples (Table 4.7). Sediment at the SS, the SETM, and the NS were collected again in October 2000 and measured to have pyrene concentrations ranging from 330 to 4200 ng/g (Table 4.8). Consistent with a harbor source, the sediment concentrations are greatest at the mouth of the river and decreased moving landward up river. There appears to have been a decrease in the sediment concentration over time, which may suggest that the sediment is indeed a source of pyrene to the overlying waters. However, Woodruff et al. (9) observed a seasonal progression in the spatial distribution of sedimentation with sediment accumulating near the mouth during the spring freshet period (April '99), and as the freshet abated, the new sediment being eroded and re-deposited further landward at the SETM (June '99). This sediment transport may also explain the change in pyrene sediment concentrations over time. These sediment concentrations are comparable to

the 1300 and 1700 ng/g of pyrene measured at 2.5 cm depth approximately 5 km north of the Battery in 1977 (90). This study's values are also comparable to the surface sediment pyrene concentration measured in the East River in August 1996 (2000 ng/g) by Mitra et al. (6).

PCB #52 sediment concentrations at the SETM were 32 and 31 ng/g in April and June, respectively. Sediment collected in October 2000 at the same site was found to have 16 and 18 ng/g of PCB#52. Again, there appears to have been a decrease in the PCB #52 sediment concentration with time. In light of the sediment movement observed by Woodruff et al. (9), this decrease may be explained by the movement of "cleaner" sediment from the harbor. The PCB #52 sediment concentrations measured here are comparable to PCB #52 surface sediment concentrations measured by Long et al. (91) along the lower estuary in 1991 ranging from 21 to 55 ng/g .

Between 2.2 and 2.9% organic carbon (OC) was measured in the 1999 sediment samples. These values are smaller than the percentage OC measured in the TSS at this site. Interestingly, however, the bottom-most TSS-associated organic carbon (3.6%) is the most similar in value. The percentage of black carbon in the SETM sediment was 0.20 and 0.21%. This value is greater than the TSS-associated black carbon measured at this site (0.08 – 0.11%). Similar to the 1999 values, sediment OC ranged from 2.6 to 3.0% organic carbon in the October 2000 sediment samples. The percentage of black carbon (BC) measured in the October sediments ranged from 0.34 to 0.79%. The relatively large BC percentage measured at the SS (0.79%) is not surprising given this site's urban nature and high boat traffic.

Estimated and Measured Dissolved Concentrations

In order to determine the direction of the thermodynamic driving force between the sediment and the overlying water, dissolved pyrene and PCB #52 concentrations were

estimated and compared to the PED-measured dissolved concentrations. First the sediment concentrations and the appropriate partitioning coefficient were used to estimate the porewater concentration in the sediment:

$$C_{porewater} = \frac{C_S}{K_d} \tag{4.1}$$

where $C_{porewater}$ is the dissolved porewater concentration (μg/L), C_S is the sediment concentration (μg/kg), and K_d is the solid-water partition coefficient (L/kg) and is estimated according to the following (59):

$$K_d = f_{OC}K_{OC} + f_{BC}K_{BC}C_w^{(\nu-1)} \tag{4.2}$$

where f_{OC} is the weight fraction of organic carbon in the solid phase, K_{OC} is the OC-normalized partitioning coefficient ([mol/kg$_{OC}$]/[mol/L]), f_{BC} is the weight fraction of BC is the solid phase, K_{BC} ([μg/kg$_{BC}$]/[μg/L]$^{\nu}$) is the BC-water partition coefficient, C_W is the dissolved concentration (μg/L), and ν is the Freundlich exponent appropriate for the specific BC-chemical pairing of interest. The porewater concentration was solved for iteratively because the solid-water partition coefficient is a function of the dissolved or porewater concentration. The f_{OC} and f_{BC} were measured (see above). A log K_{OC} value of 4.7 (69,70) was used for pyrene calculations, and a log K_{OM} value of 4.9 (42) and f_{OM} estimated as 2 times f_{OC} was used for PCB #52 calculations. K_{OC} values were adjusted for temperature affects according to the following (42):

$$K_{OC}(T_2) = K_{OC}(T_1)\left\{\frac{\Delta H_S^e}{R}\left(\frac{1}{T_1} - \frac{1}{T_2}\right)\right\} \tag{4.3}$$

where ΔH_S^e is the excess enthalpy of solution in water (kJ/mol), R is the gas constant (kJ/molK), and T is the absolute temperature (K). The ΔH_S^e's used for pyrene and PCB

#52 were 29 and 12 kJ/mol, respectively (as measured in Chapter #2). Log K_{BC} (6.4 for pyrene and 5.9 for PCB #52) values were measured by Lohmann et al. (72) in the same sediment collected at the SETM in October 2000. As Lohmann et al. used a ν of 0.7, this value has been used in the calculations here as well.

Pyrene porewater concentrations estimated with this method for April 1999 are over an order of magnitude greater than PED-measured bottom-water pyrene concentrations, suggesting a driving force out of the sediment (Table 4.9). This finding is consistent with the non-conservative behavior observed in the pyrene mixing diagram (Figure 4.10). The pyrene porewater concentration estimated for October is similar to the values measured in the bottom-waters, suggesting that the sediments and water may be close to equilibrium. This too is consistent with the conservative mixing behavior observed previously (Figure 4.11).

PCB #52 porewater concentrations estimated from sediment measurements in April 1999 are at least an order of magnitude greater than the PED-measured bottom water concentrations (Table 4.10). This finding suggests a gradient out of the sediments to the overlying water. However, this is contrary to the non-conservative mixing observed in the PCB #52 mixing diagram where the estuary appeared to be serving as a sink. The PCB #52 porewater concentrations estimated for October 2000 are similar in magnitude to the measured bottom water concentrations. In October, there may be a small driving force out of the sediment. These October estimates support the conservative behavior observed in the dissolved PCB #52-salinity correlation (Figure 4.13).

In order to assess the importance of desorption kinetics, the fraction of chemical desorbed was solved for according to the analytical solution for diffusion into a well-stirred bath with particles that are uniform in size (36):

$$\frac{M_t}{M_\infty} = 1 - \sum_{n=1}^{\infty} \frac{6\alpha(\alpha+1)\exp(-D_{eff} q_n^2 t / a^2)}{9 + 9\alpha + q_n^2 \alpha^2} \tag{4.4}$$

where M_t and M_∞ are the total amount of chemical in the water at time t and at infinite time, respectively (M), D_{eff} is the effective intraparticle diffusivity (L^2/T), t is time (T), and a is the particles' spherical radius (L). The values of q_n are the non-zero positive roots of:

$$\tan(q_n) = \frac{3q_n}{3 + \alpha q_n^2} \tag{4.5}$$

and α is the ratio of the volume of solution to the mass of solids divided by the partition coefficient:

$$\alpha = \frac{1}{K_d [TSS]} \tag{4.6}$$

The D_{eff}/a^2 used for pyrene was 1.0E-7 s^{-1} (see Chapter 3). The smallest of the D_{eff}/a^2 values measured in Chapter 3 was used in order to get a limiting case estimate. The D_{eff} for PCB #52 was estimated according to (23):

$$D_{eff} = \frac{D_m n^2}{K_d (1-n) \rho_s} \tag{4.7}$$

where D_m is the pore fluid diffusivity of the sorbate (cm^2/s), n is the porosity of the sorbent (cm^3 of fluid/cm^3 total), and ρ_S is the specific gravity of the sorbent (g/cm^3). A D_m of 4.8 E-6 cm^2/s (estimated according to (42)), an n of 0.13 (23), a ρ_s of 2.66 g/cm^3 (Chapter 3), and a K_d of 16,000 L/kg were used to estimate a D_{eff} of 2.2 E-12 cm^2/s for PCB #52.

Assuming an average particle radius of 32 μm, the D_{eff}/a^2 calculated for PCB #52 was 2.2 E-7 s^{-1}. The TSS concentration was assumed to be 390 mg/L, the K_d's for pyrene and PCB #52 were 27,000 and 16,000 L/kg, respectively.

Assuming an April spring tide residence time of 2.5 days (74), and an October spring tide residence time of 4.6 days [estimated by scaling according to the ratio of freshwater discharge in April 1999 (26,600 ft^3/s) to freshwater discharge in October 2000 (14,400 ft^3/s); (92)], the percentage of equilibrium achieved was estimated to be between 94 and 98% for both pyrene and PCB #52. This finding suggests that the desorption of pyrene and PCB #52 into the bottom-waters is not limited by the time for desorption. The estimated bottom water concentration including kinetics was estimated as the calculated equilibrium porewater concentration multiplied by the estimated fraction equilibrium (Tables 4.9 & 4.10). The combined equilibrium partitioning and desorption kinetics calculations suggest a thermodynamic gradient out of the sediments into the overlying water for pyrene and PCB #52 in April 1999, while suggesting little to no fugacity gradient between the sediments and water column in October 2000.

The apparent sediment-water disequilibrium in April 1999 and equilibrium in October 2000 along with the increase in pyrene and PCB #52 dissolved concentrations from April to October may be explained by the seasonal sediment deposition observed by Woodruff et al.(9). They observed sediment deposition in the seaward reaches of the estuary during the freshet (April 1999) followed by the "return" of this sediment, which was observed at the SETM in June 1999. One may hypothesize that older sediment was exposed at the SETM during the freshet as sediment was re-deposited seaward. This newly exposed older sediment may not have had sufficient contact time with the overlying water

to equilibrate at the time of sampling. Consequently, the April 1999 sediments and water column were observed to be in disequilibrium. In contrast, the October sediments, which are believed to have been at the SETM since the previous June, had a significant span of time in which to equilibrate. This "extra" time may have allowed for the observed equilibrium between the sediment and water column and for the elevated pyrene and PCB #52 concentrations observed in October 2000. These observations suggest the input of HOC's from the sediments (e.g. resuspension inputs) may be correlated with the seasonal movement of sediments within the estuary.

Magnitude of Sources and Sinks

The magnitude of the sources and sinks of pyrene and PCB #52 in the estuary were estimated in April of 1999 and October 2000 where the control volume during spring tides was defined as the section of the river between the Northern Site and the Southern Site. During neap tides, the NS and SS were also defined as the end-points; however, only the sources and sinks to the bottom waters (4 m from the river bottom) were estimated during neap tides due the significant salinity stratification within the estuary. The following inputs and sources were estimated: 1) desorption from or sorption to resuspended sediment, 2) advective fluxes over the Northern and Southern boundaries due to river flow, and 3) diffusive fluxes across the sediment-water boundary layer from the underlying sediment. The following outputs and sinks were estimated: 1a) advective flux across the Northern and Southern boundaries, 1b) advective fluxes from the bottom waters to the overlying waters (neap tide), and 2) air-water exchange (spring tides only).

The input and output due to river flow, F (M/T) was calculated as:

$$F = Q \cdot C_W \tag{4.8}$$

where Q is the tidally-averaged flow rate (L^3/T). A flow rate and salt balance including freshwater flow, Q_f, along with Knudsen's relation applied to the landward side of the "box" were used to estimate Q's into, out of, and between the two layers of the estuary for both neap and spring tides. Because the Hudson is a partially mixed estuary, it has a two-layer structure with freshwater at the surface overlying saline water at the bottom. In simplified terms, this dense saline water flows upriver, while the overlying fresh water flows downriver. This structure was used to create a simplified input Q at the bottom of the SS, an output Q at the surface of the SS, an input Q at the surface of the NS, and an input or output Q at the bottom of the NS depending on the distance of saltwater intrusion. Two additional Q's were estimated with respect to transport between the top and bottom boxes. The freshwater flow rate was estimated at 1.4 times the discharge at Green Island [Troy, NY; (93)]. The estimated Q's for neap and spring tides during April and October are presented in Appendix C. The C_W's were measured as discussed previously.

The input due to the diffusive flux, D (M/T), across the sediment-water boundary was estimated as:

$$D = \frac{D_m}{\delta_W}\left(\frac{C_S}{K_d} - C_w\right) \cdot A_{sed} \tag{4.9}$$

where δ_W is the diffusive boundary layer thickness at the sediment-water interface (L) and A_{sed} is the cross-sectional area over which the diffusive flux is occurring (L^2). C_W and C_S were measured. The D_m was estimated as 7.7 E-6 cm^2/s (50)and 4.8 E-6 cm^2/s (42)for pyrene and PCB #52, respectively. The diffusive boundary layer thickness was estimated

as 2 E-2 cm during both neap and spring tide. The δ_W is often between 2 E-2 and 1 E-1 cm thick and is dependent on the flow velocity of the overlying water and the surface topography of the sediment (94). Because of the larger velocities observed in the lower Hudson Estuary (95), the lower value of this range was used in this model. K_d was estimated as discussed previously. A_{sed} was estimated as 3.3 E7 m^2.

The input due to sediment resuspension, R (M/T) was estimated according to the following equation:

$$R = \left(\frac{C_S}{K_d} - C_W \right) \cdot V_W \cdot \frac{M_t}{M_\infty} \qquad (4.10)$$

where V_w is the volume of water and M_t/M_∞ is the fraction of equilibrium that has been achieved and was solved according to Eq. 4.4. The t was assumed to be 1 day as the inputs were estimated on a g/day basis.

As approximately 20% of the estuary undergoes significant sediment resuspension, this portion was used to estimate input due to sediment resuspension. A tidally-averaged surface-water and a bottom-water TSS were estimated as 71 and 390 mg/L, respectively during spring tide based on the measurements made at the SETM on October 13, 2000. The bottom-water TSS for neap tides was estimated as one-fifth of the spring tide value (78 mg/L). It may be more appropriate to estimate the TSS in the estuary as a step function with TSS at 800 mg/L for 3 hr during max flood, followed by TSS = 50 mg/L for 3 hr during slack tide, etc. This would allow for the changing "driving force" or chemical potential within the estuary to be more accurately represented.

The output due to air-water exchange, AW (M/T) was calculated according to:

$$AW = v_{tot} \cdot C_W \cdot A_{surf} \qquad (4.11)$$

where v_{tot} is the water transfer velocity (cm/s), and A_{surf} is the surface area of the water. The v_{tot} used in the calculations were 4.0 E-4 cm/s and 7.9 E-4 cm/s for pyrene and PCB #52, respectively (42). v_{tot} is defined as:

$$v_{tot} = \frac{z_w}{D_m} + \frac{z_a}{D_a K'_H} \tag{4.12}$$

where z_w is the thickness of the stagnant water film at the air-water interface (cm), z_a is the thickness of the adjacent stagnant air boundary layer (cm), D_a is the chemical's diffusion coefficient in air (cm^2/s), and K'_H is the Henry's Law constant (L_w/L_a). The z_w was estimated as 5 E-3 cm, and z_a as 0.1 cm. The z_w is a low estimate, which will allow for an upper value estimate of v_{tot}. The D_a's used in the calculations were 4.9 E-2 cm^2/s and 3.9 E-2 cm^2/s for pyrene and PCB #52, respectively and estimated according to Schwarzenbach et al. (42). The K'_H's were 3.6 E-4 and 1.2 E-2 L_a/L_w for pyrene and PCB #52, respectively (42). The surface area of the water was estimated as 4.0 E7 m^2.

For pyrene during the April 1999 spring tide, the advective inputs and outputs are of similar magnitudes, and the inputs due to diffusive and sediment resuspension input are comparable (Table 4.11). The output due to air-water exchange is two orders of magnitude lower than the other sources and sinks. The advective inputs and outputs during the April 1999 neap tide are also of similar magnitude. The sediment diffusive input during the April neap and spring tides were estimated to be equivalent; however, the neap diffusive input may in fact be smaller depending on the water velocity, and the resulting diffusive boundary layer thickness. The sediment resuspension input during the April neap tide was estimated to be approximately a factor of three less than sediment diffusive input. Much of this is due to the fact that only the desorption of pyrene from the suspended particles in the bottom waters of the estuary have been estimated during neap tide. This assumption seems

reasonable due to the stratified nature of the estuary during neap tides. During both tides in April 1999, sediment resuspension and diffusive input appear to be the predominant inputs of pyrene to the estuary.

During the October spring tide, the advective inputs and outputs are again comparable to each other (Table 4.12). Again the sediment diffusive and resuspension inputs are of similar magnitude; however, they are approximately a factor of two smaller than the input estimated for the April 1999 spring tide. This is because the sediment and water are more closely equilibrated during October than April causing less of an input from the sediment. For the October neap tide bottom waters, the advective inputs are larger than the outputs; however, they are within a factor of two. Again, there is a decrease in the sediment diffusive and resuspension inputs between April and October neap tide. During the October neap tide, the input due to sediment resuspension is a factor of ten smaller than the input due to sediment boundary-layer diffusive input, which is again partially due to the assumption of a limited height of resuspension, and the consequent decrease in the mass of particles from which pyrene desorption was estimated. During spring tide in October 2000, the sediment diffusive and resuspension inputs are still the predominant sources of pyrene to the system; however they are less important than they were in April 1999. Similarly, the input of pyrene due to diffusive and resuspension inputs have decreased between April and October. This decrease in sediment sources between April and October is the result of more closely equilibrated sediments and overlying waters present in October 2000.

As with pyrene, the April 1999 spring tide sources and sinks of PCB #52 were also dominated by diffusive and sediment resuspension input (Table 4.13). The advective inputs are slightly larger (15 vs. 6 g/day) than the advective outputs. Again, air-water

exchange does not appear to be an important sink. The neap tide advective input and output are again similar in magnitude. As in April 1999, the neap tide sediment resuspension and diffusive input appear to be the dominant sources of PCB #52 to the estuary with diffusive input three times greater than the input due to sediment resuspension (39 vs. 12 g/day).

The October 2000 spring tide PCB #52 sources appear to be dominated by sediment diffusive and resuspension inputs; however, these inputs are less than half of the April 1999 PCB #52 spring input. Again, advective inputs and outputs are of comparable magnitudes (92 vs. 110 g/day). Because of the elevated PCB #52 concentrations within the estuary in October, air-water exchange is a larger sink that in was in April 1999 (8 g/day in October vs. 0.5 g/day in April). During the October 2000 neap tide, the PCB #52 advective outputs were almost twice the advective inputs to the bottom waters. The sediment boundary-layer diffusive inputs appear to be the largest source of PCB #52 to the October neap tide bottom waters. The input due to resuspension is about four times smaller than the diffusive input to the October 2000 neap tide waters. While sediment diffusion and resuspension appear to be the most important sources of PCB #52 to the estuary, the importance of these sources appears to have diminished in October 2000 due to the more closely equilibrated sediments and overlying waters.

One-Box Model

Steady state was assumed, and a mass balance of the inputs and outputs was used to solve for the C_W within the spring tide estuary:

$$C_W = \frac{F_{IN} + \frac{C_S}{K_d}\left(V_W \frac{M_t}{M_\infty} + \frac{D_m}{\delta_W} A_{sed}\right)}{Q_{OUT} + v_{tot} A_{surf} + V_W \frac{M_t}{M_\infty} + \frac{D_m}{\delta_W} A_{sed}} \quad (4.13)$$

where F_{IN} is the advective input (M/T) and Q_{OUT} is the water flow rate out of the system (L^3/T). During the neap tide, the C_W within the bottom waters of the estuary were calculated in a similar manner:

$$C_W = \frac{F_{IN} + \frac{C_S}{K_d}\left(V_W \frac{M_t}{M_\infty} + \frac{D_m}{\delta_W} A_{sed}\right)}{Q_{OUT} + V_W \frac{M_t}{M_\infty} + \frac{D_m}{\delta_W} A_{sed}} \quad (4.14)$$

In this case air-water exchange is not considered, and Q_{OUT} includes the flow rate from the bottom waters to those above. The calculated C_W was then compared to the measured C_W in order to access the validity of the model (Tables 4.15 & 4.16). The measured C_W was estimated by averaging the PED-measured dissolved concentrations at the SETM for April 1999 and at the SETM and NETM for October 2000 within the appropriate control volume.

In April 1999 the estimated C_W for pyrene is about a factor of two larger than the measured value during the spring tide (17 vs. 8.5 ng/L). Considering all of the parameters that were estimated, these numbers are in good agreement. During the neap tide the estimated pyrene C_W is over four times larger than the PED-measured value. The inconsistency between the estimated and observed C_W's may suggest that one of the sources has been over estimated or that there is a missing sink. As this model did not include sink terms for bio- or photodegradation, which may remove pyrene from the estuary, these processes may contribute to a missing sink. The greater discrepancy between the estimated and observed values during neap tide may indicate that the inputs due to

sediment resuspension were overestimated. For example, the estimated tidally-averaged TSS vales may be too high.

During the April 1999 neap tide, the estimated PCB #52 concentration is four times larger than the PED-measured concentration. During the spring tide, the model overestimates the PCB #52 concentration by almost a factor of 30. This suggests that a source has been overestimated or that there is a missing sink. In light of the apparent driving force out of the sediments at the SETM and the apparent sink observed in the mixing diagram, "cleaner" sediments within the estuary may be scavenging PCB #52 serving as the "missing sink." This hypothesis is further supported by the fact that sediment resuspension is greater during the spring than neap tides, and that there appears to be a larger sink for pyrene (only 8.7 ng/L) during the spring tide than during the neap tide (61 ng/L).

As in April, the October 2000 estimated C_W for pyrene are about a factor of two larger than the measured C_W for spring tide, and the neap-tide estimated pyrene C_W is almost four times larger than the PED-measured value. Again considering all of the estimated parameters, the agreement is good; however, there could be a small missing sink (e.g., bio- or photodegradation) or a small overestimation of a source (e.g., an overestimate of the TSS during neap tide). The October 2000 estimates for PCB #52 C_W's are in good agreement (within 12% during spring tide and within 52% during neap tide) with the PED-measured C_W's. In this case, the sources and sinks appear to have been modeled appropriately.

Implications

In April 1999 the sediments within the lower Hudson Estuary provided for the input of pyrene to the overlying waters. However, the sediments and water appear to have been more closely equilibrated during October 2000 suggesting that the sediments may have provided for a significantly smaller source of pyrene to the waters of the Hudson. With respect to PCB #52, mixing diagrams indicate that resuspended sediments may have provided a sink for dissolved PCB #52 in April 1999; however, selected sediment samples indicate that the sediment served as a source in April 1999. One explanation may be the scavenging of PCB #52 by cleaner sediments within the estuary. October 2000 PCB #52 findings indicate that, as with pyrene, the sediments and waters of the lower Hudson are more closely equilibrated with respect to PCB #52.

Estimates of the magnitudes of the sources and sinks of pyrene and PCB #52 to the lower Hudson Estuary indicate that in April 1999, the largest sources of these chemicals was due to sediment diffusive and resuspension input. Again, in October, diffusive and resuspension provided for the largest input; however, more closely equilibrated October sediments and water provided for a smaller input of both pyrene and PCB #52 from the underlying sediments. The inputs due to these sources are of similar magnitude.

The April to October decrease in driving force observations may be explained by the removal of sediment during the spring freshet coupled to the exposure of older underlying sediments that did not have sufficient time to equilibrate with the overlying water column at the time of sampling. Sediment redeposited in June of 1999 had ample time in which to equilibrate with the overlying waters explaining the more closely equilibrated system observed in October 2000. This observation suggests that there may be

a seasonal trend in HOC inputs from underlying sediments. The dynamic changes in this estuarine system make the modeling the fate of HOCs within it a challenge. Further modeling that accounts for the dynamic as well as multi-dimensional nature of this system is needed in order to assess the fate of PAHs and PCBs within the lower Hudson Estuary.

Table 4.1. Sampling dates and coordinates.

Station	Date	Coordinates
Southern Site (SS; Battery)	April 9 – 18, 1999	40° 43.350' N 74° 01.666' W
	October 4 –14, 2000	40° 45.597' N 74° 00.931' W
Southern Estuarine Turbidity Maximum (SETM)	April 9 – 18, 1999	40° 49.231' N 73° 58.210' W
	October 4 –14, 2000	40° 49.209' N 73° 58.269' W
Northern Estuarine Turbidity Maximum (NETM)	October 4 –14, 2000	40° 53.297' N 73° 56.148' W
Northern Site (NS; Hastings)	April 9 – 18, 1999	40° 59.680' N 73° 53.799' W
	October 4 –14, 2000	40° 58.594' N 73° 54.175' W

Table 4.2. PED Depths and Length of Deployment.

Station	Date	Length of Deployment (days)		Total Water Depth (meters)[a]		PED "Depths" (meters from river bottom)[b]	
		Neap	Spring	Neap	Spring	Neap	Spring
SS	April 1999	2.90	3.13	12	12	9, 5.5, 3, 2, 1	10, 3.5, 1.5
	October 2000	1.68	1.77	15.5	15	2 (below surface), 2, 1	2 (below surface), 2, 1
SETM	April 1999	2.79	2.88	9.7	10	6.7, 5.5, 3, 2, 1	8.0, 3.5, 1.5
	October 2000	2.03	1.78	8.8	9.4	2 (below surface), 2, 1	2 (below surface), 2, 1
NETM	October 2000	1.79	1.83	6.6	5.8	2 (below surface), 2, 1	2 (below surface), 2, 1
NS	April 1999	3.00	1.96	11.5	10	8.5, 5.5, 3, 2, 1	8, 3, 1
	October 2000	1.70	1.86	8.5	7.3	2 (below surface), 2, 1	2 (below surface), 2, 1

[a]Total water depth is a function of tidal cycle with a tidal range of 1.2 to 1.6 m (95). [b]Value are meters from river bottom unless otherwise specified.

Table 4.3. Hydrographic and water sampling depths.

Station	Date	Sampling Depth (meters from surface)	
		Neap Tide	Spring Tide
SS	April 1999	1.8, 9.5, 10.5	2.0, 6.9, 7.9, 8.0, 8.9
	October 2000	—	2, 12.7, 14
			2, 13.9, 15
SETM	April 1999	—	3.0, 5.3, 6.3, 7.3
	October 2000		1.9, 6.9, 7.9
NETM	October 2000	—	2.0, 3.7, 4.8
			2, 5.5, 6.5
NS	April 1999	2.1, 9.5, 10.5	3.0, 6.7, 7.7, 8.7
	October 2000	—	2.0, 5.1, 6.3
			2, 6.3, 7.3

Table 4.4. Average PED blanks ± 1 s.d. as a percentage of the water-measured sample

Chemical	April 1999		October 2000	
	Average	Range	Average	Range
Pyrene	0.89 ± 0.76% (n = 33)	0.086 – 1.9%	0.69 ± 0.75% (n = 34)	0.023 – 2.9%
PCB #52	14 ± 10% (n = 6)	3.6 - 33%	0.33 ± 0.25% (n = 32)	0.10 – 1.0%

Table 4.5. Total suspended solids, organic and black carbon in the lower Hudson Estuary in April 1999.

Neap or Spring Tide	Station	Depth (meters from surface)	Date	Time	Flood, Ebb, or Slack	Total Suspended Solids (mg/L)	Percent Organic Carbon	Percent Black Carbon
Neap Tide	SS	10.5	4/9/99	11:02 AM	Ebb	21	3.3	
Neap Tide	SS	10.7	4/9/99	afternoon	---	43	2.4	
Spring Tide	SS	2	4/15/99	7:30 AM	Flood	68	1.9	0.10
Spring Tide	SS	6.9	4/15/99	7:25 AM	Flood	160	1.5	0.11
Spring Tide	SS	7.9	4/15/99	7:19 AM	Flood	120	1.8	0.15
Spring Tide	SETM	3	4/17/99	4:33 PM	Ebb	190	13	
Spring Tide	SETM	5.3	4/17/99	4:26 PM	Ebb	280	5.0	0.11
Spring Tide	SETM	6.3	4/17/99	4:18 PM	Ebb	320	4.6	0.08
Spring Tide	SETM	7.3	4/17/99	4:11 PM	Ebb	380	3.6	0.10
Spring Tide	NS	3	4/15/99	8:28 AM	Flood	110	6.9	0.25
Spring Tide	NS	6.7	4/15/99	~ 8:20 AM	Flood	170	3.7	0.11
Spring Tide	NS	7.7	4/15/99	8:15 AM	Flood	220	4.0	0.16
Spring Tide	NS	8.7	4/15/99	8:10 AM	Flood	180	3.1	

Table 4.6. Total suspended solids, organic and black carbon in the lower Hudson Estuary in October 2000.[a]

Neap or Spring Tide	Station	Depth (meters from surface)	Date	Time	Flood, Ebb, or Slack	Total Suspended Solids (mg/L)	Percent Organic Carbon	Percent Black Carbon
Spring Tide	SS	12.7	10/12/00	6:11 PM	Slack	26	2.2	
Spring Tide	SETM	1.9	10/13/00	8:30 AM	Flood	82	2.0	<0.3
Spring Tide	SETM	6.9	10/13/00	8:20 AM	Flood	320	2.9	<0.3
Spring Tide	SETM	7.9	10/13/00	8:05 AM	Flood	640	3.7	0.5
Spring Tide	NETM	2.0	10/12/00	3:00 PM	Ebb	180	3.6	
Spring Tide	NETM	3.7	10/12/00	2:52 PM	Ebb	300	4.6	
Spring Tide	NETM	4.8	10/12/00	2:42 PM	Ebb	420	4.7	
Spring Tide	NS	2.0	10/12/00	1:20 PM	Slack	26	3.5	
Spring Tide	NS	5.1	10/12/00	1:05 PM	Slack	44	3.0	
Spring Tide	NS	6.3	10/12/00	12:49 PM	Slack	66	3.2	

[a]These values were measured by Rainer Lohmann.

Table 4.7. Pyrene, PCB #52, organic carbon, and black carbon measured in lower Hudson Estuary sediments in April and June 1999.

Location and Date	Sediment Depth (cm)	Pyrene (ng/g)	PCB #52 (ng/g)	Percent organic carbon	Percent black carbon
S. ETM, April 1999	0 - 2	1600	32	2.2	0.21
S. ETM, June 1999	0 – 2	1600	31	2.9	0.20

Table 4.8. Pyrene, PCB #52, organic carbon, and black carbon measured in lower Hudson Estuary sediments in October 2000.

Location and Date	Sediment Depth (cm)	Pyrene (ng/g)	PCB #52 (ng/g)	Percent organic carbon	Percent black carbon
Southern Site, Oct. 2000	0 - 1	4200		3.0[a]	0.79[a]
S. ETM, Oct. 2000	0 - 1	840	16	2.6[b]	0.34[b]
S. ETM, Oct. 2000	1 - 2	1500	18	2.6[b]	0.34[b]
Northern Site, Oct. 2000	1 - 2	330			

[a]Measured in our lab by Rainer Lohmann. [b]Organic and black carbon measurements are for the 0-4 cm depth and were measured in our lab (72).

Table 4.9. Estimated porewater concentration and the corresponding bottom-water concentration at the SETM in April 1999.

Chemical	Sediment concentration (ng/g)	Estimated solid-water partitioning coefficient (L/kg)	Estimated porewater concentration (ng/L)[c]	Estimated fraction equilibrium[d]	Estimated bottom water concentration including kinetics (ng/L)[e]	PED-measured bottom-water concentration (ng/L)[f]
Pyrene	1600	11,000[a]	140	0.94	140	3 - 10
PCB #52	32	15,000[b]	2.1	0.95	2.0	0.004 – 0.3

[a]Estimated with f_{OC} = 0.022 (measured), log K_{OC} = 4.7 (69), f_{BC} = 0.0021 (measured), log K_{BC} = 6.4 (72). [b]Estimated with f_{OM} = 0.044 (estimated as 2 times f_{OC}), log K_{OM} = 4.90 (42), f_{BC} = 0.0021 (measured), log K_{BC} = 5.9 (72). [c]Estimated as C_S/K_d. [d]Estimated according to Eq. 4.4 with residence time of 2.5 days, a mass-to-volume ratio of 390 mg/L and K_d = 27,000 L/kg for pyrene and K_d = 16,000 L/kg for PCB #52. [e]Estimated as the estimated porewater concentration multiplied by the estimated fraction equilibrium. [f]PED-measured concentration range during both neap and spring tides.

Table 4.10. Estimated porewater concentration and the corresponding bottom-water concentration at the SETM in October 2000.

Chemical	Sediment depth (cm)	Sediment concentration (ng/g)	Estimated solid-water partitioning coefficient (L/kg)	Estimated porewater concentration (ng/L)[c]	Estimated fraction equilibrium[d]	Estimated bottom water concentration including kinetics (ng/L)[e]	PED-measured bottom-water concentration (ng/L)[f]
Pyrene	0 - 1	840	25,000[a]	33	0.97	31	20 - 30
	1 - 2	1500	20,000[a]	77	0.97	72	20 - 30
PCB #52	0 - 1	16	31,000[b]	0.51	0.98	0.50	0.2 - 0.3
	1 - 2	18	30,000[b]	0.59	0.98	0.58	0.2 - 0.3

[a]Estimated with f_{OC} = 0.029 (measured), log K_{OC} = 4.7 (69), f_{BC} = 0.0034 (measured), log K_{BC} = 6.4 (72). [b]Estimated with f_{OM} = 0.058 (estimated as 2 times f_{OC}), log K_{OM} = 4.90 (42), f_{BC} = 0.0034 (measured), log K_{BC} = 5.9 (72). [c]Estimated as C_S/K_d. [d]Estimated according to Eq. 4.4 with residence time of 4.6 days, a mass-to-volume ratio of 390 mg/L and K_d = 27,000 L/kg for pyrene and K_d = 16,000 L/kg for PCB #52. [e]Estimated as the estimated porewater concentration multiplied by the estimated fraction equilibrium. [f]PED-measured concentration range during both neap and spring tides.

Table 4.11. Magnitude of the sources and sinks of pyrene to the lower Hudson Estuary in April 1999[a]

Sources (g/day):	Spring Tide	Neap Tide
Advective Inputs	1400	290
Sediment Diffusive Input	2300	2300
Sediment Resuspension Input	2200	640
Sinks (g/day):		
Advective Output	1700	430
Air-Water Exchange	30	---

[a]Neap tide sources and sinks are only for the bottom-water box.

Table 4.12. Magnitude of the sources and sinks of pyrene to the lower Hudson Estuary in October 2000[a]

Sources (g/day):	Spring Tide	Neap Tide
Advective Inputs	7200	2200
Sediment Diffusive Input	900	620
Sediment Resuspension Input	800	62
Sinks (g/day):		
Advective Output	8000	1100
Air-Water Exchange	130	---

[a]Neap tide sources and sinks are only for the bottom-water box.

Table 4.13. Magnitude of the sources and sinks of PCB #52 to the lower Hudson Estuary in April 1999[a]

Sources (g/day):	Spring Tide	Neap Tide
Advective Inputs	15	4.8
Sediment Diffusive Input	39	39
Sediment Resuspension Input	32	12
Sinks (g/day):		
Advective Output	6	4.7
Air-Water Exchange	0.5	---

[a]Neap tide sources and sinks are only for the bottom-water box.

Table 4.14. Magnitude of the sources and sinks of PCB #52 to the lower Hudson Estuary in October 2000[a]

Sources (g/day):	Spring Tide	Neap Tide
Advective Inputs	92	5.1
Sediment Diffusive Input	18	18
Sediment Resuspension Input	10	4.4
Sinks (g/day):		
Advective Output	110	9.6
Air-Water Exchange	8	---

[a]Neap tide sources and sinks are only for the bottom-water box.

Table 4.15. Mass-balance estimated C_W and PED-measured C_W for April 1999.

Chemical	Spring Tide		Neap Tide	
	Mass-balance estimated C_W[a]	PED-measured C_W[b]	Mass-balance estimated C_W[c]	PED-measured C_W[d]
Pyrene (ng/L)	17	8.5	15	3.4
PCB #52 (pg/L)	230	8.7	270	61

[a]Calculated according to Eq. 4.13. [b]The average of the PED measurements in the vertical at the SETM. [c]Calculated according to Eq. 4.14. [d]The average of the PED measurements in the bottom waters at the SETM.

Table 4.16. Mass-balance estimated C_W and PED-measured C_W for October 2000.

Chemical	Spring Tide		Neap Tide	
	Mass-balance estimated C_W[a]	PED-measured C_W[b]	Mass-balance estimated C_W[c]	PED-measured C_W[d]
Pyrene (ng/L)	23	13	57	16
PCB #52 (pg/L)	280	250	440	290

[a]Calculated according to Eq. 4.13. [b]The average of the PED measurements in the vertical at the SETM and NETM. [c]Calculated according to Eq. 4.14. [d]The average of the PED measurements in the bottom waters at the SETM and NETM.

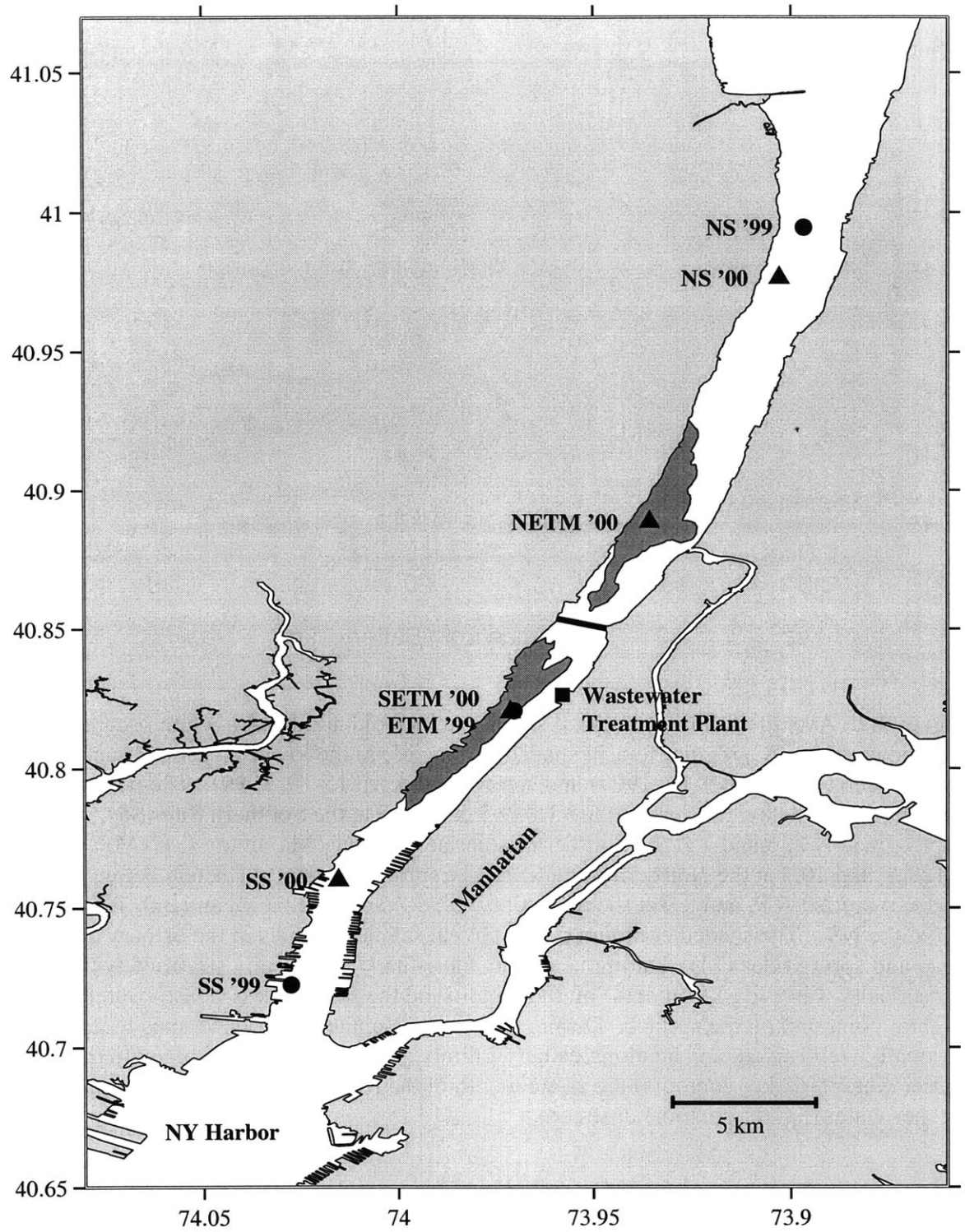

Figure 4.1. Sampling locations in the lower Hudson Estuary. The first set of stations (circles): the Southern Site (SS); the Southern Estuarine Turbidity Maximum (SETM); and the Northern Site (NS) were sampled in April 1999. The second set of stations (triangles): SS, SETM, the Northern Estuarine Turbidity Maximum (NETM), and NS were sampled in October 2000. The dark areas in the river are areas of high turbidity.

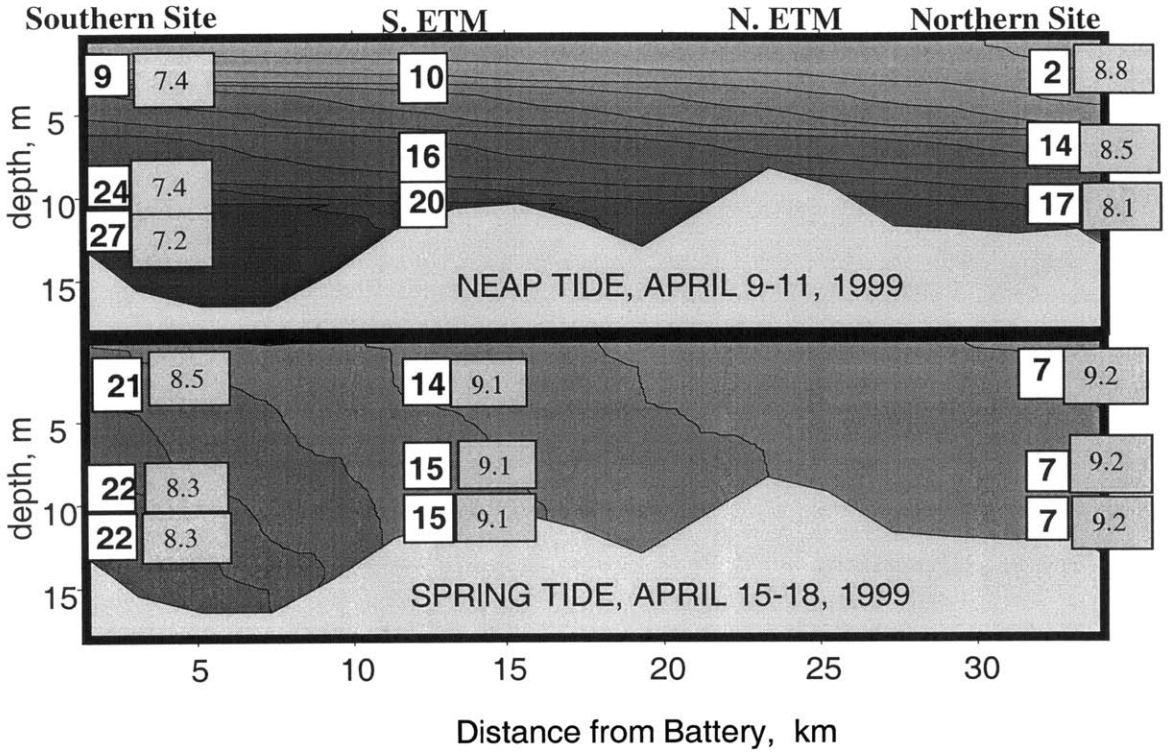

Figure 4.2. Average salinity (practical salinity units; bold numbers in white squares) and temperature (°C; regular font in shaded rectangles) in the lower Hudson Estuary during neap tide (April 9-11, 1999) and spring tide (April 15-18, 1999). The neap tide depths (meters below the surface) are 1.8, 9.5, and 10.5 at the Southern Site (SS), approximately 2, 6,and 7 at the Southern Estuarine Turbidity Maximum (SETM) and 2.1, 9.5, and 10.5 at the Northern Site (NS). The spring tide depths (meters below the surface) are 2.0, 7.9, and 8.9 at the SS, 3.0, 6.3, and 7.3 at the SETM, and 3.0, 7.7, and 8.7 at the NS. The shaded contours depict typical salinity profiles in the estuary during neap and spring tides (74). During neap tide, the estuary is vertically stratified with the denser salty water (dark contours) on the bottom and the fresher (less-dense) water (lighter contours) on the surface. During the spring tide, the estuary becomes more vertically well-mixed, and an along estuary salinity gradient is more visible with the saltier waters (darker contours) are at the mouth of the river near the Battery and the fresher water (lighter contour) upstream.

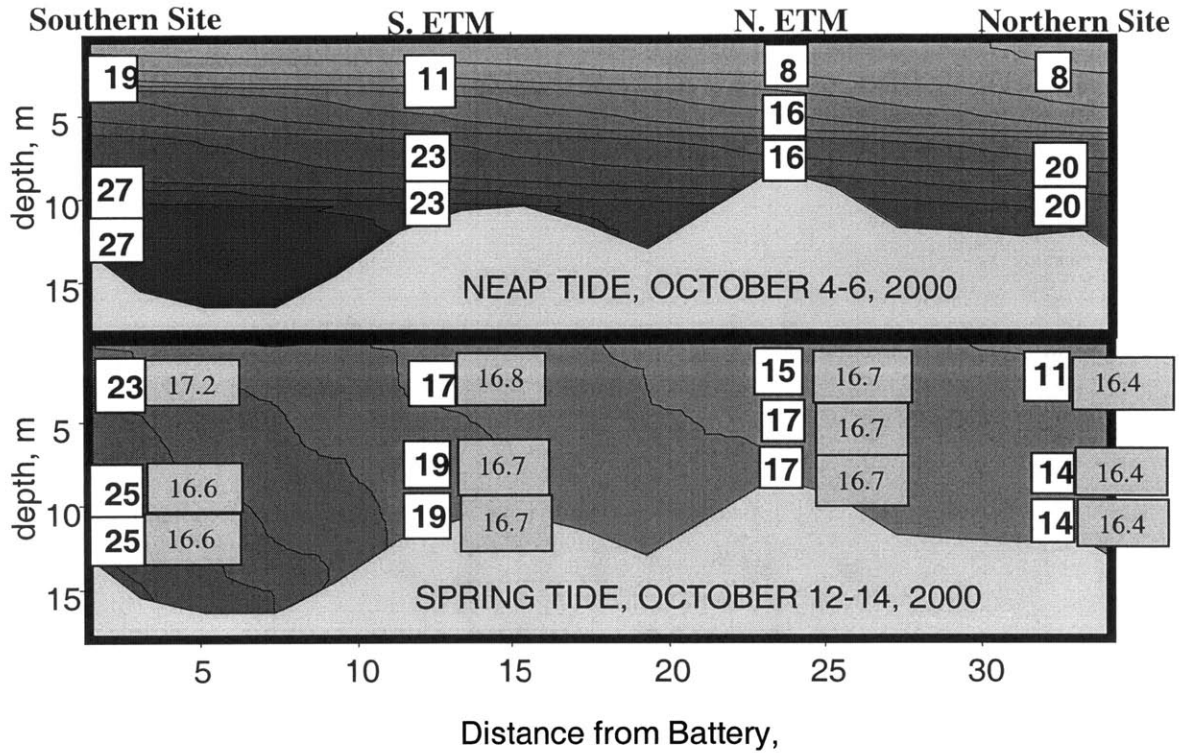

Figure 4.3. Average salinity (practical salinity units; bold numbers in white squares) and temperature (°C; regular font in shaded rectangles) in the lower Hudson Estuary during neap tide (October 4-6, 2000) and spring tide (October 12-14, 2000). The neap tide depths (meters below the surface) are 2, 13, and 14 at the Southern Site (SS), 2, 7,and 8 at the Southern Estuarine Turbidity Maximum (SETM), 2, 4, and 5 at the Northern Estuarine Turbidity Maxiumum (NETM), and 2, 5, and 6 at the Northern Site (NS). The spring tide depths (meters below the surface) are 2, 12.7, and 14 at the SS, 1.9, 6.9, and 7.9 at the SETM, 2.0, 3.7, and 4.8 at the NETM, and 2.0, 5.1, and 6.3 at the NS. The contours depict representative salinity gradients during the neap and spring tides in the estuary with darker shades representing saltier water and lighter shades depicting fresher water (74).

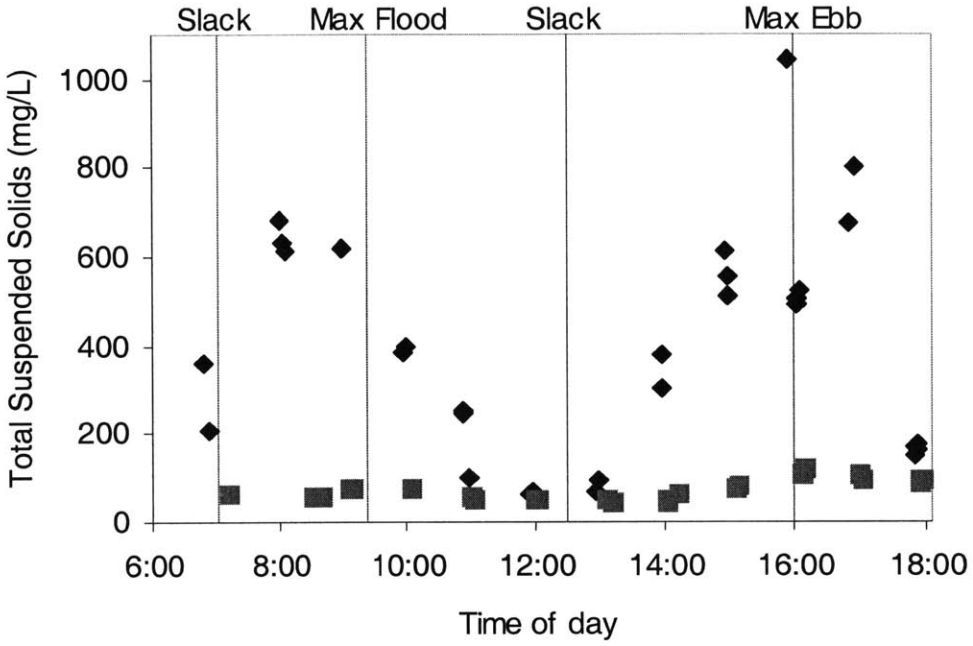

Figure 4.4. Total suspended solids (TSS) as a function of time at the SETM on 10/13/00 measured with the Hydrolab over the course of one tidal cycle. The TSS measured at between 6.5 and 8 m depth (diamonds) averaged 390 mg/L over the tidal cycle, while the TSS measured at approximately 2 m depth (squares) averaged 71 mg/L. The slack tide, maximum flood, and maximum ebb times are for the George Washington Bridge which is approximately 4 km upriver and were predicted with Xtide, a tide-prediction program.

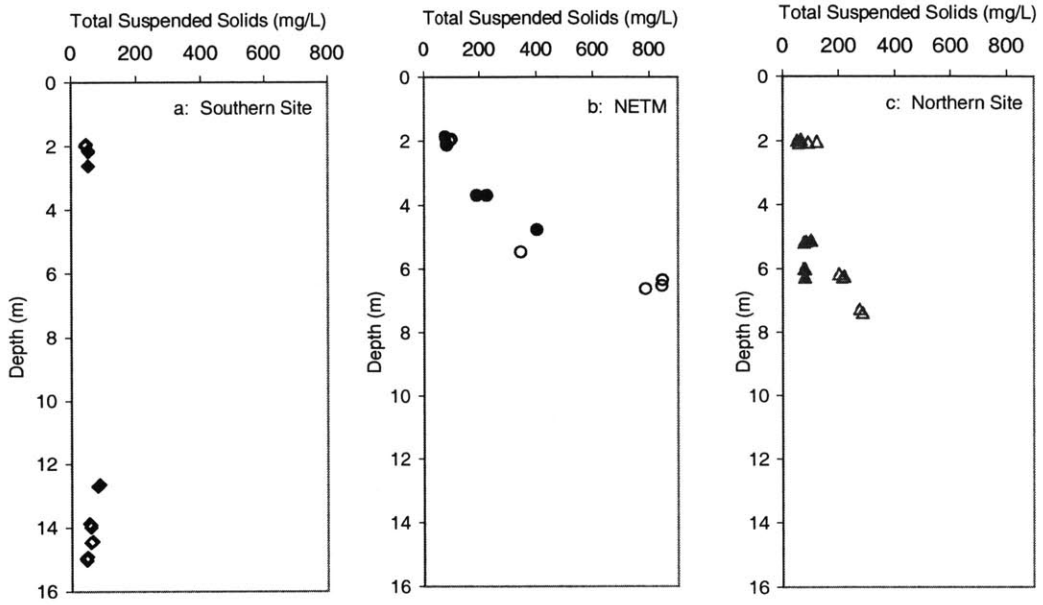

Figure 4.5. Total suspended solids concentrations at the Southern Site (SS; a), the Northern Estuarine Maximum (NETM; b), and the Northern Site (NS; c) as a function of depth. The TSS concentrations at the SS were measured during slack tide on 10/12/00 between 18:11 and 18:38 (solid diamond) and during slack tide on 10/14/00 between 13:54 and 14:22 (open diamonds). TSS was measured at the NETM during ebb tide on 10/12/00 between 14:41 and 15:07 (closed circles) and during flood tide on 10/14/00 between 10:55 and 11:13 (open circles). The TSS measurements at the NS were collected during slack tide on 10/12/00 between 12:48 and 13:22 (solid triangles) and during flood tide on 10/14/00 between 9:15 and 9:28 (open triangles).

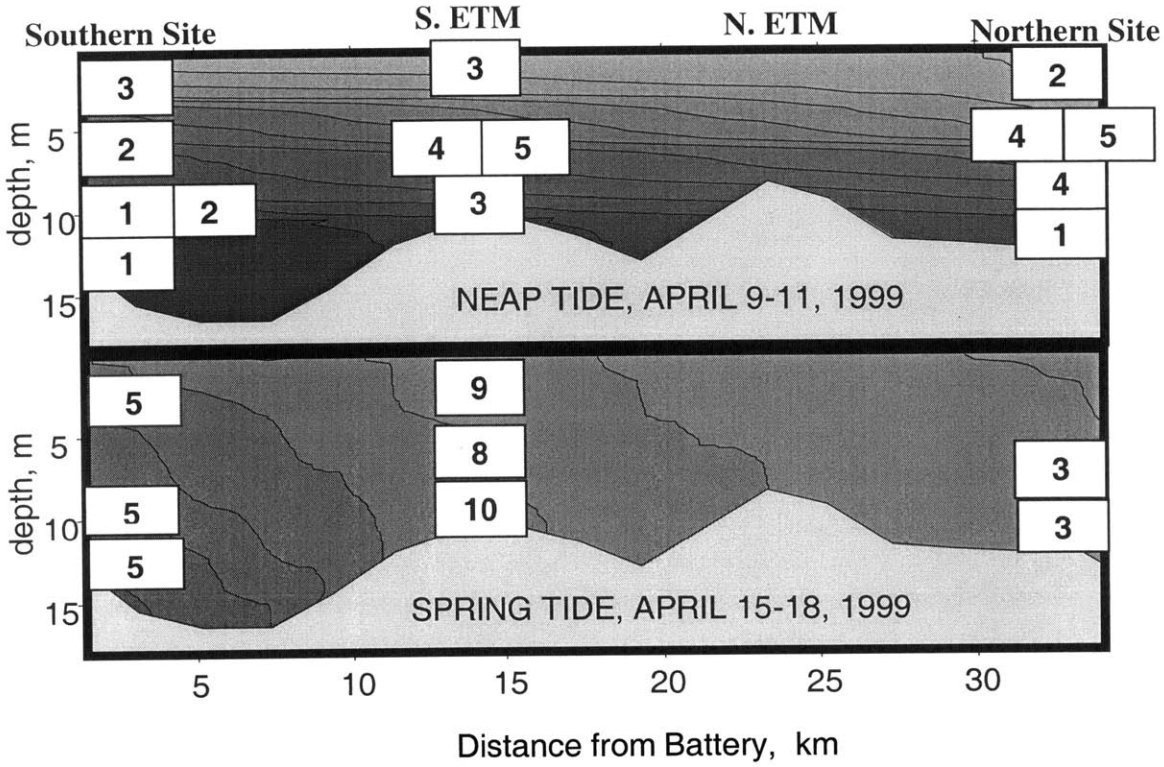

Figure 4.6. PED-measured dissolved pyrene concentration (ng/L) in the lower Hudson Estuary during neap tide (April 9-11, 1999) and spring tide (April 15-18, 1999). The neap tide depths (meters from the river bottom) are 9, 5.5, 2, and 1 at the Southern Site (SS), 6.7, 2, and 1 at the Southern Estuarine Turbidity Maximum (SETM), and 8.5, 5.5, 2, and 1at the Northern Site (NS). The spring tide depths (meters from the river bottom) are 10, 3.5, and 1.5 at the SS, 8, 3.5, and 1.5 at the SETM, and 3 and 1 at the NS. Contours depict representative salinity gradients within the estuary during neap and spring tides with darker contours representing more saline water and the lighter contours depicting fresher water (74).

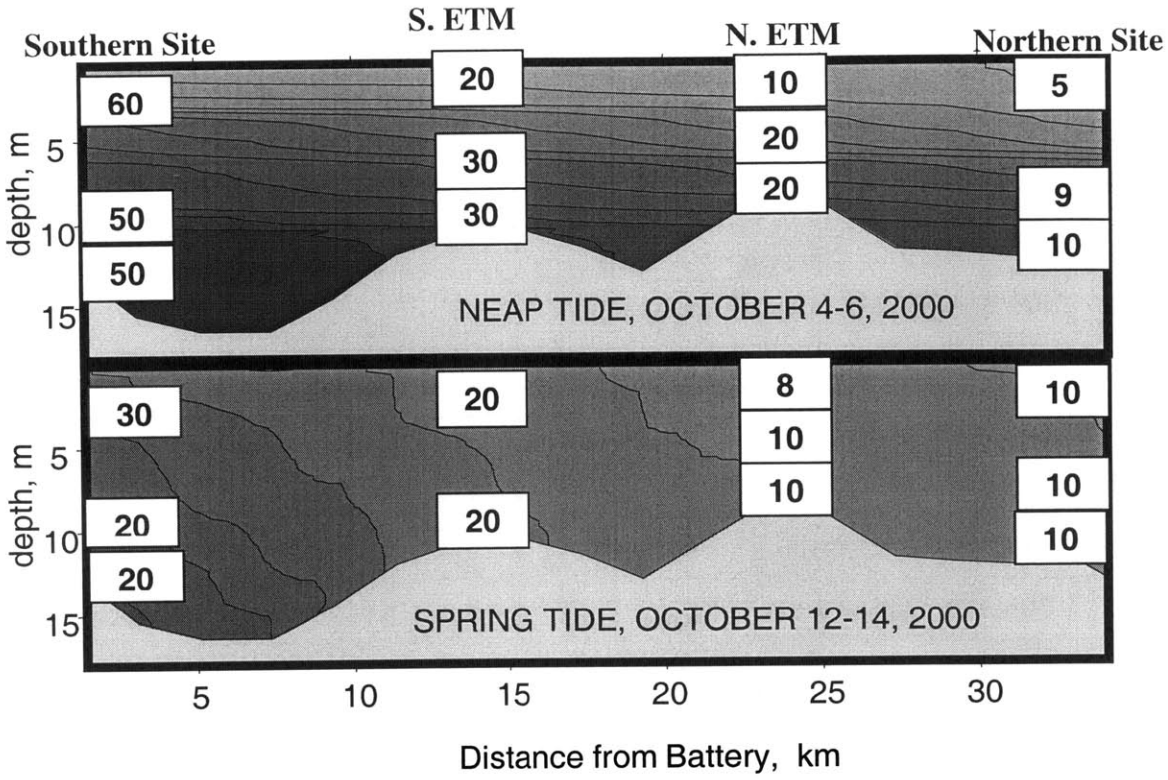

Figure 4.7. PED-measured dissolved pyrene concentration (ng/L) in the lower Hudson Estuary during neap tide (October 4-6, 2000) and spring tide (October 12-14, 2000). The upper-most PEDs are 2 m below the surface, and the deeper PEDs are 2 and 1 m from the river bottom. Unfortunately, the spring PED 2 m from the bottom at the Southern Estuarine Turbidity Maximum was contaminated. Contours depict representative salinity gradients within the estuary during neap and spring tides with darker contours representing more saline water and the lighter contours depicting fresher water (74).

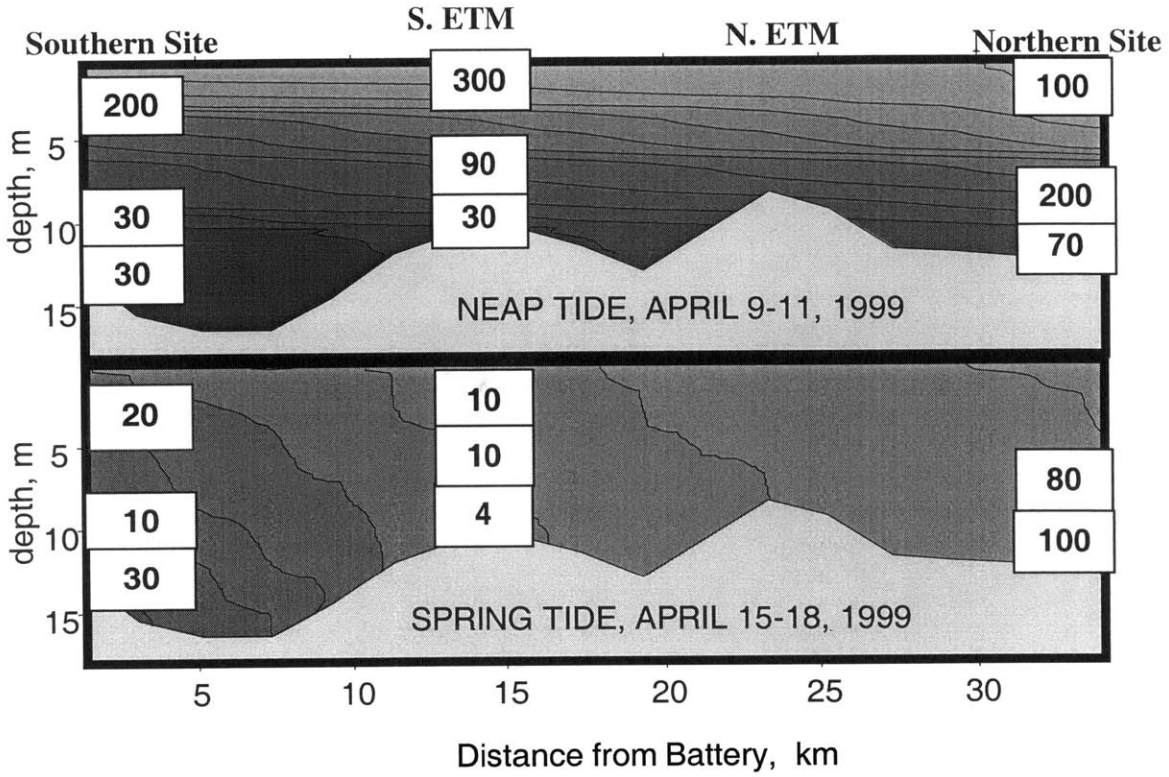

Figure 4.8. PED-measured dissolved PCB #52 concentration (pg/L) in the lower Hudson Estuary during neap tide (April 9-11, 1999) and spring tide (April 15-18, 1999). The neap tide depths (meters from the river bottom) are 9, 3, and 1 at the Southern Site (SS), 6.7, 3, and 1 at the Southern Estuarine Turbidity Maximum (SETM), and 8.5, 3, and 1at the Northern Site (NS). The spring tide depths (meters from the river bottom) are 10, 3.5, and 1.5 at the SS, 8, 3.5, and 1.5 at the SETM, and 3 and 1 at the NS. Contours depict representative salinity gradients within the estuary during neap and spring tides with darker contours representing more saline water and the lighter contours depicting fresher water (74).

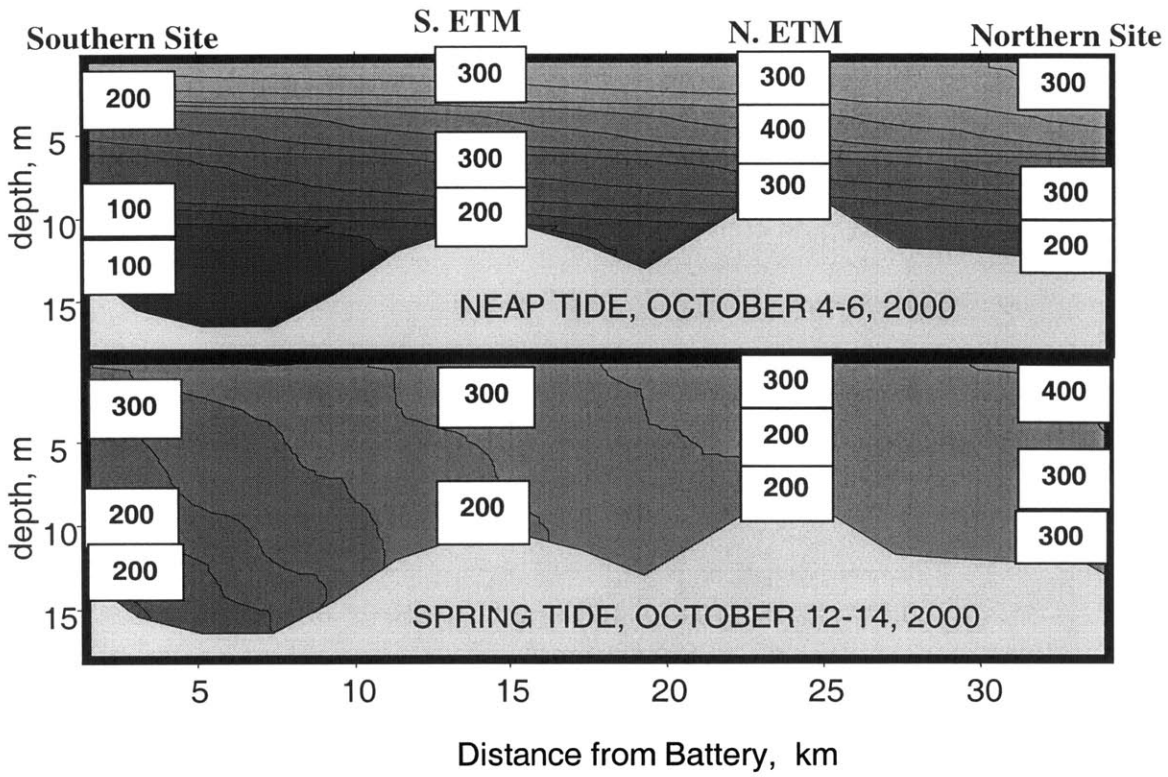

Figure 4.9. PED-measured dissolved PCB #52 (pg/L) in the lower Hudson Estuary during neap tide (October 4-6, 2000) and spring tide (October 12-14, 2000). The upper-most PEDs are 2 m below the surface, and the deeper PEDs are 2 and 1 m from the river bottom. Unfortunately, the spring PED 2 m from the bottom at the Southern Estuarine Turbidity Maximum was contaminated. Contours depict representative salinity gradients within the estuary during neap and spring tides with darker contours representing more saline water and the lighter contours depicting fresher water (74).

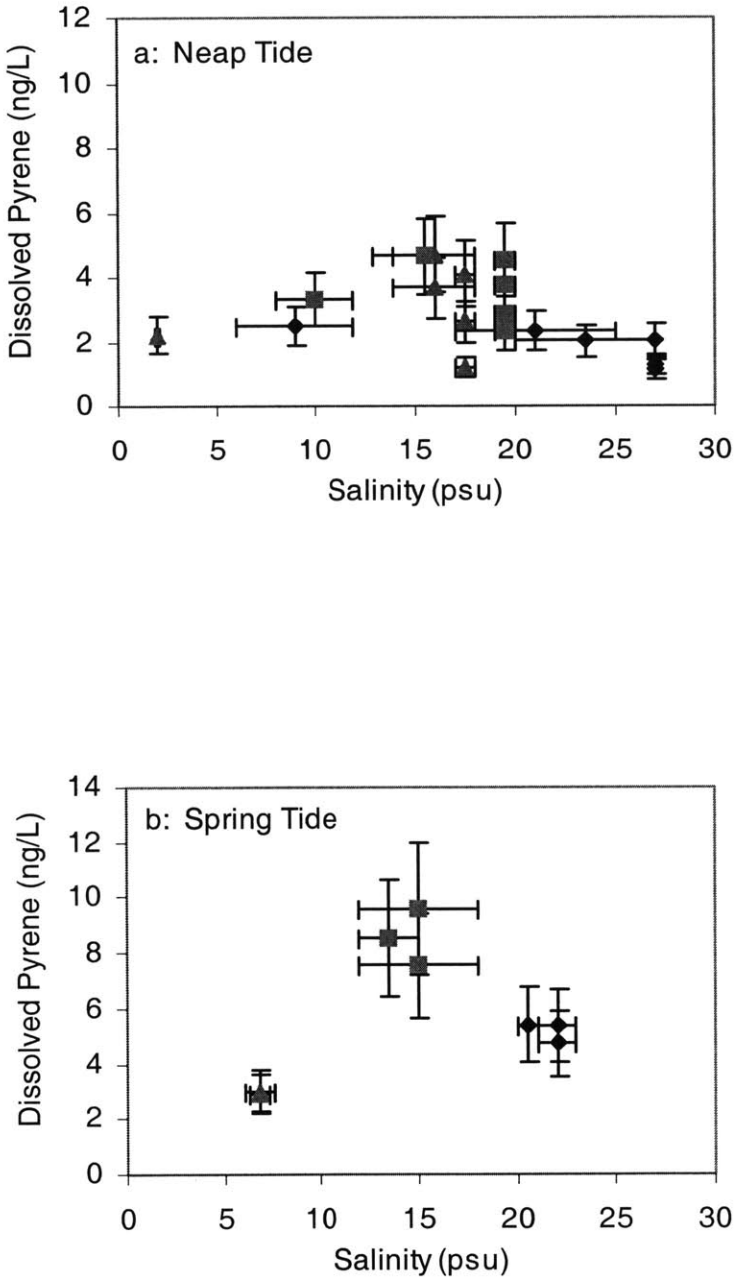

Figure 4.10. Dissolved pyrene concentration (ng/L) as a function of salinity (psu) measured at the Northern Site (triangle), the S. ETM (square), and the Southern Site (diamond) during neap tide (a) and spring tide (b) during the April 1999 sampling campaign. "Error" bars in the x-direction depict the salinity range observed at this location. Error bars in the y-direction represent a 25% measurement error.

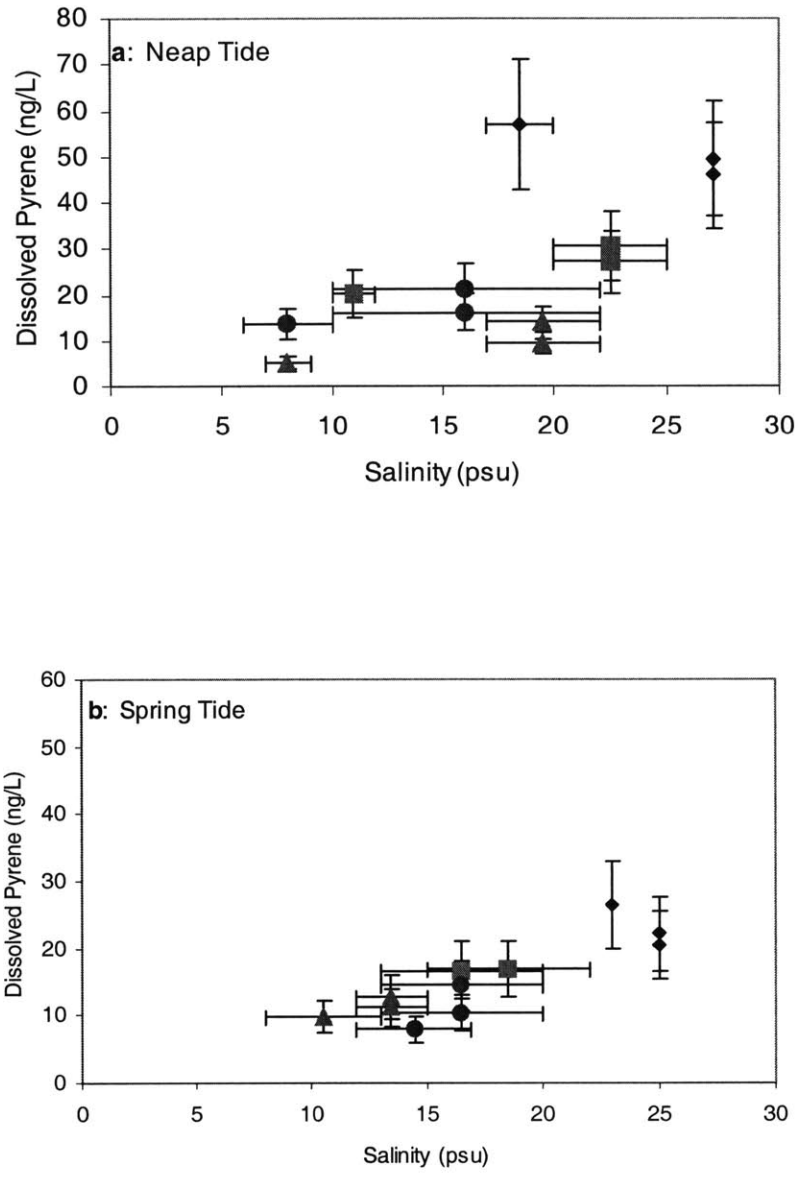

Figure 4.11. Dissolved pyrene concentration (ng/L) as a function of salinity (psu) measured at the Northern Site (triangle), the N. ETM (circle), the S. ETM (square), and the Southern Site (diamond) during neap tide (a) and spring tide (b) during the October 2000 sampling campaign. "Error" bars in the x-direction depict the salinity range observed at this location. Error bars in the y-direction represent a 25% measurement error.

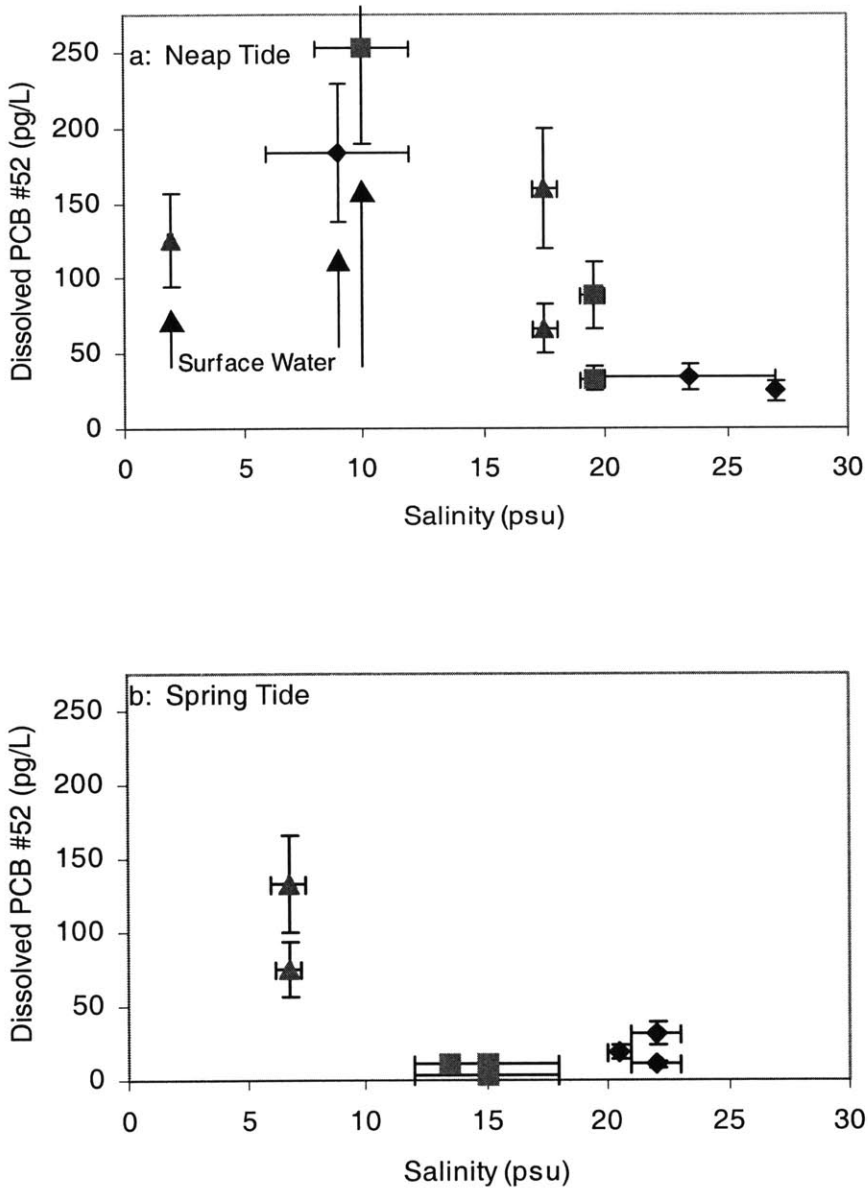

Figure 4.12. Dissolved PCB #52 concentration (ng/L) as a function of salinity (psu) measured at the Northern Site (triangle), the S. ETM (square), and the Southern Site (diamond) during neap tide (a) and spring tide (b) during the April 1999 sampling campaign. "Error" bars in the x-direction depict the salinity range observed at this location. Error bars in the y-direction represent a 25% measurement error.

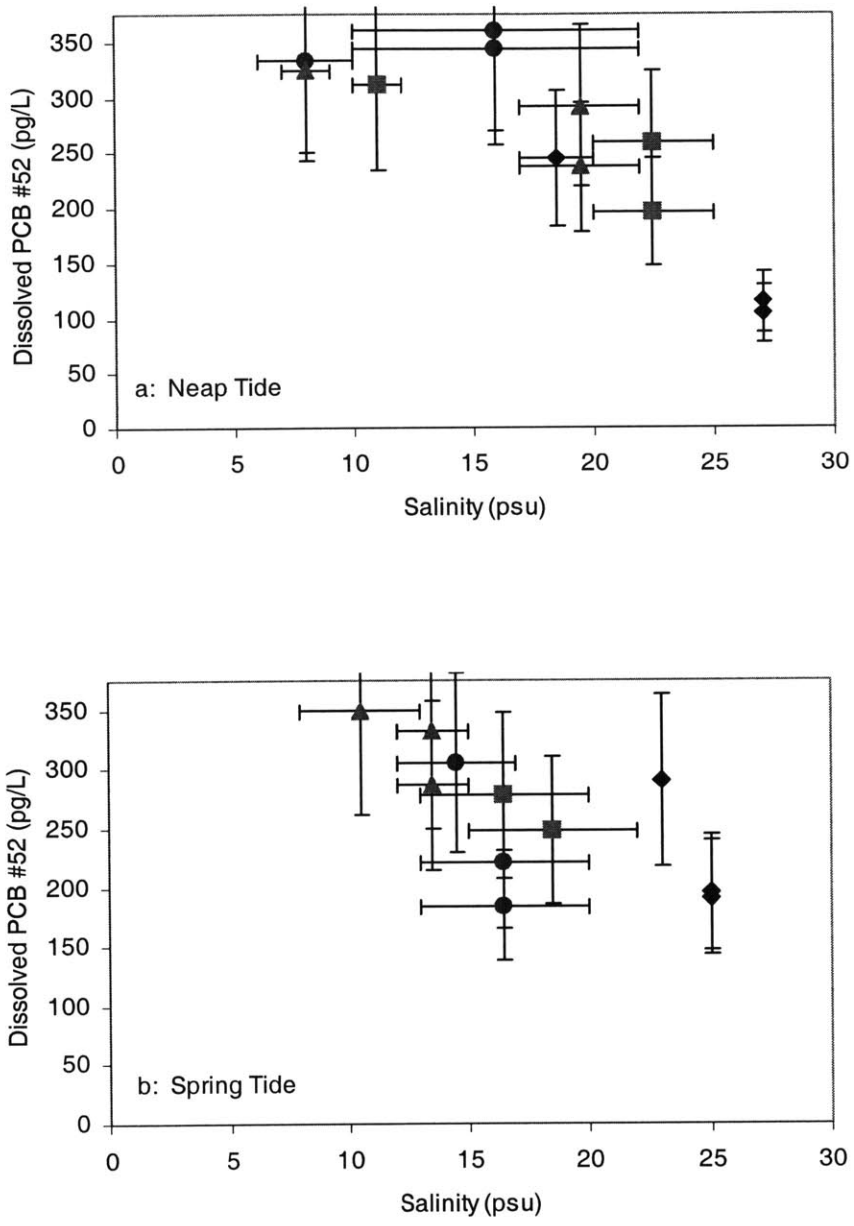

Figure 4.13. Dissolved PCB #52 concentration (ng/L) as a function of salinity (psu) measured at the Northern Site (triangle), the N. ETM (circle), the S. ETM (square), and the Southern Site (diamond) during neap tide (a) and spring tide (b) during the October 2000 sampling campaign. "Error" bars in the x-direction depict the salinity range observed at this location. Error bars in the y-direction represent a 25% measurement error.

CHAPTER 5: CONCLUSIONS AND AREAS OF FUTURE WORK

CONCLUSIONS

The overall goal of this thesis was to assess the importance of sediment resuspension to the input of PAHs and PCBs to the lower Hudson Estuary. In order to accomplish this, three areas of work were pursued: 1) a passive sampler for the measurement of "truly dissolved" HOCs was developed; 2) the desorption kinetics of pyrene from native Hudson River sediments was measured and modeled with a physically-based desorption model (23,24); and 3) the inputs of pyrene and PCB #52 into the lower Hudson Estuary were examined with respect to sediment resuspension, and the resultant inputs were quantified.

Initial experiments indicate that PEDs are useful devices for the measurement of dissolved HOCs in the water column. Polyethylene is readily available in varying thicknesses and is inexpensive. K_{PEW}s can be estimated with K_{OW}s and adjusted for temperature and salinity. Diffusivities can be used to estimate the time for equilibrium. PEDs can be impregnated with internal standards so that the rate of desorption within the surrounding environment can be measured and used to correct for the uptake rate of the chemicals of interest.

As PEDs require days (depending on the chemical and temperature) to reach equilibrium with the surrounding water, they allow for a time-averaged measurement. This is useful for determining the level of pollutant exposure for organisms living in the sampled environment. Using different PED thicknesses will allow for the measurement of varying lengths of time. For example, decreasing the PED thickness from 80 to 40 μm cuts the uptake time by 75%.

The physically- and chemically-based model for effective diffusivity put forth by Wu and Gschwend (23,24) appears to be appropriate for estimating the desorption kinetics of pyrene in native sediments. Despite the fact that between 66 and 98% of the pyrene is believed to have been desorbing from black carbon, the retarded radial diffusion model allowed for the estimation of an effective diffusivity that fit experimental results. An improved understanding of the pyrene desorption rates in native sediments is important for predicting pyrene inputs resulting from the disequilibrium observed between the pyrene fractions in the sediments and overlying water column.

In April 1999 the sediments within the lower Hudson Estuary provided for the input of pyrene into the overlying waters. However, the sediments and water appear to have been more closely equilibrated during October 2000 suggesting that the sediments may have provided for a significantly smaller source of pyrene to the waters of the Hudson. With respect to PCB #52, mixing diagrams indicate that resuspended sediments may have provided a sink for dissolved PCB #52 in April 1999; however, the limited sediment samples collected for this study indicate that the sediment served as a source in April 1999. One explanation for this observation may be the scavenging of PCB #52 by cleaner sediments within the estuary. October 2000 PCB #52 findings indicate that, as with pyrene, the sediments and waters of the lower Hudson are more closely equilibrated with respect to PCB #52.

Estimates of the magnitudes of the sources and sinks of pyrene and PCB #52 to the lower Hudson Estuary indicate that in April 1999, the largest sources of these chemicals was due to sediment diffusive and resuspension input, which are of comparable magnitudes. The April to October decrease in driving force observations

may be explained by the removal of sediment during the spring freshet coupled to the exposure of older underlying sediments that did not have sufficient time to equilibrate with the overlying water column at the time of sampling. Sediment redeposited in June of 1999 had ample time in which to equilibrate with the overlying waters explaining the more closely equilibrated system observed in October 2000. This observation suggests that there may be a seasonal trend in HOC inputs from underlying sediments. The dynamic changes in this estuarine system make the modeling the fate of HOCs within it a challenge.

FUTURE WORK

As is often the case, the findings from this research have brought to light many areas where an improved understanding and, consequently, future work is needed. The following is a list of future work that should be pursued to further our understanding within each of the areas of study pursued here.

PEDs

- Further experiments are needed to explain the causes for increasing D_{PE} with time. The plasticizer theory could be further tested by measuring the pyrene sorption into a PED, and repeating the experiment with the same pyrene-sorbed PED. If the pyrene is acting as a plasticizer, one would expect to see less of an increase in uptake rate as the "plasticizer" concentration increases.

- The lower-than-literature D_{PE}'s measured in this study need to be further investigated. An additional method for D_{PE} measurement may remove sampling artifacts that are resulting in the lower-than-literature values.

- Further research is needed to verify that PEDs can be consistently impregnated with internal standards so that the rate of desorption within the surrounding environment can be measured and used to correct for the uptake rate of the chemicals of interest.

Desorption Kinetics

- The pyrene desorption experiment should be repeated with greater sampling points during the first 2 hr of the experiment, allowing for a more accurate measurement for the rate of pyrene desorption.
- Further pyrene desorption experiments should be performed with varying solid-to-water ratios to verify and/or illustrate the importance of this parameter to desorption rates.
- Desorption experiments for PCB #52 should be completed on native Hudson River sediments in order measure a desorption rate constant for this chemical as well as assess the validity of Wu and Gschwend (23,24) with respect to PCB's sorbed to native sediments.

Hudson Sediment-Water Exchange

- Further modeling that accounts for the multi-dimensional nature of this system is needed in order to assess the fate of PAHs and PCBs within the lower Hudson Estuary. The model used here accounts for vertical variations on a limited scale, and does little to account for across river variability.
- A more representative model that accounts for the cyclic nature of sediment resuspension is needed to more accurately predict the input of HOCs due to sediment resuspension. A series of step functions (over a particular time window, e.g., a residence

time) representing the on-off nature of the tidal influence on resuspension events may be a good first step.

LITERATURE CITED

(1) Karickhoff, S. W.; Brown, D. S.; Scott, T. A. 1979. Sorption of hydrophobic pollutants on natural sediments. *Water Res.*, *13*, 241-248.

(2) Chen, H.-W. *Fluxes of Organic Pollutants from Sediments in Boston Harbor*; Massachusetts Institute of Technology: Cambridge, MA, 1993, pp 145.

(3) Achman, D. R.; Brownawell, B. J.; Zhang, L. 1996. Exchange of polychlorinated biphenyls between sediment and water in the Hudson River Estuary. *Estuaries*, *19*, 950-965.

(4) Flores, A. E. *Assessing the Fate of PAHs in the Boston Inner Harbor Using Semipermeable Membrane Devices (SPMDs)*; Massachusetts Institute of Technology: Cambridge, MA, 1998, pp 121.

(5) Petroni, R. N.; Israelsson, P. H. *Mass Balance of 3D Model of PAHs in Boston's Innner Harbor*; Massachusetts Institute of Technology: Cambridge, MA, 1998, pp 224.

(6) Mitra, S.; Dellapenna, T. M.; Dickhut, R. M. 1999. Polycyclic aromatic hydrocarbon distribution within lower Hudson River estuarine sediments: physical mixing vs. sediment geochemistry. *Estuar Coast Shelf S*, *49*, 311-326.

(7) Hirschberg, D.; Bokuniewicz, H. J. "Measurements of water temperature, salinity and suspended sediment concentrations along the axis of the Hudson River estuary 1980-1981," Marine Sciences Research Center, State University of New York, Stony Brook, 1981.

(8) Geyer, W. R. "Final Report: Particle Trapping in the Lower Hudson Estuary," Hudson River Foundation, 1995.

(9) Woodruff, J. D.; Geyer, W. R.; Sommerfield, C. K.; Driscoll, N. W. 2001. Seasonal variation of sediment deposition on the Hudson River Estuary. *Marine Geology*, *179*, 105-119.

(10) Adams, R. G. *Sediment-Water Exchange of Polycyclic Aromatic Hydrocarbons in the Lower Hudson Estuary*; Massachusetts Institute of Technology: Cambridge, 2000, pp 112.

(11) U.S.EPA "Technical basis for deriving sediment quality criteria for nonionic organic contaminants for the protection of benthic organisms by using equilibrium partitioning," U.S. EPA Office of Water, 1993.

(12) U.S.EPA "EPA's contaminated sediment management strategy.," U.S. EPA Office of Water, 1998.

(13) N.O.A.A. "Sediment Toxicity in U.S. Coastal Waters," National Oceanic and Atmospheric Administration, Coastal Monitoring and Bioeffects Division, Office of Ocean Resources Conservation and Assessment, Coastal Ocean Program, 1998.

(14) Baker, J. E.; Eisenreich, S. J. 1989. PCBs and PAHs as tracers of particulate dynamics in large lakes. *J. Great Lakes Res.*, *15*, 84-103.

(15) Baker, J. E.; Eisenreich, S. J.; Eadie, B. J. 1991. Sediment trap fluxes and benthic recycling of organic carbon, polycyclic aromatic hydrocarbons, and polychlorinated biphenyl congeners in Lake Superior. *Environ. Sci. Technol.*, *25*, 500-509.

(16) Sanders, G.; Hamilton-Taylor, J.; Jones, K. C. 1996. PCB and PAH dynamics in a small rural lake. *Environ. Sci. Technol.*, *30*, 2958-2966.

(17) Zhou, J. L.; Fileman, T. W.; Evans, S.; Donkin, P.; Fauzi, R.; Mantoura, C.; Rowland, S. J. 1996. Seasonal distribution of dissolved pesticides and polynuclear aromatic hydrocarbons in the Humber Estuary in Humber coastal zone. *Mar. Pollut. Bull.*, *32*, 599-608.

(18) Fernandes, M. B.; Sicre, M.-A.; Boireau, A.; Tronczynski, J. 1997. Polyaromatic hydrocarbon (PAH) distribution in the Seine River and its estuary. *Mar. Pollut. Bull.*, *11*, 857-867.

(19) Zhou, J. L.; Fileman, T. W.; Evans, S.; Donkin, P.; Readman, J. W.; Mantoura, R. F. C.; Rowland, S. 1999. The partition of fluoranthene and pyrene between suspended particles and dissolved phase in the Humber Estuary: a study of the controlling factors. *Sci. Total Environ.*, *243/244*, 305-321.

(20) Jeremiason, J. D.; Eisenreich, S. J.; Baker, J. E.; Eadie, B. J. 1998. PCB Decline in settling particles and benthic recycling of PCBs and PAHs in Lake Superior. *Environ. Sci. Technol.*, *32*, 3249-3256.

(21) Capel, P. D.; Eisenreich, S. J. 1985. PCBs in Lake Superior, 1978-1980. *J. Great Lakes Res.*, *11*, 447-461.

(22) Maskaoui, K.; Zhou, J. L.; Hong, H. S.; Zhang, Z. L. 2002. Contamination by polycyclic aromatic hydrocarbons in the Jiulong River Estuary and Western Xiamen Sea, China. *Environ. Pollut.*, *118*, 109-122.

(23) Wu, S.-C.; Gschwend, P. M. 1986. Sorption kinetics of hydrophobic organic compounds to natural sediments and soils. *Environ. Sci. Technol.*, *20*, 717-725.

(24) Wu, S.-C.; Gschwend, P. M. 1988. Numerical modeling of sorption kinetics of organic compounds to soil and sediment particles. *Water Resour. Res.*, *8*, 1373-1383.

(25) Farrington, J. W.; Goldberg, E. D.; Risebrough, R. W.; Martin, J. H.; Bowen, V. T. 1983. U.S. "Mussel Watch" 1976-1978: An overview of the trace-metal, DDE, PCB, hydrocarbons, and artificial radionuclide data. *Environ. Sci. Technol.*, *17*, 490-496.

(26) Huckins, J. N.; Tubergen, M. W.; Manuweera, G. K. 1990. Semipermeable membrane devices containing model lipid: A new approach to monitoring the bioavailability of lipophilic contaminants and estimating their bioconcentration potential. *Chemosphere*, *20*, 533-552.

(27) Arthur, C. L.; Pawliszyn, J. 1990. Solid phase microextraction with thermal desorption using fused silica optical fibers. *Anal. Chem.*, *62*, 2145-2148.

(28) Gale, R. W.; Huckins, J. N.; Petty, J. D.; Peterman, P. H.; Schwartz, T. R.; Tillitt, D. E. 1997. Comparison of the uptake of dioxin-like compounds by caged channel catfish and semipermeable membrane devices in the Saginaw River, Michigan. *Environ. Sci. Technol.*, *31*, 178-187.

(29) Huckins, J. N.; Manuweera, G. K.; Petty, J. D.; Mackay, D.; Lebo, J. A. 1993. Lipid-containing semipermeable membrane devices for monitoring organic contaminants in water. *Environ. Sci. Technol.*, *27*, 2488-2496.

(30) Gale, R. W. 1998. Three-compartment model for contaminant accumulation by semipermeable membrane devices. *Environ. Sci. Technol.*, *32*, 2292-2300.

(31) Vrana, B.; Schüürmann, G. 2002. Calibrating the uptake kinetics of semipermeable membrane devices in water: Impact of hydrodynamics. *Environ. Sci. Technol.*, *36*, 290-296.

(32) Petty, J. D.; Orazio, C. E.; Huckins, J. N.; Gale, R. W.; Lebo, J. A.; Meadows, J. C.; Echols, K.; Cranor, W. L. 2000. Considerations involved with the use of semipermeable membrane devices for monitoring environmental contaminants. *J. Chromatogr. A.*, *879*, 83-94.

(33) Huckins, J. N.; Petty, J. D.; Lebo, J. A.; Almeida, F. V.; Booij, K.; Alvarez, D. A.; Cranor, W. L.; Clark, R. C.; Mogensen, B. B. 2002. Development of permeability/performance reference compound approach for in situ calibration of semipermeable membrane devices. *Environ. Sci. Technol.*, *36*, 85-91.

(34) Potter, D. W.; Pawliszyn, J. 1994. Rapid determination of polycyclic aromatic hydrocarbons and polychlorinated biphenyls in water using solid-phase microextraction and GC/MS. *Environ. Sci. Technol.*, *28*, 298-305.

(35) de Fatima Alpendurada, M. 2000. Solid-phase microextraction: a promising technique for sample preparation in environmental analysis. *J. Chromatogr. A*, *889*, 3-14.

(36) Crank, J. *The Mathematics of Diffusion*; Oxford University Press: London, 1975.

(37) Vo-Dinh, T. *Synchronous Excitation Spectroscopy*; Wehry, E. L., Ed.; Plenum Press: New York, 1981, pp 167-192.

(38) Hawker, D. W.; Connell, D. W. 1988. Octanol-water partition coefficients of polychlorinated biphenyl congeners. *Environ. Sci. Technol.*, *22*, 382-387.

(39) Sangster, J. 1989. Octanol-water partition coefficients of simple organic compounds. *J. Phys. Chem. Ref. Data.*, *18*, 1111-1229.

(40) Mackay, D.; Shiu, W.-Y.; Ma, K.-C. *Illustrated Handbook of Physical-Chemical Properties and Environmental Fate of Organic Compounds*; Lewis Publishers: Boca Raton, 1992; Vol. 2.

(41) Hansch, C.; Leo, A.; Hoekman, D. *Exploring QSAR: Hydrophobic, Electronic, and Steric Constants*; American Chemical Society: Washington, DC, 1995; Vol. 2.

(42) Schwarzenbach, R. P.; Gschwend, P. M.; Imboden, D. M. *Environmental Organic Chemistry*; 1st ed.; John Wiley & Sons, Inc.: New York, 1993.

(43) Shiu, W.-Y.; Ma, K.-C. 2000. Temperature dependence of physical-chemical properties of selected chemicals of environmental interest. II. Chlorobenzenes, polychlorinated biphenyls, polychlorinated dibenzo-p-dioxins, and dibenzofurans. *J. Phys. Chem. Ref. Data*, *29*, 387-462.

(44) Flynn, J. H. 1982. A collection of kinetic data for the diffusion of organic compounds in polyolefins. *Polymer*, *23*, 1325-1344.

(45) Asfour, A.-F. A.; Saleem, M.; DeKee, D. 1989. Diffusion of saturated hydrocarbons in low density polyethylene (LDPE) films. *J. Appl. Polym. Sci.*, *38*, 1503-1514.

(46) Doong, S. J.; Ho, W. S. 1992. Diffusion of hydrocarbons in polyethylene. *Ind. Eng. Chem. Res.*, *31*, 1050-1060.

(47) Aminabhavi, T. M.; Naik, H. G. 1998. Chemical compatibility study of geomembranes--sorption/desorption, diffusion and swelling phenomena. *J. Hazard. Mater.*, *60*, 175-203.

(48) Šimko, P.; Šimon, P.; Khunová, V. 1999. Removal of polycyclic aromatic hydrocarbons from water by migration into polyethylene. *Food Chemistry*, *64*, 157-161.

(49) Barrer, R. M. *Diffusion and permeation in heterogeneous media*; Crank, J. and Park, G. S., Ed.; Academic Press: London, 1968, pp 165-217.
(50) Hayduk, W.; Laudie, H. 1974. Prediction of diffusion coefficients for non-electrolytes in dilute aqueous solutions. *AIChE J.*, *20*, 611-615.
(51) Rudnick, S. M. *In Situ Fluorescence Detection of Polycyclic Aromatic Hydrocarbons (PAH) in the Marine Environment*; University of Massachusetts: Boston, MA, 1998, pp 181.
(52) Gustafsson, Ö., personal communication.
(53) Karickhoff, S. W.; Morris, K. R. 1985. Impact of Tubificid Oligochaetes on Pollutants Transport in Bottom Sediments. *Environ. Sci. Technol.*, *19*, 51-56.
(54) Lamoureux, E.; Brownawell, B. J. 1999. Chemical and biological availability of sediment-sorbed hydrophobic organic contaminants. *Environ. Toxicol. Chem.*, *18*, 1733-1741.
(55) Gustafsson, Ö.; Gschwend, P. M.; Buesseler, K. O. 1997. Settling removal rate of PCBs into the Northwestern Atlantic derived from ^{238}U-^{234}Th Disequilibria. *Environ. Sci. Technol.*, *31*, 3544-3550.
(56) Schneider, A. R.; Eadie, B. J.; Baker, J. E. 2002. Episodic particle transport events controlling PAH and PCB cycling in Grand Traverse Bay, Lake Michigan. *Environ. Sci. Technol.*, *36*, 1181-1190.
(57) McGroddy, S. E.; Farrington, J. W.; Gschwend, P. M. 1996. Comparison of the in situ and desorption sediment-water partitioning of polycyclic aromatic hydrocarbons and polychlorinated biphenyls. *Environ. Sci. Technol*, *30*, 172-177.
(58) Gustafsson, Ö.; Haghseta, F.; Chan, C.; MacFarlane, J.; Gschwend, P. M. 1997. Quantification of the dilute sedimentary soot phase: implications for PAH speciation and bioavailability. *Environ. Sci. Technol.*, *31*, 203-209.
(59) Accardi-Dey, A.; Gschwend, P. M. 2002. Assessing the combined roles of natural organic matter and black carbon as sorbents in sediments. *Environ. Sci. Technol.*, *36*, 21-29.
(60) Carroll, K. M.; Harkness, M. R.; Bracco, A. A.; Balcarcel, R. R. 1994. Application of a permeant/polymer diffusion model to the desorption of polychlorinated biphenyls from Hudson River Sediments. *Environ. Sci. Technol*, *28*, 251-258.
(61) Pignatello, J. J.; Xing, B. 1996. Mechanisms of slow sorption of organic chemicals to natural particles. *Environ. Sci. Technol.*, *30*, 1-11.
(62) Brusseau, M. L.; Suresh, P.; Rao, C. 1991. Influence of sorbate sturcture of nonequilibrium sorption of organic compounds. *Environ. Sci. Technol.*, *25*, 1501-1508.
(63) Karickhoff, S. W.; Morris, K. R. 1985. Sorption dynamics of hydrophobic pollutants in sediment suspensions. *Environ. Toxicol. Chem.*, *4*, 469-479.
(64) Blake, G. R. *Particle Density*; Black, C. A., Ed.; American Society of Agronomy, Inc.: Madison, 1965; Vol. 1, pp 770.
(65) Rudnick, S. M.; Chen, R. F. 1998. Laser-induced fluorescence of pyrene and other polycyclic aromatic hydrocarbons (PAH) in seawater. *Talanta*, *47*, 907-919.
(66) Gauthier, T. D.; Shane, E. C.; Guerin, W. F.; Seitz, W. R.; Grant, C. L. 1986. Fluorescence quenching method for determining equilibrium constants for

polycyclic aromatic hydrocarbons binding to dissolved humic materials. *Environ. Sci. Technol.*, *20*, 1162-1166.

(67) Chin, Y.-P.; Gschwend, P. M. 1992. Partitioning of polycyclic aromatic hydrocarbons to marine porewater organic colloids. *Environ. Sci. Technol.*, *26*, 1621-1626.

(68) Peters, D. G.; Hayes, J. M.; Hieftje, G. M. *Chemical Separations and Measurements: Theory and Practice of Analytical Chemistry*; W.B. Saunders Co.: Philadelphia, 1974.

(69) Karickhoff, S. W. 1981. Semiempirical estimation of sorption of hydrophobic pollutants on natural sediments and soils. *Chemosphere*, *10*, 833-846.

(70) Gawlik, B. M.; Sotiriou, N.; Feicht, E. A.; Schulte-Hostede, S.; Kettrup, A. 1997. Alternatives for the determination of the soil adsorption coefficient, Koc, of non-ionic organic compounds - A Review. *Chemosphere*, *34*, 2525-2551.

(71) Bucheli, T. D.; Gustafsson, Ö. 2000. Quantification of the soot-water distribution coefficient of PAHs provides mechanistic basis for enhanced sorption observations. *Environ. Sci. Technol.*, *34*, 5144-5151.

(72) Lohmann, R.; MacFarlane, J. K.; Gschwend, P. M. in prep. On the importance of black carbon to sorption coefficients of native PAHs, PCBs, and PCDDs in contaminated sediments. .

(73) Ullman, W. J.; Aller, R. C. 1982. Diffusion coefficients in nearshore marine sediments. *Limnol. Oceanogr.*, *27*, 552-556.

(74) Geyer, W. R.; Gschwend, P. M.; Adams, R. G. *Sediment-water column exchange of toxic organic compounds*; Office of Naval Research: Arlington, VA, 1999.

(75) Wolfe, D. A., E.R. Long, G.B. Thursby. 1996. Sediment toxicity in the Hudson-Raritan Estuary: Distribution and correlations with chemical contamination. *Estuaries*, *19*, 901-912.

(76) Bopp, R. F.; Simpson, H. J.; Olsen, C. R.; Kostyk, N. 1981. Polychlorinated biphenyls in sediments of the tidal Hudson River, New York. *Environ. Sci. Technol.*, *15*, 210-216.

(77) Brown, M. P.; Werner, M. B.; Sloan, R. J.; Simpson, K. W. 1985. Polychlorinated biphenyls in the Hudson River. *Environ. Sci. Technol.*, *19*, 657-661.

(78) Peven, C. S.; Uhler, A. D.; Hillman, R. E.; Steinhauer, W. G. 1996. Concentrations of organic contaminants in *Mytilus edulis* from the Hudson-Raritan Estuary and Long Island Sound. *Sci. Tot. Environ.*, *179*, 135-147.

(79) N.O.A.A. *Geometric mean and high concentrations*, 2000.

(80) U.S.EPA "Hudson River PCB Superfund site (New York) Superfund Proposed Plan," , 2000.

(81) Geyer, W. R.; Woodruff, J. D.; Traykovski, P. 2001. Sediment transport and trapping in the Hudson River Estuary. *Estuaries*, *24*, 670-679.

(82) Abood, K. A. "Hudson River hydrodynamic and water quality characteristics: Prospectives on the New York Bight Symposium," , 1978.

(83) Cooper, J. C.; Cantelmo, F. R.; Newton, C. E. 1988. Overview of the Hudson River Estuary. *American Fisheries Society Mongraph*, *4*, 11-24.

(84) Bothner, M.; Gill, P.; Boothman, W.; Taylor, B.; Karl, H. "Chemical and textural characteristics of sediments at an EPA reference site for dredged material on the

continental slope SW of the Farallon Islands," U.S. Geological Survey, Woods Hole Field Center, 1997.

(85) Mitra, S.; Bianchi, T. S.; McKee, B. A.; Sutula, M. 2002. Black carbon from the Mississippi River: Quantities, sources , and potential implications for the global carbon cycle. *Environ. Sci. Technol.*, *36*, 2296-2302.

(86) Gigliotti, C. L.; Brunciak, P. A.; Dachs, J.; Glenn, T. R.; Nelson, E. D.; Totten, L. A.; Eisenreich, S. J. 2002. Air-water exchange of polycyclic aromatic hydrocarbons in the New York-New Jersey, USA, Harbor Estuary. *Environ. Toxicol. Chem.*, *21*, 235-244.

(87) Litten, S., New York State Department of Environmental Conservation.

(88) Totten, L. A.; Brunciak, P. A.; Gigliotti, C. L.; Dachs, J.; Glenn, T. R.; Nelson, E. D.; Eisenreich, S. J. 2001. Dynamic air-water exchange of polychlorinated biphenyls in the New York-New Jersey Harbor Estuary. *Environ. Sci. Technol.*, *35*, 3834-3840.

(89) Schulz, D. E.; Petrick, G.; Duinker, J. C. 1989. Complete characterization of polychlorinated biphenyl congeners in commercial Aroclor and Clophen mixtures by multidimensional gas chromatography-electron capture detection. *Environ. Sci. Technol.*, *23*, 852-859.

(90) Keane, D. P.; Bopp, R. F. "Chronologies of PAH Levels in Hudson Sediments," Hudson River Foundation, 1999.

(91) Long, E. R.; Wolfe, D. A.; Scott, K. J.; Thursby, G. B.; Tern, E. A.; Peven, C.; Schwartz, T. "Magnitude and Extent of Sediment Toxicity in the Hudson-Raritan Estuary," National Oceanic and Atmospheric Administration, 1995.

(92) U.S.G.S. *Hudson River freshwater discharge at New York, NY*; http://ny.usgs.gov/htdocs/dialer_plots/Hudson_R_at_NYC_Freshwater_Discharge.htm, 2001.

(93) U.S.G.S. *Daily Streamflow for New York; USGS 01358000 Hudson River at Green Island New York*; http://waterdata.usgs.gov/ny/nwis/discharge/?site_no=01358000, 2000; Vol. 2002.

(94) Jorgensen, B. B.; Marias, D. J. D. 1990. The diffusive boundary layer of sediments; Oxygen microgradients over a microbial mat. *Limnol. Oceanogr.*, *35*, 1343-1355.

(95) Geyer, W. R.; Trowbridge, J. H.; Bowen, M. M. 2000. The dynamics of a partially mixed estuary. *J. Phys. Oceanogr.*, *30*, 2035-2048.

APPENDIX A: MATLAB CODE FOR PROCESSING LASER-INDUCED FLUORESCENCE

CSMA SOFTWARE OUTPUT

Directions for processing fluorescence data

Create a "home" directory (e.g. RachelDesorp)
in the C:\matlab directory. Put all data and
matlab data (*.mat) and scripts (*.m) files
in this home directory.

Put all *.spe data files in the csma\ra\
directory.

Run "processdata" in matlab to generate figures
in postprocess\figs*.eps and peaks data in
postprocess\data\peaks.dat.

Run "plotmulti" in matlab to generate figures
with multiple spectra on a single plot.

```
% driver file for fluorescence data
%processdata.m

% Input the directory where the *.spe data files are
datadir1='ra'

% Number of first file in ra###*.spe sequence
firstnum=1054;

% Enter the first number in the ra###*.spe file sequence that
% is to be processed
firstfile=1054;

% Enter the last number in the ra###*.spe file sequence that
% is to be processed
lastfile=1164;

% This queries the filenames contained in the data directory
datadir2=['csma\' datadir1];
D=dir(datadir2);
[Ntot,m]=size(D);

% Check to see if DATA file exists in POSTPROCESS/DATA/
fid=fopen('POSTPROCESS\DATA\peaks.dat');
if fid < 0
   peaks=zeros(Ntot-2,4);
   save POSTPROCESS\DATA\peaks.dat peaks -ascii
else
   fclose(fid);
end
load ('POSTPROCESS/DATA/peaks.dat')

%if fid >0
%   dataflag=1;               % File already exists
%   fclose(fid) ;
%   load ('POSTPROCESS/DATA/peaks.dat')
%else
%   dataflag=0;               % File doesn't exist
%  peaks=zeros(Ntot-2,4);
%end

ii=firstfile-firstnum+1;
for fileindex = (firstfile+3-firstnum) : (lastfile+3-firstnum)

   filename=getfield(D(fileindex),'name');

   [pks]=plot13sub(datadir1,filename,ii);

   peaks(ii,:)=pks;

   ii=ii+1;
end

%save POSTPROCESS\DATA\peaks.mat peaks
%save POSTPROCESS\DATA\peaks.dat peaks -ascii
```

```
size(peaks)

fid=fopen('POSTPROCESS\DATA\peaks.dat','w');
for i=1:Ntot-2
   %  fprintf(fid,'%6i %6i %6.1f %15.6e \n', peaks(i,:));
   fprintf(fid,'%7i %6i %6.1f %15.6e \n', peaks(i,:));

end
fclose(fid);
```

```
function [pks]=plot13sub(dirc, filnm, ii)

%plot13.m
% This code was modified by Steve Margulis to make
% it a subroutine as part of a postprocessing program

% plot1 script for spectrometry
% plots single curve of exact filename - 300 grating
% requires center wavelength and title

% NOTE: This program changed by Steve Margulis so that
% all files (csma, temp, etc.) can be put in a single
% "home" directory and run from there.  All calls below are
% now referenced to this home directory.  However because the
% mvarget.exe program is hardwired to create the varpas.dat
% file in C:\matlab\temp directory a 'temp' directory must
% be created within the matlab directory before running.
% An additional line is added to copy the varpas.dat file
% to the proper working directory.

load mcorfact;
load ffs1;
%dirc = input ('Directory: ', 's');
%filnm = input ('File Name? XXXNNN:  ','s');
%%filepas = ['\csma\',dirc];  %Original line

filepas = ['csma\',dirc];
filepas = [filepas, '\'];
filepas = [filepas, filnm];
%filepas = [filepas,'.spe'];
combuf = ['temp\mvarget.exe ', filepas];
dos (combuf);
% added by S.M.
%!copy C:\matlab\temp\varpas.dat temp\varpas.dat
dos ('copy C:\matlab\temp\varpas.dat temp\varpas.dat');
%!del C:\matlab\temp\varpas.dat
dos ('del C:\matlab\temp\varpas.dat');

load temp\varpas.dat;
yvals = varpas;
yvals = yvals.*mgcorr3;
yvals = filtfilt(b7,a7,yvals);
dos ('del temp\varpas.dat');
xval = mxgen3(450);
```

```
% Compute wavelength and intensity of peak/s
%[ymax1,imax]=max(yvals);
%xmax1=xval(imax);

%[ymax1,imax]=max(yvals(135:185))
%xmax1=xval(imax+134)

%plot (xval, yvals,'.')
%XLABEL ('Wavelength (nm)')
%YLABEL ('Response')
%TITLE (filnm)
%text(xmax1+10,ymax1,['Peak: x= ' num2str(xmax1) '; y= '
num2str(ymax1)])
%grid;

[mm,nn]=size(filnm);
%if nn == 9
if nn == 10
   %file=filnm(1:5);
   file=filnm(1:6);
   ext=0;
   [ymax1,imax]=max(yvals);
   xmax1=xval(imax);

else
   %file=filnm(1:6);
   file=filnm(1:7);
   ext=1;
   [ymax1,imax]=max(yvals(135:185));
   xmax1=xval(imax+134);

end


plot (xval, yvals)
XLABEL ('Wavelength (nm)')
YLABEL ('Response')
TITLE (filnm)
text(xmax1+10,ymax1,['Peak: x= ' num2str(xmax1) '; y= '
num2str(ymax1)])
grid;


%filenum=str2num(filnm(3:5));
filenum=str2num(filnm(3:6));

eval(['print -depsc POSTPROCESS\FIGS\' file '.eps'])

pks=[filenum ext xmax1 ymax1];

%save POSTPROCESS\DATA\peaks.mat peaks
%save POSTPROCESS\DATA\peaks.dat peaks -ascii
```

```
%mxgen3.m
function y = xgen3(ctr)
% generates x-axis for plots based on center wavelength - 300 grating
y = ctr - 107.56:.3136:ctr + 107.58;
```

```
%plotmulti

clear all
% Input the directory where the *.spe data files are
datadir1='ra'

% Number of first file in ra###*.spe sequence
firstnum=100;

% Rachel: type the numbers of the files you want
%        to run here. Separate entries by a semi-colon.
files=[158; 183; 234; 261; 288; 345; 374];

Nfiles=length(files);
filestr=num2str(files);

% This queries the filenames contained in the data directory
datadir2=['csma\' datadir1];
D=dir(datadir2);
[Ntot,m]=size(D);

figure(1)
clf
hold on

S=['b' 'm' 'g' 'k' 'c' 'r' 'y'];

for i=1:Nfiles

   fileindex = files(i)+3-firstnum;

   filename=getfield(D(fileindex),'name')

   [yvals,xval]=plotsub(datadir1,filename);

   plot (xval, yvals,S(i))

end

XLABEL ('Wavelength (nm)')
YLABEL ('Response')
grid;
legend(filestr);
```

```
function [yvals,xval]=plotsub(dirc, filnm)

%plotsub.m
% This code was modified by Steve Margulis to make
% it a subroutine as part of a postprocessing program

% plot1 script for spectrometry
% plots single curve of exact filename - 300 grating
% requires center wavelength and title

% NOTE: This program changed by Steve Margulis so that
% all files (csma, temp, etc.) can be put in a single
% "home" directory and run from there.  All calls below are
% now referenced to this home directory.  However because the
% mvarget.exe program is hardwired to create the varpas.dat
% file in C:\matlab\temp directory a 'temp' directory must
% be created within the matlab directory before running.
% An additional line is added to copy the varpas.dat file
% to the proper working directory.

load mcorfact;
load ffs1;
%dirc = input ('Directory: ', 's');
%filnm = input ('File Name? XXXNNN:  ','s');
%%filepas = ['\csma\',dirc];  %Original line

filepas = ['csma\',dirc];
filepas = [filepas, '\'];
filepas = [filepas, filnm];
%filepas = [filepas,'.spe'];
combuf = ['temp\mvarget.exe ', filepas];
dos (combuf);
% added by S.M.
%!copy C:\matlab\temp\varpas.dat temp\varpas.dat
dos ('copy C:\matlab\temp\varpas.dat temp\varpas.dat');
%!del C:\matlab\temp\varpas.dat
dos ('del C:\matlab\temp\varpas.dat');

load temp\varpas.dat;
yvals = varpas;
yvals = yvals.*mgcorr3;
yvals = filtfilt(b7,a7,yvals);
dos ('del temp\varpas.dat');
xval = mxgen3(450);


return
```

APPENDIX B: PED-MEASURED DISSOLVED PAH AND PCB CONCENTRATIONS FOR APRIL 1999 AND OCTOBER 2000

April 1999 Lower Hudson Estuary PED-measured Dissolved Concentrations
Rachel Adams

R (KJ/mol/K):	0.00831451
PED I (old; cm):	3.50E-03
PED I (new; cm):	2.70E-03

Chemical	log K_{PEW} log (Lw/kgpe) (23 C)	Excess Enthalpy (kJ/mol)	mult. factor 23C --> 9C	log K_{PEW} log (Lw/kgpe) (9 C)	Ks	LeBas Vol. (cm^3/mol)	Diffusivity (cm^2/s)	Diffusivity @ 8 C (cm^2/s)
Phenanthrene	4.3	18	1.44	4.46	0.28	199	1.00E-10	3.69E-11
Pyrene	5	29	1.79	5.25	0.29	214	2.00E-11	7.37E-12
Benzo(a)pyrene	6.2	11	1.25	6.30	0.48	265	7.00E-12	2.58E-12

	Time (d)	Mt/Minf (new PED) (t = 3.0 days)	Mt/Minf (new PED) (t = 2.79 days)	Mt/Minf (new PED) (t = 2.90 days)	Mt/Minf (new PED) (t = 1.96 days)
Hastings - Neap:	3	0.968	0.960	0.964	0.902
S. Conv. - Neap:	2.79	0.575	0.555	0.566	0.467
Battery - Neap:	2.90	0.342	0.330	0.336	0.276
Hastings - Spring:	1.96				
S. Conv. - Spring:	2.88				
Battery - Spring:	3.13				

	Mt/Minf (old PED) (t = 3.0 days)	Mt/Minf (old PED) (t = 2.79 days)	Mt/Minf (old PED) (t = 2.90 days)	Mt/Minf (old PED) (t = 1.96 days)
	0.882	0.865	0.874	0.770
	0.446	0.430	0.438	0.360
	0.264	0.254	0.259	0.213

April 1999 Lower Hudson Estuary PED-measured Dissolved Concentrations
Rachel Adams

Location	Time	Depth	Old or New PE	Salinity Range (from Rocky) (psu)		Average Salinity (psu)	Salinity Error (psu)	Salinity (Molarity)
Hastings	Neap (April 8-11)	8.5 m from bottom	new	1.9	2.1	2	0.1	0.03
Hastings	Neap (April 8-11)	5.5 m from bottom	new	14	18	16	2	0.24
Hastings	Neap (April 8-11)	5.5 m from bottom	old	14	18	16	2	0.24
Hastings	Neap (April 8-11)	3 m from bottom	new	17	18	17.5	0.5	0.27
Hastings	Neap (April 8-11)	2 m from bottom	new	17	18	17.5	0.5	0.27
Hastings	Neap (April 8-11)	1 m from bottom	new	17	18	17.5	0.5	0.27
Hastings	Spring (April 15-18)	8 m from bottom	old	6	7	6.5	0.5	0.10
Hastings	Spring (April 15-18)	3 m from bottom	old	6	7.5	6.75	0.75	0.10
Hastings	Spring (April 15-18)	1 m from bottom	old	6	7.5	6.75	0.75	0.10
S. Conv.	Neap (April 8-11)	6.7 m from bottom	old	8	12	10	2	0.15
S. Conv.	Neap (April 8-11)	5.5 m from bottom	old	13	18	15.5	2.5	0.23
S. Conv.	Neap (April 8-11)	3 m from bottom	new	19	20	19.5	0.5	0.30
S. Conv.	Neap (April 8-11)	2 m from bottom	old	19	20	19.5	0.5	0.30
S. Conv.	Neap (April 8-11)	2 m from bottom	new	19	20	19.5	0.5	0.30
S. Conv.	Neap (April 8-11)	1 m from bottom	old	19	20	19.5	0.5	0.30
S. Conv.	Spring (April 15-18)	8 m from bottom	new	12	15	13.5	1.5	0.20
S. Conv.	Spring (April 15-18)	3.5 m from bottom	new	12	18	15	3	0.23
S. Conv.	Spring (April 15-18)	1.5 m from bottom	new	12	18	15	3	0.23
Battery	Neap (April 8-11)	9 m from bottom	old	6	12	9	3	0.14
Battery	Neap (April 8-11)	5.5 m from bottom	old	17	25	21	4	0.32
Battery	Neap (April 8-11)	3 m from bottom	old	20	27	23.5	3.5	0.36
Battery	Neap (April 8-11)	2 m from bottom	old	27	27	27	0	0.41
Battery	Neap (April 8-11)	2 m from bottom	new	27	27	27	0	0.41
Battery	Neap (April 8-11)	1 m from bottom	old	27	27	27	0	0.41
Battery	Spring (April 15-18)	10 m from bottom	old	20	21	20.5	0.5	0.31
Battery	Spring (April 15-18)	3.5 m from bottom	old	21	23	22	1	0.33
Battery	Spring (April 15-18)	1.5 m from bottom	old	21	23	22	1	0.33

April 1999 Lower Hudson Estuary PED-measured Dissolved Concentrations
Rachel Adams

			ng/g PED			ng/L		
Location	Time	Depth	Phenanthrene	Pyrene	Benzo(a)pyrene	Phenanthrene	Pyrene	Benzo(a)pyrene
Hastings	Neap (April 8-11)	8.5 m from bottom	90	234			2.2	
Hastings	Neap (April 8-11)	5.5 m from bottom	120	569	7		4.7	
Hastings	Neap (April 8-11)	5.5 m from bottom	98	345	4	3.3	3.7	0.006
Hastings	Neap (April 8-11)	3 m from bottom	127	323			2.6	
Hastings	Neap (April 8-11)	2 m from bottom	118	504	6	3.6	4.1	0.006
Hastings	Neap (April 8-11)	1 m from bottom	72	148			1.2	
Hastings	Spring (April 15-18)	8 m from bottom						
Hastings	Spring (April 15-18)	3 m from bottom	68	200	5	2.9	2.9	0.010
Hastings	Spring (April 15-18)	1 m from bottom	22	209	4	0.9	3.0	0.009
S. Conv.	Neap (April 8-11)	6.7 m from bottom	91	284	5		3.3	
S. Conv.	Neap (April 8-11)	5.5 m from bottom	149	421	4	5.2	4.7	0.006
S. Conv.	Neap (April 8-11)	3 m from bottom	79	285	6		2.3	
S. Conv.	Neap (April 8-11)	2 m from bottom	108	354	4	3.6	3.8	0.006
S. Conv.	Neap (April 8-11)	2 m from bottom	143	553	7	4.3	4.5	0.008
S. Conv.	Neap (April 8-11)	1 m from bottom		269			2.9	
S. Conv.	Spring (April 15-18)	8 m from bottom	83	994	9	2.6	8.5	0.010
S. Conv.	Spring (April 15-18)	3.5 m from bottom	60	892	12	1.9	7.5	0.014
S. Conv.	Spring (April 15-18)	1.5 m from bottom	104	1134	39	3.3	9.6	0.046
Battery	Neap (April 8-11)	9 m from bottom	90	213			2.5	
Battery	Neap (April 8-11)	5.5 m from bottom	64	229	3	2.1	2.4	0.004
Battery	Neap (April 8-11)	3 m from bottom	64	201			2.0	
Battery	Neap (April 8-11)	2 m from bottom	42	119	2	1.3	1.2	0.003
Battery	Neap (April 8-11)	2 m from bottom	60	271	4	1.7	2.0	0.004
Battery	Neap (April 8-11)	1 m from bottom	48	132			1.3	
Battery	Spring (April 15-18)	10 m from bottom	75	531	8	2.4	5.4	0.011
Battery	Spring (April 15-18)	3.5 m from bottom	72	471	6	2.3	4.7	0.008
Battery	Spring (April 15-18)	1.5 m from bottom	71	538		2.3	5.4	

April 1999 Lower Hudson Estuary PED-measured Dissolved Concentrations -- PCBs

	(mS/cm)	(Molarity)	(psu)
Spring Tide Salinity near surface:	27.8	0.23	17
Spring Tide Salinity near bottom:	32.6	0.27	19
Neap Tide Salinity near surface:		0.10	7
Neap Tide Salinity near bottom:		0.30	21

PCB Congener	from Hawker & Connell, 1988 Kow (Lw/Lo)	Kpe (est.) (Lw/kgPE)	Excess Enthalpy of sol.* (kJ/mol)	Kpe @ 8 C (Lw/kgPE)	Ks**	Kpe @ 8 C & @ 0.10 M	Kpe @ 8 C & @ 0.23 M	Kpe @ 8 C & @ 0.27 M	Kpe @ 8 C & 0.30 M	Kom (L/kg)	Dpe est. @ 23C (cm^2/s)	Dpe est @ 8 C (cm^2/s)
52	6.92E+05	2.51E+05	12	3.26E+05	0.48	3.64E+05	4.19E+05	4.39E+05	4.55E+05	3.70E+04	7.0E-12	2.8E-12
95	1.35E+06	1.36E+06	20	2.10E+06	0.52	2.36E+06	2.75E+06	2.89E+06	3.00E+06	1.48E+05	4.0E-12	1.6E-12
105	4.47E+06	1.17E+07	20	1.81E+07	0.52	2.04E+07	2.37E+07	2.50E+07	2.59E+07	8.66E+05	4.0E-12	1.6E-12
128	5.50E+06	1.71E+07	14	2.29E+07	0.56	2.60E+07	3.06E+07	3.24E+07	3.37E+07	1.18E+06	1.0E-12	4.0E-13

Old PED length (cm):	3.50E-03
New PED length (cm):	2.55E-03
R (kJ/mol/K):	0.0083145
T (C):	8

* Excess enthalpy of solution of liquid = excess enthalpy of solution of a solid - enthalpy of melting
PCB #52 measured experimentally; the remaining values calculated according to above eqn. with values from Shiu & Ma, 2000.
**Ks = 0.0018 * LeBas Molar Volume according to Xie et al., 1997

April 1999 Lower Hudson Estuary PED-Measured Dissolved Concentrations -- PCBs

		4 Cl			5 Cl				6 Cl		7 Cl	
		D19-52	D23-44	D32-66	D32-95	D39-99	D46-110	D54-105	D53-146	D63-128	D66-174	D67-177
NEAP TIDE PED's at the Battery (SS)												
							Area Cmpd. in extract (not %recovery corrected)					
0222BNP9	9 m	5.61E+06	2.74E+06	1.54E+06	1.48E+06	6.17E+05	1.52E+06	1.19E+05	6.47E+04	4.07E+04	1.80E+04	2.18E+04
Tot.Xtr.Vol. (uL)	75											
New or Old	Old						**Mass Cmpd. (pg) / (g) PED dry wgt.**					
PED dry wgt (g)	2.17	18291	8937	5040	7036	2944	7253	567	408	257	141	171
Exposure Time (d)	2.9				Concentration calculated based on Kpe and time for diffusion into PED (pg/L)							
Salinity (psu)	9	**183**			**14**			**0.14**		**0.10**		
Salinity "Error" (psu)	3	0.27			0.21			0.21		0.10		
Distance from bottom:							Area Cmpd. in extract (not %recovery corrected)					
0222BNP3	3 m	1.21E+06	5.85E+05	4.27E+05	4.43E+05	1.73E+05	3.88E+05	6.72E+04				
Tot.Xtr.Vol. (uL)	200											
New or Old	Old						**Mass Cmpd. (pg) / (g) PED dry wgt.**					
PED dry wgt (g)	1.96	4385	2121	1549	2349	916	2055	356				
Exposure Time (d)	2.9				Concentration calculated based on Kpe and time for diffusion into PED (pg/L)							
Salinity (psu)	23.5	**34**			**3**			**0.07**				
Salinity "Error" (psu)	3.5	0.27			0.21			0.21				
Distance from bottom:							Area Cmpd. in extract (not %recovery corrected)					
0222BNP1	1 m	9.29E+05	5.17E+05	3.64E+05	4.63E+05	1.17E+05	3.09E+05					
Tot.Xtr.Vol. (uL)	200											
New or Old	Old						**Mass Cmpd. (pg) / (g) PED dry wgt.**					
PED dry wgt (g)	2.07	3191	1776	1249	2323	587	1552					
Exposure Time (d)	2.90				Concentration calculated based on Kpe and time for diffusion into PED (pg/L)							
Salinity (psu)	27	**24**			**3**							
Salinity "Error" (psu)	0	0.27			0.21							

April 1999 Lower Hudson Estuary PED-Measured Dissolved Concentrations -- PCBs

		4 Cl			5 Cl				6 Cl		
		D19-52	D23-44	D32-66	D32-95	D39-99	D46-110	D54-105	D53-146	D63-128	D66-174
SPRING TIDE PED's at the Battery (SS)											
Distance from bottom:							Area Cmpd. in extract (not %recovery corrected)				
0222BSP1	10	6.49E+05	3.49E+05	2.41E+05	2.35E+05	8.89E+04	2.17E+05				
Tot.Xtr.Vol. (uL)	175										
New or Old	Old						**Mass Cmpd. (pg) / (g) PED dry wgt.**				
PED dry wgt (g)	1.96	2354	1266	872	1244	471	1152				
Exposure Time (d)	3.125				Concentration calculated based on Kpe and time for diffusion into PED (pg/L)						
Salinity (psu)	21	**18**			**1.6**						
Salinity "Error" (psu)	0.5	0.28			0.21						
Distance from bottom:							Area Cmpd. in extract (not %recovery corrected)				
0222BSP4	3.5	4.11E+05	2.60E+05	1.55E+05	1.28E+05	5.75E+04	1.42E+05	2.65E+04			
Tot.Xtr.Vol. (uL)	125										
New or Old	Old						**Mass Cmpd. (pg) / (g) PED dry wgt.**				
PED dry wgt (g)	1.78	1638	1037	619	743	335	828	154			
Exposure Time (d)	3.125				Concentration calculated based on Kpe and time for diffusion into PED (pg/L)						
Salinity (psu)	22	**12**			**0.7**			**0.03**			
Salinity "Error" (psu)	1	0.28			0.21			0.21			
Distance from bottom:							Area Cmpd. in extract (not %recovery corrected)				
0222BSP2	1.5	1.18E+06	6.76E+05	4.64E+05	3.92E+05	1.60E+05	4.02E+05	3.52E+04			
Tot.Xtr.Vol. (uL)	175										
New or Old	Old						**Mass Cmpd. (pg) / (g) PED dry wgt.**				
PED dry wgt (g)	1.73	4825	2772	1903	2348	959	2411	211			
Exposure Time (d)	3.125				Concentration calculated based on Kpe and time for diffusion into PED (pg/L)						
Salinity (psu)	22	**38**			**3.3**			**0.04**			
Salinity "Error" (psu)	1	0.28			0.21			0.21			
BATTERY FIELD BLANK PED											
							Area Cmpd. in extract (not %recovery corrected)				
0222BSPB		4.36E+04			5.64E+04						
Tot.Xtr.Vol. (uL)	175										
New or Old	Old						**Mass Cmpd. (pg) / (g) PED dry wgt.**				
PED dry wgt (g)	1.78	174			328						
Exposure Time (d)											

April 1999 Lower Hudson Estuary PED-Measured Dissolved Concentrations -- PCBs

		4 Cl			5 Cl				6 Cl		7 Cl	
		D19-52	D23-44	D32-66	D32-95	D39-99	D46-110	D54-105	D53-146	D63-128	D66-174	D67-177
NEAP TIDE PED's at the SETM												
	Distance from Bottom:						Area Cmpd. in extract (not %recovery corrected)					
0228CNP7	6.7 m	6.65E+06	2.83E+06	1.80E+06	1.92E+06	8.60E+05	1.87E+06	1.45E+05	8.18E+04	4.12E+04	3.36E+04	2.88E+04
Tot.Xtr.Vol. (uL)	200											
New or Old	New						**Mass Cmpd. (pg) / (g) PED dry wgt.**					
PED dry wgt (g)	1.63	32782	13965	8895	14957	6706	14587	1129	887	447	481	412
Exposure Time (d)	2.79						Concentration calculated based on Kpe and time for diffusion into PED (pg/L)					
Salinity (psu)	10	**253**			**22**			**0.21**		**0.13**		
							Fraction of Equilibrium					
Salinity "Error" (psu)	2	0.37			0.28			0.28		0.14		
	Distance from Bottom:						Area Cmpd. in extract (not %recovery corrected)					
0228CNP3	3 m	3.77E+06	1.73E+06	1.08E+06	1.11E+06	4.54E+05	1.11E+06	1.31E+05	5.65E+04	5.18E+04		
Tot.Xtr.Vol. (uL)	175											
New or Old	New						**Mass Cmpd. (pg) / (g) PED dry wgt.**					
PED dry wgt (g)	2.07	14684	6756	4218	6866	2795	6861	809	484	443		
Exposure Time (d)	2.79						Concentration calculated based on Kpe and time for diffusion into PED (pg/L)					
Salinity (psu)	19.5	**88**			**7**			**0.12**		**0.10**		
							Fraction of Equilibrium					
Salinity "Error" (psu)	0.5	0.37			0.28			0.28		0.14		
	Distance from Bottom:						Area Cmpd. in extract (not %recovery corrected)					
0228CNP1	1 m	1.19E+06	5.89E+05	3.92E+05	4.53E+05	1.67E+05	3.90E+05	3.22E+04				
Tot.Xtr.Vol. (uL)	200											
New or Old	Old						**Mass Cmpd. (pg) / (g) PED dry wgt.**					
PED dry wgt (g)	2.28	4179	2077	1383	2524	930	2175	179				
Exposure Time (d)	2.79						Concentration calculated based on Kpe and time for diffusion into PED (pg/L)					
Salinity (psu)	19.5	**33**			**3**			**0.04**				
							Fraction of Equilibrium					
Salinity "Error" (psu)	0.5000	0.27			0.20			0.20				

April 1999 Lower Hudson Estuary PED-Measured Dissolved Concentrations -- PCBs

		4 Cl			5 Cl			6 Cl		
		D19-52	D23-44	D32-66	D32-95	D39-99	D46-110	D54-105	D53-146	D63-128	D66-174
SPRING TIDE PED's at the SETM											
	Distance from Bottom:						Area Cmpd. in extract (not %recovery corrected)				
0228CSP8	8 m	4.02E+05	1.88E+05	2.30E+04	7.02E+05	8.14E+04	1.63E+05				
Tot.Xtr.Vol. (uL)	200										
New or Old	New						**Mass Cmpd. (pg) / (g) PED dry wgt.**				
PED dry wgt (g)	1.85	1752	817	100	4830	560	1125				
Exposure Time (d)	2.88						Concentration calculated based on Kpe and time for diffusion into PED (pg/L)				
Salinity (psu)	13.5	**11**			**6**						
							Fraction of Equilibrium				
Salinity "Error" (psu)	1.5	0.37			0.28						
	Distance from Bottom:						Area Cmpd. in extract (not %recovery corrected)				
0228CSP3	3.5 m	3.37E+05	2.00E+05	8.68E+04	1.10E+05	5.30E+04	1.06E+05				
Tot.Xtr.Vol. (uL)	200										
New or Old	New						**Mass Cmpd. (pg) / (g) PED dry wgt.**				
PED dry wgt (g)	1.52	1783	1055	459	923	443	884				
Exposure Time (d)	2.88						Concentration calculated based on Kpe and time for diffusion into PED (pg/L)				
Salinity (psu)	15	**11**									
							Fraction of Equilibrium				
Salinity "Error" (psu)	3	0.37			0.28						
	Distance from Bottom:						Area Cmpd. in extract (not %recovery corrected)				
0228CSP1	1.5 m	1.90E+05	1.02E+05	2.89E+04	9.10E+05	1.76E+04	9.46E+04				
Tot.Xtr.Vol. (uL)	200										
New or Old	New						**Mass Cmpd. (pg) / (g) PED dry wgt.**				
PED dry wgt (g)	1.96	779	421	1190	5912	114	615				
Exposure Time (d)	2.88						Concentration calculated based on Kpe and time for diffusion into PED (pg/L)				
Salinity (psu)	15	**4**			**7**						
							Fraction of Equilibrium				
Salinity "Error" (psu)	3	0.37			0.28						
CONVERGENCE FIELD BLANK PED											
							Area Cmpd. in extract (not %recovery corrected)				
0228CBLK		6.30E+04	3.40E+04	7.12E+04	1.59E+05	3.27E+04	8.38E+04				
Tot.Xtr.Vol. (uL)	175										
							Mass Cmpd. (pg) / (g) PED dry wgt.				
PED dry wgt (g)	1.96	259	140	293	1035	213	545				

April 1999 Lower Hudson Estuary PED-Measured Dissolved Concentrations -- PCBs

		4 Cl			5 Cl				6 Cl		
		D19-52	D23-44	D32-66	D32-95	D39-99	D46-110	D54-105	D53-146	D63-128	D66-174
NEAP TIDE PED's at Hastings (NS)											
	Distance from Bottom:						Area Cmpd. in extract (not %recovery corrected)				
0226HNP9	8.5 m	3.43E+06	1.38E+06	7.76E+05	1.07E+06	3.54E+05	7.95E+05	4.65E+04	4.65E+04	1.98E+04	
Tot.Xtr.Vol. (uL)	300										
New or Old	Old						**Mass Cmpd. (pg) / (g) PED dry wgt.**				
PED dry wgt (g)	2.17	11779	4725	2661	5468	1803	4047	237	326	139	
Exposure Time (d)	3.00						Concentration calculated based on Kpe and time for diffusion into PED (pg/L)				
Salinity (psu)	2	**125**			**12**			**0.06**		**0.05**	
							Fraction of equilibrium				
Salinity "Error" (psu)	0.1	0.28			0.21			0.21		0.21	
	Distance from Bottom:						Area Cmpd. in extract (not %recovery corrected)				
0226HNP3	3 m	5.80E+06	2.78E+06	1.49E+06	1.62E+06	6.38E+05	1.55E+06	1.59E+05			
Tot.Xtr.Vol. (uL)	300										
New or Old	New						**Mass Cmpd. (pg) / (g) PED dry wgt.**				
PED dry wgt (g)	1.63	26534	12728	6807	10975	4331	10495	1077			
Exposure Time (d)	3.00						Concentration calculated based on Kpe and time for diffusion into PED (pg/L)				
Salinity (psu)	17.5	**159**			**13**			**0.15**			
							Fraction of equilibrium				
Salinity "Error" (psu)	0.5	0.38			0.29			0.29			
	Distance from Bottom:						Area Cmpd. in extract (not %recovery corrected)				
0226HNP1	1 m	2.48E+06	1.24E+06	6.46E+05	7.09E+05	2.66E+05	6.56E+05				
Tot.Xtr.Vol. (uL)	300										
New or Old	Old						**Mass Cmpd. (pg) / (g) PED dry wgt.**				
PED dry wgt (g)	2.28	8088	4036	2109	3434	1288	3180				
Exposure Time (d)	3.00										
Salinity (psu)	18	**67**			**6**						
							Fraction of equilibrium				
Salinity "Error" (psu)	0.5	0.28			0.21						

April 1999 Lower Hudson Estuary PED-Measured Dissolved Concentrations -- PCBs

		4 Cl			5 Cl				6 Cl		
		D19-52	D23-44	D32-66	D32-95	D39-99	D46-110	D54-105	D53-146	D63-128	D66-174
SPRING TIDE PED's at Hastings (NS)											
Distance from Bottom:							Area Cmpd. in extract (not %recovery corrected)				
0226HSP8	8 m	5.58E+04	2.01E+04	4.32E+04	1.29E+05		2.10E+04				
Tot.Xtr.Vol. (uL)	300										
New or Old	Old						**Mass Cmpd. (pg) / (g) PED dry wgt.**				
PED dry wgt (g)	2.17	191	68.9	148	655		107				
Exposure Time (d)	1.96						Concentration calculated based on Kpe and time for diffusion into PED (pg/L)				
Salinity (psu)	7	**2**			**2**						
							Fraction of equilibrium				
Salinity "Error" (psu)	0.5	0.22			0.17						
***This sample (Spring Hastings PED @ 8 m is **suspect; i**t may have been switched wit							Area Cmpd. in extract (not %recovery corrected)				
0226HSP3	3 m	1.68E+06	7.01E+05	4.44E+05	5.62E+05	1.80E+05	4.26E+05	5.01E+04			
Tot.Xtr.Vol. (uL)	300										
New or Old	Old						**Mass Cmpd. (pg) / (g) PED dry wgt.**				
PED dry wgt (g)	2.07	6064	2529	1603	3008	966	2280	268			
Exposure Time (d)	1.96						Concentration calculated based on Kpe and time for diffusion into PED (pg/L)				
Salinity (psu)	6.75	**75**			**8**			**0.08**			
								Fraction of equilibrium			
Salinity "Error" (psu)	0.75	0.22			0.17			0.17			
Distance from Bottom:							Area Cmpd. in extract (not %recovery corrected)				
0226HSP1	1 m	3.12E+06	1.45E+06	8.48E+05	8.63E+05	3.41E+05	7.55E+05	5.28E+04			
Tot.Xtr.Vol. (uL)	300										
New or Old	Old						**Mass Cmpd. (pg) / (g) PED dry wgt.**				
PED dry wgt (g)	2.17	10699	4962	2910	4392	1737	3844	269			
Exposure Time (d)	1.96						Concentration calculated based on Kpe and time for diffusion into PED (pg/L)				
Salinity (psu)	6.75	**132**			**11**			**0.08**			
								Fraction of equilibrium			
Salinity "Error" (psu)	0.75	0.22			0.17			0.17			

October 2000 Lower Hudson Estuary PED-measured Dissolved Concentrations--PAHs
Rachel Adams

PED I (cm): 2.70E-03

Chemical	log K_{PEW} log (Lw/kgpe) (23 C)	Excess Enthalpy (kJ/mol)	mult. factor 23C --> 17C	log K_{PEW} log (Lw/kgpe) (17 C)	Ks	LeBas Vol. (cm^3/mol)
Phenanthrene	4.3	18	1.16	4.37	0.28	199
Pyrene	5	29	1.28	5.11	0.29	214
Benzo(a)pyrene	6.2	11	1.10	6.24	0.48	265

	Time (d)
Battery- Neap:	1.68
Battery- Spring:	1.77
Conv S.- Neap:	2.03
Conv S.- Neap-Spring:	6.26
Conv S.- Spring	1.78
Conv N.- Neap:	1.79
Conv N.- Neap-Spring:	6.26
Conv N.- Spring	1.83
Hastings - Neap:	1.70
Hastings - Spring:	1.86

Chemical	Diffusivity (cm^2/s)	Diffusivity @ 1 (cm^2/s)	Mt/Minf (t = 1.68 days)	Mt/Minf (t = 2.03 days)	Mt/Minf (t = 6.26 days)	Mt/Minf (t = 1.78 days)
Phenanthrene	1.00E-10	6.9E-11	0.972	0.986	1.000	0.977
Pyrene	1.00E-11	6.9E-12	0.417	0.458	0.769	0.429
Benzo(a)pyrene	7.00E-12	4.8E-12	0.349	0.383	0.663	0.359

October 2000 Lower Hudson Estuary PED-measured Dissolved Concentrations--PAHs

Rachel Adams

Location	Time	Depth	Salinity Range (from Rocky) (psu)		Average Salinity (psu)	Salinity "Error" (psu)	Salinity (Molarity)
Battery	Neap (Oct 4-6)	2 m below surf.	17	20	18.5	1.5	0.16
Battery	Neap (Oct 4-6)	2 m from bottom	27	27	27	0	0.23
Battery	Neap (Oct 4-6)	1 m from bottom	27	27	27	0	0.23
Batt. Field Blank	Neap (Oct 4-6)	Field Blank					
Battery	Spring (Oct 12-14)	2 m below surf.	23	23	23	0	0.20
Battery	Spring (Oct 12-14)	2 m from bottom	25	25	25	0	0.21
Battery	Spring (Oct 12-14)	1 m from bottom	25	25	25	0	0.21
Batt. Field Blank	Spring (Oct 12-14)	Field Blank					
S. Conv.	Neap (Oct 4-6)	2 m below surf.	10	12	11	1	0.09
S. Conv.	Neap (Oct 4-6)	2 m from bottom	20	25	22.5	2.5	0.19
S. Conv.	Neap (Oct 4-6)	1 m from bottom	20	25	22.5	2.5	0.19
S. Conv. Field Blank	Neap (Oct 4-6)	Field Blank					
S. Conv.	Neap-Spring (Oct 6-12)	2 m below surf.	10	24	17	7	0.14
S. Conv.	Neap-Spring (Oct 6-12)	2 m from bottom	14	26	20	6	0.17
S. Conv.	Neap-Spring (Oct 6-12)	1 m from bottom	14	26	20	6	0.17
S. Conv. Field Blank	Neap-Spring (Oct 6-12)	Field Blank					
S. Conv.	Spring (Oct 12-14)	2 m below surf.	13	20	16.5	3.5	0.14
S. Conv.	Spring (Oct 12-14)	2 m from bottom	15	22	18.5	3.5	0.16
S. Conv.	Spring (Oct 12-14)	1 m from bottom	15	22	18.5	3.5	0.16
S. Conv. Field Blank	Spring (Oct 12-14)	Field Blank					

October 2000 Lower Hudson Estuary PED-measured Dissolved Concentrations--PAHs

Rachel Adams

Location	Time	Depth	Salinity Range (from Rocky) (psu)		Average Salinity (psu)	Salinity "Error" (psu)	Salinity (Molarity)
N. Conv.	Neap (Oct 4-6)	2 m below surf.	6	10	8	2	0.07
N. Conv.	Neap (Oct 4-6)	2 m from bottom	10	22	16	6	0.14
N. Conv.	Neap (Oct 4-6)	1 m from bottom	10	22	16	6	0.14
N. Conv. Field Blank	Neap (Oct 4-6)	Field Blank					
N. Conv.	Neap-Spring (Oct 6-12)	2 m below surf.	6	17	11.5	5.5	0.10
N. Conv.	Neap-Spring (Oct 6-12)	2 m from bottom	10	20	15	5	0.14
N. Conv.	Neap-Spring (Oct 6-12)	1 m from bottom	10	20	15	5	0.14
N. Conv. Field Blank	Neap-Spring (Oct 6-12)	Field Blank					
N. Conv.	Spring (Oct 12-14)	2 m below surf.	12	17	14.5	2.5	0.12
N. Conv.	Spring (Oct 12-14)	2 m from bottom	13	20	16.5	3.5	0.14
N. Conv.	Spring (Oct 12-14)	1 m from bottom	13	20	16.5	3.5	0.14
N. Conv. Field Blank	Spring (Oct 12-14)	Field Blank					
Hastings	Neap (Oct 4-6)	2 m below surf.	7	9	8	1	0.07
Hastings	Neap (Oct 4-6)	2 m from bottom	17	22	19.5	2.5	0.17
Hastings	Neap (Oct 4-6)	1 m from bottom	17	22	19.5	2.5	0.17
Hastings-Field Blank	Neap (Oct 4-6)	Field Blank					
Hastings	Spring (Oct 12-14)	2 m below surf.	8	13	10.5	2.5	0.09
Hastings	Spring (Oct 12-14)	2 m from bottom	12	15	13.5	1.5	0.12
Hastings	Spring (Oct 12-14)	1 m from bottom	12	15	13.5	1.5	0.12
Hastings-Field Blank	Spring (Oct 12-14)	Field Blank					

October 2000 Lower Hudson Estuary PED-measured Dissolved Concentrations--PAHs

Rachel Adams

			ng/g PED			ng/L		
Location	Time	Depth	Phenanthrene	Pyrene	Benzo(a)pyrene	Phenanthrene	Pyrene	Benzo(a)pyrene
Battery	Neap (Oct 4-6)	2 m below surf.	59	3357	60	2.4	57	0.083
Battery	Neap (Oct 4-6)	2 m from bottom	20	2846	47	0.8	46	0.061
Battery	Neap (Oct 4-6)	1 m from bottom	31	3076	43	1.2	50	0.056
Batt. Field Blank	Neap (Oct 4-6)	Field Blank	14	9.9	b.d.l.			
Battery	Spring (Oct 12-14)	2 m below surf.	43	1653	34	1.7	26	0.044
Battery	Spring (Oct 12-14)	2 m from bottom	32	1290	25	1.2	20	0.031
Battery	Spring (Oct 12-14)	1 m from bottom	32	1402	26	1.2	22	0.032
Batt. Field Blank	Spring (Oct 12-14)	Field Blank	7					
S. Conv.	Neap (Oct 4-6)	2 m below surf.	25	1254	19	1.0	20	0.026
S. Conv.	Neap (Oct 4-6)	2 m from bottom	14	2035	22	0.5	31	0.027
S. Conv.	Neap (Oct 4-6)	1 m from bottom	12	1803	24	0.5	27	0.029
S. Conv. Field Blank	Neap (Oct 4-6)	Field Blank	7.9	30	b.d.l.			
S. Conv.	Neap-Spring (Oct 6-12)	2 m below surf.	72	6438	315	2.8	60	0.233
S. Conv.	Neap-Spring (Oct 6-12)	2 m from bottom	68	6194	222	2.6	56	0.160
S. Conv.	Neap-Spring (Oct 6-12)	1 m from bottom	77	10285	269	3.0	94	0.194
S. Conv. Field Blank	Neap-Spring (Oct 6-12)	Field Blank	5.1	2.4	b.d.l.			
S. Conv.	Spring (Oct 12-14)	2 m below surf.	37	1010	35.2	1.5	17	0.048
S. Conv.	Spring (Oct 12-14)	2 m from bottom	--	--	--	--	--	--
S. Conv.	Spring (Oct 12-14)	1 m from bottom	41	1032	31.6	1.6	17	0.043
S. Conv. Field Blank	Spring (Oct 12-14)	Field Blank	6	1.90	b.d.l.			

October 2000 Lower Hudson Estuary PED-measured Dissolved Concentrations--PAHs
Rachel Adams

			ng/g PED			ng/L		
Location	Time	Depth	Phenanthrene	Pyrene	Benzo(a)pyrene	Phenanthrene	Pyrene	Benzo(a)pyrene
N. Conv.	Neap (Oct 4-6)	2 m below surf.	16	781	27	0.67	14	0.040
N. Conv.	Neap (Oct 4-6)	2 m from bottom	15	964	26	0.61	16	0.036
N. Conv.	Neap (Oct 4-6)	1 m from bottom	16	1285	34	0.65	21	0.047
N. Conv. Field Blank	Neap (Oct 4-6)	Field Blank	61	13	b.d.l.			
N. Conv.	Neap-Spring (Oct 6-12)	2 m below surf.	11	777	38	0.4	7	0.030
N. Conv.	Neap-Spring (Oct 6-12)	2 m from bottom	10	897	52	0.4	8	0.039
N. Conv.	Neap-Spring (Oct 6-12)	1 m from bottom	17	1783	65	0.7	17	0.049
N. Conv. Field Blank	Neap-Spring (Oct 6-12)	Field Blank						
N. Conv.	Spring (Oct 12-14)	2 m below surf.	6	472	12	0.24	8	0.017
N. Conv.	Spring (Oct 12-14)	2 m from bottom	4	627	14	0.17	10	0.019
N. Conv.	Spring (Oct 12-14)	1 m from bottom	5	869	16	0.19	14	0.022
N. Conv. Field Blank	Spring (Oct 12-14)	Field Blank						
Hastings	Neap (Oct 4-6)	2 m below surf.	8	290	14	0.33	5	0.021
Hastings	Neap (Oct 4-6)	2 m from bottom	2	558	10	0.10	9	0.014
Hastings	Neap (Oct 4-6)	1 m from bottom	2	832	17	0.10	14	0.023
Hastings-Field Blank	Neap (Oct 4-6)	Field Blank						
Hastings	Spring (Oct 12-14)	2 m below surf.	10	565	21	0.41	10	0.031
Hastings	Spring (Oct 12-14)	2 m from bottom	9	664	19	0.36	11	0.026
Hastings	Spring (Oct 12-14)	1 m from bottom	9	755	19	0.36	13	0.027
Hastings-Field Blank	Spring (Oct 12-14)	Field Blank						

October 2000 Lower Hudson Estuary PED-measured Dissolved Concentrations--PCBs

Rachel Adams

PED l (cm): 2.70E-03

Chemical	from Hawker & Connell, 1988 Kow (Lw/Lo)	Kpe (est.) (Lw/kgPE)	Excess Enthalpy of sol.* (kJ/mol)	mult. factor 23C --> 17C	log K_{PEW} log (Lw/kgpe) (17 C)	LeBas Volume (cm^3/mol.)	Ks**	log K_{PEW} w/0.15 M salt (Conv. S)	log K_{PEW} w/0.20 M salt (Battery)	Dpe est. @ 23((cm^2/s)	Dpe est @ 17 ((cm^2/s)
PCB #52	6.92E+05	2.51E+05	12	1.11	5.44	268.0	0.48	5.52	5.54	7.0E-12	4.8E-12
PCB #95	1.35E+06	1.36E+06	20	1.18	6.21	289.1	0.52	6.28	6.31	4.0E-12	2.7E-12
PCB #105	4.47E+06	1.17E+07	20	1.18	7.14	289.1	0.52	7.22	7.25	4.0E-12	2.7E-12
PCB #128	5.50E+06	1.71E+07	14	1.12	7.28	310.0	0.56	7.37	7.39	1.0E-12	6.9E-13

	Time (d)
Battery-Neap:	1.68
Conv S.- Neap:	2.03
Conv S.- Neap-Spring	6.26
Conv S.- Spring	1.78
Conv N.- Neap:	1.79
Conv N.- Neap-Spring	6.26
Conv N.- Spring	1.83

	Time (d)
Hastings - Neap	1.70
Hastings - Spring	1.86

Chemical	Mt/Minf (t = 1.68 days)	Mt/Minf (t = 2.03 days)	Mt/Minf (t = 6.26 days)	Mt/Minf (t = 1.78 days)
PCB #52	0.349	0.383	0.663	0.359
PCB #95	0.264	0.290	0.508	0.272
PCB #105	0.264	0.290	0.508	0.272
PCB #128	0.133	0.145	0.254	0.136

October 2000 Lower Hudson Estuary PED-measured Dissolved Concentrations--PCBs

Rachel Adams

Location	Time	Depth	Salinity Range (from Rocky) (psu)		Average Salinity (psu)	Salinity Error (psu)	Salinity (Molarity)
Battery	Neap (Oct 4-6)	2 m below surf.	17	20	19	2	0.16
Battery	Neap (Oct 4-6)	2 m from bottom	27	27	27	0	0.23
Battery	Neap (Oct 4-6)	1 m from bottom	27	27	27	0	0.23
Batt. Field Blank	Neap (Oct 4-6)	Field Blank					
Battery	Spring (Oct 12-14)	2 m below surf.	23	23	23	0	0.20
Battery	Spring (Oct 12-14)	2 m from bottom	25	25	25	0	0.21
Battery	Spring (Oct 12-14)	1 m from bottom	25	25	25	0	0.21
Batt. Field Blank	Spring (Oct 12-14)	Field Blank					
S. Conv.	Neap (Oct 4-6)	2 m below surf.	10	12	11	1	0.09
S. Conv.	Neap (Oct 4-6)	2 m from bottom	20	25	23	3	0.19
S. Conv.	Neap (Oct 4-6)	1 m from bottom	20	25	23	3	0.19
S. Conv. Field Blank	Neap (Oct 4-6)	Field Blank					
S. Conv.	Neap-Spring (Oct 6-12)	2 m below surf.	10	24	17	7	0.14
S. Conv.	Neap-Spring (Oct 6-12)	2 m from bottom	14	26	20	6	0.17
S. Conv.	Neap-Spring (Oct 6-12)	1 m from bottom	14	26	20	6	0.17
S. Conv. Field Blank	Neap-Spring (Oct 6-12)	Field Blank					
S. Conv.	Spring (Oct 12-14)	2 m below surf.	13	20	17	4	0.14
S. Conv.	Spring (Oct 12-14)	2 m from bottom	15	22	19	4	0.16
S. Conv.	Spring (Oct 12-14)	1 m from bottom	15	22	19	4	0.16
S. Conv. Field Blank	Spring (Oct 12-14)	Field Blank					

October 2000 Lower Hudson Estuary PED-measured Dissolved Concentrations--PCBs

Rachel Adams

Location	Time	Depth	Salinity Range (from Rocky) (psu)		Average Salinity (psu)	Salinity Error (psu)	Salinity (Molarity)
N. Conv.	Neap (Oct 4-6)	2 m below surf.	6	10	8	2	0.07
N. Conv.	Neap (Oct 4-6)	2 m from bottom	10	22	16	6	0.14
N. Conv.	Neap (Oct 4-6)	1 m from bottom	10	22	16	6	0.14
N. Conv. Field Blank	Neap (Oct 4-6)	Field Blank					
N. Conv.	Neap-Spring (Oct 6-12)	2 m below surf.	6	17	12	6	0.10
N. Conv.	Neap-Spring (Oct 6-12)	2 m from bottom	10	20	15	5	0.13
N. Conv.	Neap-Spring (Oct 6-12)	1 m from bottom	10	20	15	5	0.13
N. Conv. Field Blank	Neap-Spring (Oct 6-12)	Field Blank					
N. Conv.	Spring (Oct 12-14)	2 m below surf.	12	17	15	3	0.12
N. Conv.	Spring (Oct 12-14)	2 m from bottom	13	20	17	4	0.14
N. Conv.	Spring (Oct 12-14)	1 m from bottom	13	20	17	4	0.14
N. Conv. Field Blank	Spring (Oct 12-14)	Field Blank					
Hastings (C7)	Neap (Oct 4-6)	2 m below surf.	7	9	8	1	0.07
Hastings (C7)	Neap (Oct 4-6)	2 m from bottom	17	22	20	3	0.17
Hastings (C7)	Neap (Oct 4-6)	1 m from bottom	17	22	20	3	0.17
Hastings (C7)	Neap (Oct 4-6)	Field Blank					
Hastings (C7)	Spring (Oct 12-14)	2 m below surf.	8	13	11	3	0.09
Hastings (C7)	Spring (Oct 12-14)	2 m from bottom	12	15	14	2	0.12
Hastings (C7)	Spring (Oct 12-14)	1 m from bottom	12	15	14	2	0.12
Hastings (C7)	Spring (Oct 12-14)	Field Blank					

October 2000 Lower Hudson Estuary PED-measured Dissolved Concentrations--PCBs

Rachel Adams

			ng/g PED				pg/L			
Location	Time	Depth	PCB #52	PCB #95	PCB #105	PCB #128	PCB #52	PCB #95	PCB #105	PCB #128
Battery	Neap (Oct 4-6)	2 m below surf.	28	15	1.4	0.51	245	29	0.306	0.163
Battery	Neap (Oct 4-6)	2 m from bottom	13	8	1.1	0.28	104	14	0.218	0.081
Battery	Neap (Oct 4-6)	1 m from bottom	14	9	1.2	0.29	115	16	0.240	0.086
Batt. Field Blank	Neap (Oct 4-6)	Field Blank	0.15	0.14	0.0	b.d.l.				
Battery	Spring (Oct 12-14)	2 m below surf.	35	19	1.4	0.51	291	36	0.292	0.155
Battery	Spring (Oct 12-14)	2 m from bottom	24	13	1.1	0.28	196	24	0.222	0.083
Battery	Spring (Oct 12-14)	1 m from bottom	23	15	1.2	0.29	191	27	0.245	0.088
Batt. Field Blank	Spring (Oct 12-14)	Field Blank	0.05	0.09	0.006	b.d.l.				
S. Conv.	Neap (Oct 4-6)	2 m below surf.	37	19.0	2	0.667	312	36	0.417	0.198
S. Conv.	Neap (Oct 4-6)	2 m from bottom	34	15.3	2	0.549	260	26	0.353	0.163
S. Conv.	Neap (Oct 4-6)	1 m from bottom	26	11.1	1	0.441	196	19	0.275	0.131
S. Conv. Field Blank	Neap (Oct 4-6)	Field Blank	0.1	0.1	b.d.l.	b.d.l.				
S. Conv.	Neap-Spring (Oct 6-12)	2 m below surf.	72	40	5	1.64	332	41	0.54	0.280
S. Conv.	Neap-Spring (Oct 6-12)	2 m from bottom	54	31	4	1.25	242	31	0.43	0.206
S. Conv.	Neap-Spring (Oct 6-12)	1 m from bottom	58	33	4	1.34	260	33	0.51	0.222
S. Conv. Field Blank	Neap-Spring (Oct 6-12)	Field Blank	0.1	0.1	b.d.l.	b.d.l.				
S. Conv.	Spring (Oct 12-14)	2 m below surf.	32	17	1.9	0.62	278	34	0.425	0.196
S. Conv.	Spring (Oct 12-14)	2 m from bottom	--	--	--	--	--	--	--	--
S. Conv.	Spring (Oct 12-14)	1 m from bottom	30	16	2.0	0.65	249	30	0.444	0.205
S. Conv. Field Blank	Spring (Oct 12-14)	Field Blank	0.10	0.10	b.d.l.	b.d.l.				

October 2000 Lower Hudson Estuary PED-measured Dissolved Concentrations--PCBs

Rachel Adams

			ng/g PED				pg/L			
Location	Time	Depth	PCB #52	PCB #95	PCB #105	PCB #128	PCB #52	PCB #95	PCB #105	PCB #128
N. Conv.	Neap (Oct 4-6)	2 m below surf.	36	18	1.9	0.61	334	20	0.25	0.115
N. Conv.	Neap (Oct 4-6)	2 m from bottom	42	21	2.1	0.72	361	22	0.25	0.124
N. Conv.	Neap (Oct 4-6)	1 m from bottom	40	20	2.1	0.80	344	21	0.25	0.138
N. Conv. Field Blank	Neap (Oct 4-6)	Field Blank	0.1	0.1	b.d.l.	b.d.l.				
N. Conv.	Neap-Spring (Oct 6-12)	2 m below surf.	72	40	5	1.64	349	43	0.57	0.297
N. Conv.	Neap-Spring (Oct 6-12)	2 m from bottom	54	31	4	1.25	254	32	0.45	0.217
N. Conv.	Neap-Spring (Oct 6-12)	1 m from bottom	58	33	4	1.34	273	35	0.54	0.234
N. Conv. Field Blank	Neap-Spring (Oct 6-12)	Field Blank	0.1	0.1	b.d.l.	b.d.l.				
N. Conv.	Spring (Oct 12-14)	2 m below surf.	35	18	1.5	0.59	305	35	0.333	0.193
N. Conv.	Spring (Oct 12-14)	2 m from bottom	26	13	1.3	0.44	221	25	0.287	0.139
N. Conv.	Spring (Oct 12-14)	1 m from bottom	22	11	1.1	0.39	185	22	0.248	0.123
N. Conv. Field Blank	Spring (Oct 12-14)	Field Blank	0.09	0.10	0.015	b.d.l.				
Hastings (C7)	Neap (Oct 4-6)	2 m below surf.	35.0	16.1	1.1	0.4	325	34	0.263	0.150
Hastings (C7)	Neap (Oct 4-6)	2 m from bottom	35.2	17.1	1.4	0.5	293	32	0.296	0.158
Hastings (C7)	Neap (Oct 4-6)	1 m from bottom	28.5	14.1	1.2	0.4	237	26	0.256	0.139
Hastings (C7)	Neap (Oct 4-6)	Field Blank	0.2	0.1	0.0	b.d.l.				
Hastings (C7)	Spring (Oct 12-14)	2 m below surf.	38.6	16.5	1.4	0.6	350	34	0.334	0.206
Hastings (C7)	Spring (Oct 12-14)	2 m from bottom	37.7	16.0	1.4	0.6	333	32	0.334	0.205
Hastings (C7)	Spring (Oct 12-14)	1 m from bottom	32.5	14.3	1.3	0.5	287	28	0.303	0.182
Hastings (C7)	Spring (Oct 12-14)	Field Blank	0.1	0.1	b.d.l.	b.d.l.				

APPENDIX C: ESTIMATED FLOW RATES USED IN MODELING CALCULATIONS

Lower Hudson Estuary Flow Rates

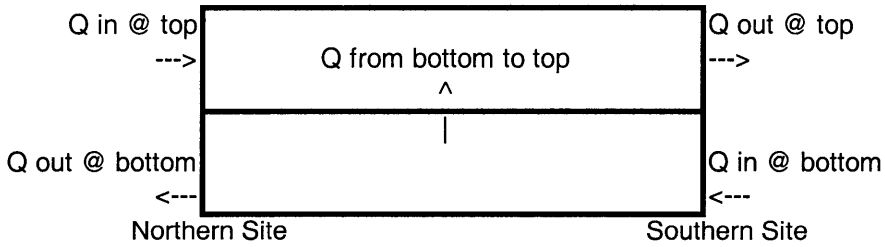

Time of Year	Tide	Q in @ top (m^3/s)	Q in @ bottom (m^3/s)	Q out @ top (m^3/s)	Q out @ bottom (m^3/s)	Q from bottom to top (m^3/s)
April 9 - 11, 1999	Neap	2000	2200	3400	800	1400
April 15 - 18, 1999	Spring	580	2850	3550	-120	---
October 4 - 6, 2000	Neap	380	530	760	150	380
October 12 - 14, 2000	Spring	1280	3160	3440	1010	---